REMARKS

Claims 1-3, 10-19, 36-38 and 42–50 are pending and under consideration. With this Amendment, claims 1 – 3, 10 – 17, 38, 42 – 43, 45 – 50 are being canceled; claims 51 – 70 are being added; and claims 18, 19, 36, 37, and 44 are being amended. Thus, after entry of this Amendment, claims 18 – 19, 36 – 37, 44, and 51 – 70 are pending and under consideration. The amendments to the specification and claims and the various rejections raised in the Office Action are discussed in more detail below.

The Specification Amendments

Although redundant over the priority claim timely made in applicants' application data sheet, 37 C.F.R. § 1.76, in an abundance of caution applicants have added an explicit recitation of the priority claim to the specification. No new matter has been added.

The definition of rhodobacteriochlorin at lines 23 – 25 on page 1 of the specification has been amended to correct the location of one of the 4 methyl groups, from position 8 (which is correctly reported in line 25 to have an ethyl, rather than methyl, substituent), to position 18. The location of each of the four methyl groups is correctly and unambiguously shown in reaction scheme **1** on pages 37 – 38. This clerical amendment adds no new matter.

The specification has also been amended to correct the reference number ascribed to the compound, Pd-Bpheid, at line 31 on page 20. The correct reference number is unambiguously provided on page 19, line 34. This clerical amendment does not introduce new matter.

The Amendments To The Claims

The claims have been amended to focus prosecution on a single species of bacteriochlorophyll derivative, palladium 3^1-oxo-15-methoxycarbonylmethyl-rhodobacteriochlorin 13^1-(2-sulfoethyl) amide, which is designated in the specification as compound **4**.

Claims 18 and 51 – 53 are drawn to the compound *per se*. Independent claim 18, as amended herein, now recites:

> 18. Palladium 3^1-oxo-15-methoxycarbonylmethyl-rhodobacteriochlorin 13^1-(2-sulfoethyl) amide, or pharmaceutically acceptable salt thereof.

Claims 51 – 52, which depend directly or indirectly from claim 18, further limit the counterion in the salt, with claim 53, in independent form, drawn to the dipotassium salt. Claim 53 is identical in scope to original claim 18. Exemplary support for these claims can be found in original claim 18 and in the

specification at page 20, lines 1 – 2; Example 1; and page 11, lines 29 – 31, the latter of which provides specific support for various of the cationic counterions.

Claim 19 is drawn to pharmaceutical compositions comprising the compound of claim 18. Claim 19 has been amended by deleting the adjectival modifier, "bacteriochlorophyll", for increased clarity, and has been amended to adjust its dependency, consequent to cancellation of claim 1. Exemplary support can be found in original claim 19, and in the specification additionally at page 6, line 30 – page 7, line 2; and in the *in vivo* studies reported beginning at page 30, line 6.

Claims 36 and claims 54 – 67 are drawn to methods of using the compound of claim 18 for vascular-targeted photodynamic therapy (VTP) of tumors. Claim 36 is independent; each of claims 54 – 67, newly added by amendment herein, depends directly or indirectly from claim 36. Claim 36, as amended herein, now reads:

> 36. A method for vascular-targeted photodynamic therapy (VTP) of a tumor, which comprises:
> (a) administering the compound according to claim 18 to an individual having a tumor; and
> (b) irradiating the local area of the tumor with light.

Claim 36 has been amended (*i*) to depend from claim 18, (*ii*) to ensure proper antecedent basis for recitation of "tumor" in step "(b)", and (*iii*) to clarify that in this method of "*photo*dynamic therapy", the local irradiation is irradiation with *light*. The other amendments, including deletion of the adjectival modifier, "bacteriochlorophyll", are for increased clarity. Exemplary support can be found in original claim 36 and throughout the specification. Each of new claims 54 – 63 depends directly from claim 36, further reciting the type of tumor to be treated. Exemplary support for these claims can found in the specification at page 16, lines 7 – 10, and Examples 14 – 17. Claims 64 and 65 respectively depend directly and indirectly from claim 36, further specifying that the photosensitizing compound is administered systemically (claim 64), and more specifically, intravenously (claim 65). Support for claims 64 and 65 may be found, *e.g.*, at page 17, lines 9 – 12 of the specification. Claim 66 depends directly from claim 36 and recites that "the irradiation wavelength approximates an absorption maximum of the [administered] compound." Support for this limitation can be found throughout the specification, and particularly at page 17, lines 13 – 16. Claim 67, which depends from claim 66, further recites that the wavelength used to irradiate the tumor is about 670 – 780 nm. Specific support may be found, *e.g.*, at page 18, lines 18 – 21 of the specification.

Claim 37 is drawn to a method of using the compound of claim 18 for treating age-related macular degeneration (AMD). As amended, claim 37 recites:

37. A method for photodynamic therapy of age-related macular degeneration by vascular occlusion, which comprises:

(a) administering the compound according to claim 18 to an individual in need thereof; and

(b) irradiating the local area of the macular degeneration with light.

Claim 37 has been amended to depend from claim 18 rather than claim 1 and, in fashion analogous to claim 36, has also been amended for clarity. Support can be found, *inter alia*, in original claim 37.

Claim 68 is new and is drawn to methods of using the compound of claim 18 for treatment of benign prostatic hypertrophy. Claim 68 reads:

68. A method of treating benign prostatic hypertrophy by vascular-targeted photodynamic therapy, comprising:

(a) administering the compound according to claim 18 to an individual having benign prostatic hypertrophy; and

(b) irradiating the local area of the prostate with light.

Exemplary support can be found in the specification at page 16, lines 32 – 33.

Claim 70 is new, and is multiply dependent from method of treatment claims 36, 37, and 68, further specifying that the pharmaceutically acceptable salt of the compound according to claim 18 is the dipotassium salt.

Claims 44 and 49 recite methods of synthesizing compound **4**. Claim 44, as amended herein, recites:

44. A method for preparation of a pharmaceutically acceptable salt of palladium 3^1-oxo-15-methoxycarbonylmethyl-rhodobacteriochlorin 13^1-(2-sulfoethyl) amide, which comprises: (i) reacting Pd-bacteriopheophorbide a with taurine of the formula H_2N-$(CH_2)_2$-SO_3H in a buffer containing a pharmaceutically acceptable cation; and (ii) isolating the compound.

Claim 44 had earlier depended from claim 43, drawn to a "method for the preparation of compounds of formula II"; it has been rewritten in independent form to account for cancellation of claim 43. The claim has been further amended to broaden the scope of permissible buffer cations so that the claimed method results in synthesis of salts of compound **4** commensurate in scope with claim 18. Claim 49, which depends from claim 44, is drawn specifically to preparation of the dipotassium salt, and is commensurate in scope with claim 44 prior to the amendments made herein. Exemplary support for these two claims can be found in original claims 43 and 44, Example 1, and page 11, lines 29 – 31.

As noted above, the various amendments focus prosecution on compound **4**, with claims drawn to the compound *per se*, pharmaceutical compositions comprising the compound, methods for using the

compound, and methods for its synthesis. The amendments have been made solely to expedite prosecution of a species that is currently of particular commercial interest to applicants; the amendments have been made without acquiescence to the rejections or prejudice to applicants' pursuit of claims identical to those canceled or amended, or claims of commensurate scope, in one or more continuation applications.

No new matter has been added.

Supplemental IDS

Applicants file concurrently herewith a Supplemental IDS that cites several categories of documents: (*i*) references identified in applicants' specification that had not formally been made of record (cite nos. A2 and C4 – C9); (*ii*) references cited in an office action in the Japanese counterpart of the instant application (cite nos. B2 – B6, C10 – C12); (*iii*) the three exhibits specifically discussed in this response (cite nos. C1 – C3); (*iv*) Bommer *et al.*, U.S. Pat. No. 5,004,811, the disclosure of which is further discussed in various sections below (cite no. A1); and (*v*) an English language translation of the German language reference DE 4121876 A1 that has been applied in the currently outstanding rejections (cite no. B1).

Objections to the claims

Objection to claims 45-50 for recitation of "corresponding" has been obviated by cancellation of the respective claims.

Rejections under 35 U.S.C. § 112, ¶ 2

Claims 1 – 3, 10 – 19, 36 – 38 and 42 – 50 stand rejected under 35 U.S.C. § 112, ¶ 2 as indefinite, based on recital of "residue of an amino acid, peptide or protein." The rejection has been obviated by amendment.

Rejections Under 35 U.S.C. § 102(b)

All of the examined claims stand rejected as anticipated under 35 U.S.C. § 102(b) by each of four references: (1) Scherz *et al.*, WO 97/19081 ("WO '081")[1]; (2) Scheer *et al.*, WO 01/040232 ("WO '232")[2]; (3) Scherz *et al.*, WO 00/33833 ("WO '833")[3]; and (4) Scheer *et al.*, DE 4121876 ("DE '876").

---

[1] The U.S. national phase counterpart of WO '081 issued as U.S. Pat. No. 6,333,319.

[2] The U.S. national phase counterpart of WO '232 issued as U.S. Pat. No. 7,169,753.

Applicants have now focused the claims on the species of compound **4**. None of the four references discloses this chemical species. In addition, as further elaborated at length below, none of these references discloses a genus that includes compound **4**. Because compound **4** is excluded from the disclosed genera, none of these references can be said to have constructively disclosed the species by disclosure of a genus from which one might "at once envisage" the specific compound within the generic chemical formula, *In re Petering*, 301 F.2d 676, 133 USPQ 275 (CCPA 1962).[4] Because none of the references discloses each and every element of the present claims, none of the references anticipates applicants' now-pending claims, and the rejections under 35 U.S.C. § 102(b) should be withdrawn.

Compound 4

To facilitate the more detailed discussion that follows, the structure of compound **4**, palladium 3^1-oxo-15-methoxycarbonylmethyl-rhodobacteriochlorin 13^1-(2-sulfoethyl) amide, is presented immediately below, shown in its un-ionized state with the tetrapyrrole ring atoms numbered according to standard IUPAC nomenclature, which will be adhered to throughout the following discussion.

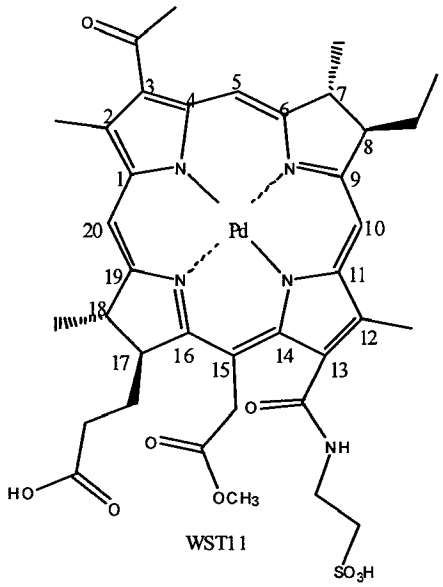

WST11

---

[3] The U.S. national phase counterpart of WO '833 issued as U.S. Pat. No. 6,569,846, and a divisional thereof issued as U.S. Pat. No. 7,045,117.

[4] *See* MPEP §2131.02 (8th ed., rev. 6).

WO '081

WO '081 does not disclose applicants' compound **4**. Neither does WO '081 disclose a genus that includes compound **4**.

WO '081 discloses processes for preparing metal-containing ("metalated") bacteriochlorophyll derivatives by transmetalation. In each case, the metalated bacteriochlorophyll derivatives so prepared are esterified at the 17^3 position:

> [t]he present invention thus relates to a new process for the preparation of synthetic metalated bacteriochlorophyll derivatives of the formula [M]-BChl wherein BChl represents the residue of a demetalated natural or synthetic bacteriochlorophyll derivative carrying at position 17^3 a group $-COOR_1$ **wherein R_1 is a C1-C25 hydrocarbyl residue**....

WO '081, page 5, lines 20 – 26 (emphasis added). Although the method is applied to the preparation of several different metalated BChl genera, **in no case is R_1 permitted to be hydrogen**. As a consequence, none of the genera disclosed in WO '081 includes applicants' compound **4**.

In greater detail, WO '081 discloses that "the process of the invention is applied to the preparation of metalated BChl derivatives of the formula I, II, or III:

I **II** **III**

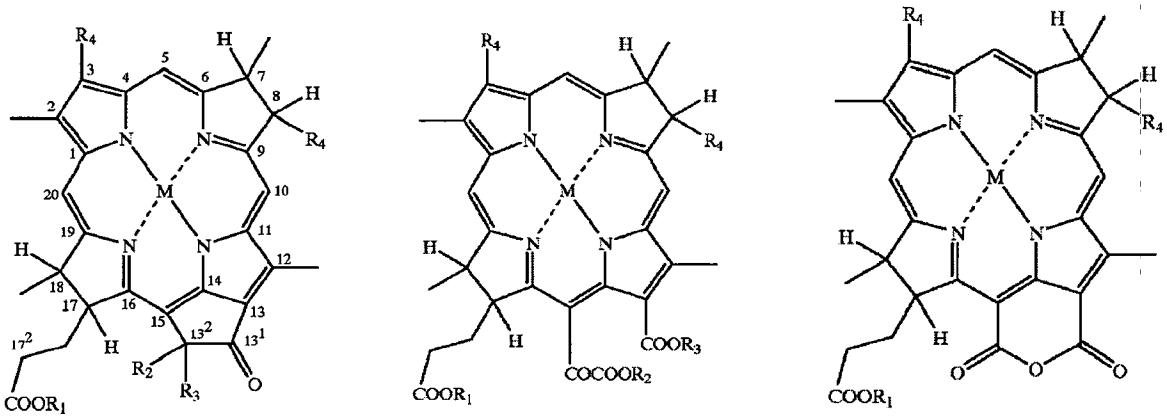

wherein R_1 is a C_1-C_{25} hydrocarbyl residue...." WO '081, page 6, line 10 – page 7, line 11 (emphasis added).

"From the above [M]-BChl derivatives of formulas I, II and III further derivatives can be obtained by transesterification at position 17^3 and thus, in another aspect, the invention relates to a process for the preparation of compounds of the formulas I', II' and III':

I' II' III'

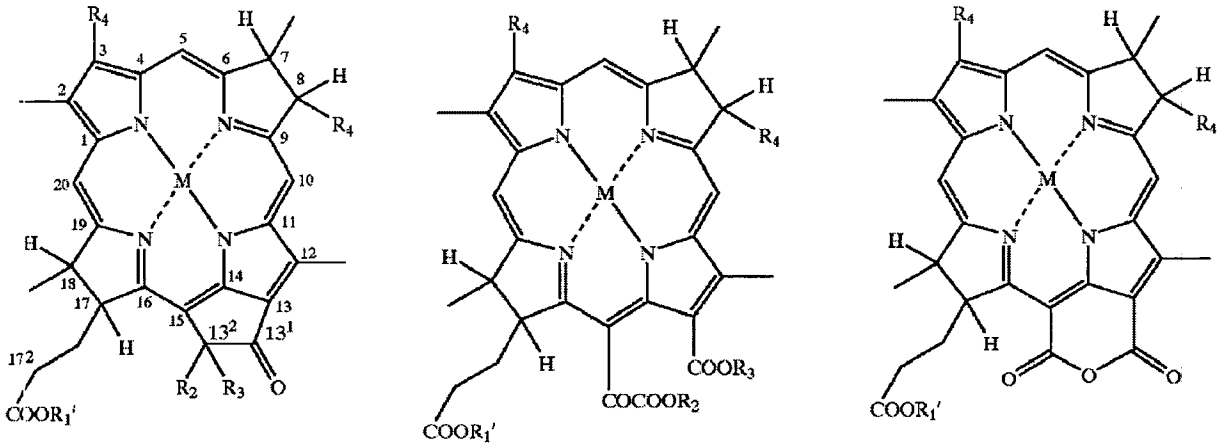

wherein R'$_1$ is selected from the group consisting of: (i) **a C_1-C_{25} hydrocarbyl residue** optionally substituted by halogen, oxo (=O), OH, CHO, COOH,[5] or NH_2, or such a residue interrupted by one or more heteroatoms selected from O, S and NH, or by a phenyl ring...." WO '081, page 7 line 21 – page 8, line 29 (emphasis added). *See also* WO '081, page 11, lines 11 – 22. "Further modifications in the periphery of the tetrapyrrole ring system" are described at WO '081 page 12, lines 10 – 26, but none of these further modifications permit R_1 or R'$_1$ to be hydrogen.

Further structural differences that exclude applicants' compound from the scope of the genera disclosed in WO '081 include the fifth ring in WO '081 formulae I, I', III, and III', and the absence of an amide at 13^1 in the four-ring tetrapyrrole genera of formulae II and II'.

To anticipate a claim, a prior art reference must disclose each and every element of the claimed invention, either expressly or by inherency. *Verdegaal Bros. v. Union Oil co. of California*, 814 F.2d 628, 2 USPQ2d 1051, 1053 (Fed. Cir. 1987).

Claims 18 and 51 – 53 as now pending are drawn to compound **4**, palladium 3^1-oxo-15-methoxycarbonylmethyl-rhodobacteriochlorin 13^1-(2-sulfoethyl) amide, and various pharmaceutically acceptable salts thereof. WO '081 does not disclose the species of compound **4**. Neither does WO '081 disclose a genus that includes compound **4**, and the reference cannot, as a consequence, be said to have disclosed a genus from which one might "at once envisage" the specific compound within the generic chemical formula, *In re Petering*, 301 F.2d 676, 133 USPQ 275 (CCPA 1962). Accordingly, claims 18

---

[5] Although R'$_1$ may permissibly be a single carbon further substituted by COOH, the 17^3 position is nonetheless esterified; R'$_1$ is not hydrogen.

and 51 – 53, as amended herein, are novel over WO '081. Claim 19 is drawn to pharmaceutical compositions comprising the compound of claim 18, and claims 36, 37, and 54 – 68 are drawn to methods of using the compound of claim 18. Because WO '081 does not disclose applicants' compound **4**, it cannot and does not disclose compositions that comprise the compound nor methods for the compound's use, and claims 19, 36-37 and 54– 68 are not anticipated by WO '081.

Finally, claims 44 and 49 recite methods of synthesizing compound **4**, comprising, as a first step, reacting Pd-bacteriopheophorbide a with taurine. No such single-step aminolysis reaction with taurine is disclosed in WO '081, and claims 44 and 49 are novel thereover.

WO '232

WO '232 does not specifically disclose applicants' compound **4**, palladium 3^1-oxo-15-methoxycarbonylmethyl-rhodobacteriochlorin 13^1-(2-sulfoethyl) amide. The reference also does not disclose a genus that includes this compound.

WO '232 discloses "novel chlorophyll and bacteriochlorophyll derivatives of the general formula I:

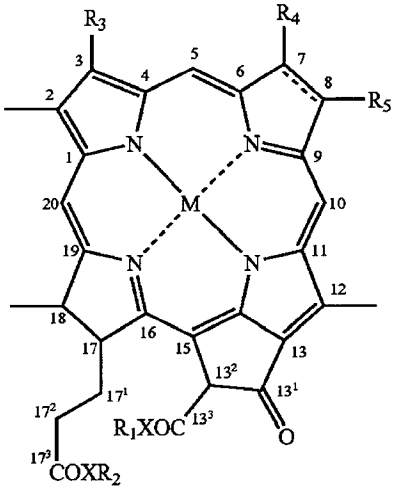

and *pyro*-derivatives thereof wherein the radical $COXR_1$ at position 13^2 is absent...." WO '232, page 5, lines 19 – 29.

All of the bacteriochlorophyll derivatives within the scope of the disclosed genus include a fifth, isocyclic, ring (13-13^1-13^2-15-14), absent from applicants' 4-ring compound **4**. As in the genera disclosed in WO '081, the 17^3 position is always esterified: R_2 is never hydrogen. *See* WO '232, page 6, line 5 – page 7, line 4. In addition, there is no 13^1 amide. The genus disclosed in WO '232 thus excludes applicants' compound **4**.

WO '232 does not disclose applicants' compound **4**, either specifically or by disclosure of a genus from which one might "at once envisage" the specific compound within the generic chemical formula. WO '232 does not disclose compositions comprising compound **4**, methods of using compound **4**, and WO '232 does not disclose the aminolysis reaction of Pd-bacteriopheophorbide a with taurine to synthesize applicants' compound **4**. Accordingly, all of applicants' now-pending claims are novel over WO '232.

WO '833

WO '833 does not specifically disclose applicants' compound **4**. The reference also does not disclose a genus that includes compound **4**.

WO '833 discloses bacteriochlorophyll compounds derivatized at the 17 position with "a substituent capable of allowing an efficient plasma transfer" – that is, efficient blood-borne circulation following systemic administration – "and cell membrane penetration," for use in photodynamic therapy. WO '833, page 4, lines 18 – 22. "The invention thus concerns the compounds of formula I, I' or I'':

I

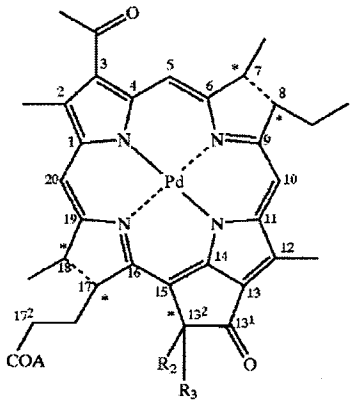

I'

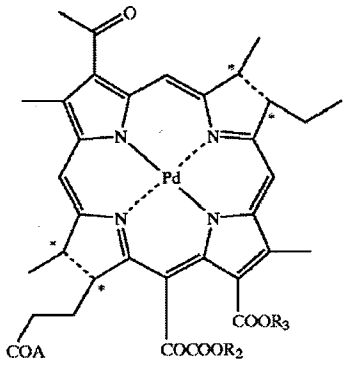

I''

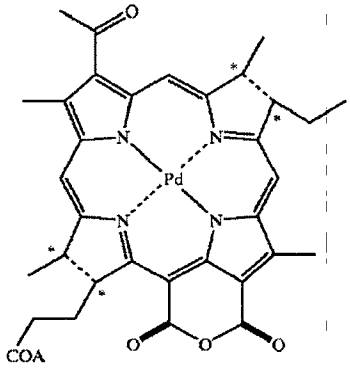

WO '833, page 4, line 25 – page 5.

In contrast to the genera disclosed in WO '081 and WO '232, the 17^3 position of the genera disclosed in WO '833 need not be esterified; as described at p. 6, line 2, "A" can be OH. Indeed, in the preferred embodiment, Pd-Bpheid, substituent "A" *is* hydroxyl:

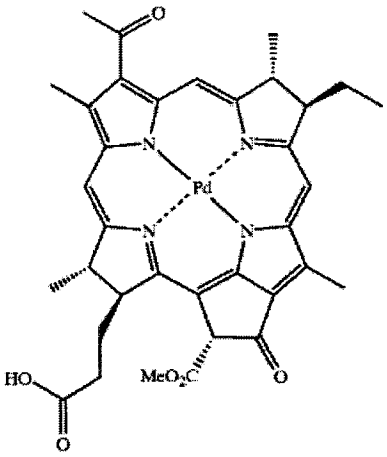

Nonetheless, each of the genera disclosed in WO '833 excludes applicants' compound **4**: formulae I and I'' have five rings, and the four-ring compounds of formula I' lack a 13^1 amide. Applicants' compound **4** is thus excluded from all three genera disclosed in WO '833.

Pending claims 18 and 51 – 53 are drawn to compound **4**, palladium 3^1-oxo-15-methoxycarbonylmethyl-rhodobacteriochlorin 13^1-(2-sulfoethyl) amide, and various pharmaceutically acceptable salts thereof. WO '833 does not disclose compound **4**, either specifically or by disclosure of a genus from which one might "at once envisage" the specific compound within the generic chemical formula. Claims 18 and 51 – 53 are thus novel over the WO '833 disclosure. Claim 19 is drawn to pharmaceutical compositions comprising the compound of claim 18, and claims 36, 37, and 54 – 68 are drawn to methods of using the compound of claim 18. Because WO '833 does not disclose applicants' compound **4**, it cannot and does not disclose compositions that comprise the compound nor methods for its use; claims 19, 36-37 and 54 – 68 are not anticipated by WO '833.

Finally, claims 44 and 49 recite methods of synthesizing compound **4**, comprising, as a first step, reacting Pd-bacteriopheophorbide a with taurine. WO '833 discloses one of the initial reactants, Pd-bacteriopheophorbide a; indeed, Pd-Bpheid a is the preferred embodiment of the WO '833 disclosure. Nonetheless, the reference does not disclose the reaction of Pd-Bpheid a with taurine. Currently pending claims 44 and 49 are thus novel thereover.

DE '876

DE '876[6] does not disclose the chemical species, palladium 3^1-oxo-15-methoxycarbonylmethyl-rhodobacteriochlorin 13^1-(2-sulfoethyl) amide, applicants' compound **4**.

The reference also does not disclose a genus that includes the compound.

German patent publication DE '876 describes bacteriochlorophyll derivatives in which modified esters at positions 13^2 and 17^3 are obtained by transesterification. Three genera of such derivatives are defined by formulae I, II, and III:

I

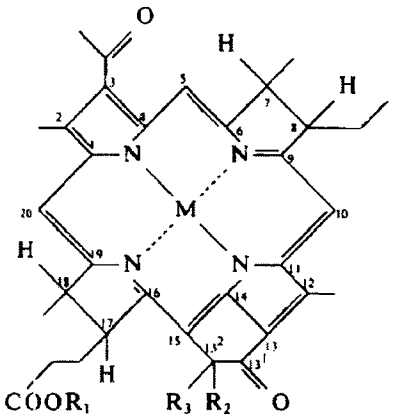

II

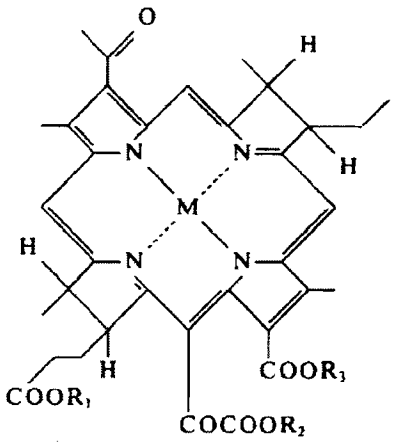

III

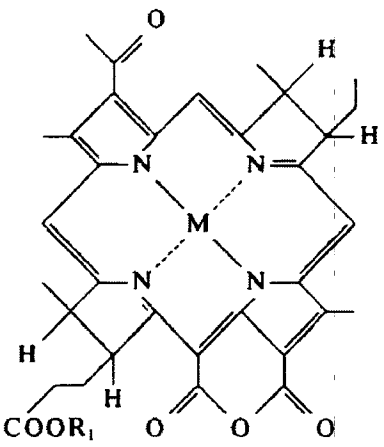

None of these genera includes applicants' compound **4**: the genera defined by formulae I and III include a 5^{th} ring; with respect to the 4-ring compounds of Formula II, the 17^3 position is always esterified; R_1 is never hydrogen[7]. All three genera lack a 13^1 amide.

"The invention also relates to a method for preparing modified bacteriochlorophylls of the general formula Ia, IIa or IIIa

---

[6] All citations to DE '876 herein are made with respect to the English language translation provided with the supplemental IDS filed concurrently herewith.

[7] DE '876 (translation) p. 3.

Ia **IIa** **IIIa**

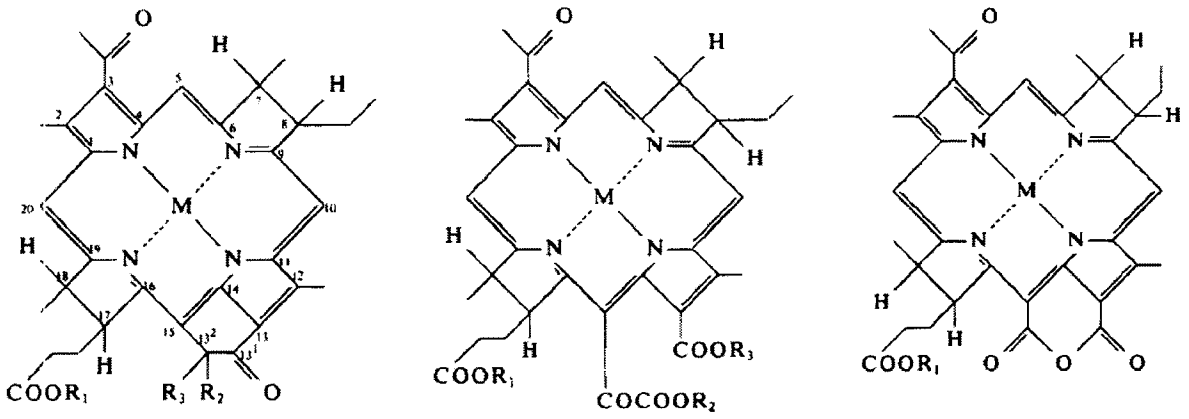

DE '876, pages 4 – 5. Although the definition of R_1 in these formulae, otherwise the same as for compounds I, II, III, "can also denote a methyl, ethyl, ethylene glycol or phytyl group or a residue of a diterpine alcohol," DE '876 p. 5, R_1 is *not* hydrogen.

DE '876 thus does not disclose a genus that includes applicants' compound **4**

Claims 18 and 51 – 53 are now drawn specifically to compound **4**, and various pharmaceutically acceptable salts thereof. Because DE '876 does not disclose compound **4**, either specifically or by disclosure of a genus from which one could at once envisage applicants' compound **4**, claims 18 and 51 – 53 are novel thereover. Claim 19 is drawn to pharmaceutical compositions comprising the compound of claim 18, and claims 36, 37, and 54 – 68 are drawn to methods of using the compound of claim 18. Because DE '876 does not disclose the compound, it cannot and does not disclose compositions that comprise the compound nor methods for its use; claims 19, 36-37 and 54 – 68 are not anticipated by DE '876. Finally, claims 44 and 49 recite methods of synthesizing compound **4**, comprising, as a first step, reacting Pd-bacteriopheophorbide **a** with taurine. DE '876 does not describe such reaction. Claims 44 and 49 are thus novel thereover.

Thus, for the reasons advanced above, *none* of the references applied by the Examiner in rejections under § 102(b) discloses each and every element of applicants' now-pending claims. The claims are novel over each of the references, and the rejections under 35 U.S.C. § 102(b) should be withdrawn.

The Claims Are Also Novel Over The '811 Patent

Applicants' claims are also novel over Bommer *et al.*, U.S. Pat. No. 5,004,811 ("the '811 patent"), newly made of record in the supplemental IDS filed concurrently herewith.

The '811 patent discloses "amino acid derivatives of compounds which contain the chromophore of porphyrins, chlorins or bacteriochlorins.... The amide linkage involves an amino group of the specified amino acid and a carboxy group of the tetrapyrrole." '811, col. 4, lines 18-23.[8]

The permissible chromophores "include the major classes of tetrapyrroles: carboxy-containing porphyrins, chlorins, and bacteriochlorins...." '811, 4:24-28. At least one free carboxylic acid moiety is required, and "[t]he preferred tetrapyrrole carboxylic acids are those wherein at least three carboxylic acid groups are present in the tetrapyrrole." '811, 7:23-25. The amino acids

> employed in the present invention are primary or secondary amino acids. The specific position of the amino group in the carbon atom chain is not critical; the only requirement is that the amino group be available to form the requisite amide linkage with the carboxyl group of the selected porphyrin. When the amino acid is primary, it must contain at least one sulfonic acid group, *i.e.*, SO_3H. It is to be understood that the sulfonic acid group is attached to the main chain through the sulfur atom.... α-sulfo-β-alanine is an example of this class of amino acids.

'811, 4:52-68. These derivatives are said to "possess greater fluorescence in tumors than do the corresponding basic tetrapyrroles," to "more uniformly distribute throughout the tumor than the basic tetrapyrrole permitting the use of considerably lower dosage," and are readily "excreted by the host." '811, 11:39-50.

The '811 patent does not specifically disclose applicants' compound **4**. Amino acid-derivatized tetrapyrrole compounds that were actually synthesized are described in Examples 1 – 7. Additional compounds that are specifically prophesied to be likewise obtainable are listed in Examples 8 – 21. None is applicants' compound **4**, palladium 31-oxo-15-methoxycarbonylmethyl-rhodobacteriochlorin 131-(2-sulfoethyl) amide.

The '811 patent also does not include a genus from which one might "at once envisage" applicants' specific compound within the generic chemical formula.

The structurally-defined genus described in '811 columns 1 – 3 lacks a centrally coordinated metal atom,

---

[8] " '811, 4:18-23."

The present invention is directed to novel fluroescent mono-, di-, tri-, or tetraamide of an amino acid and a carboxy containing tetrapyrrole compound of the formula:

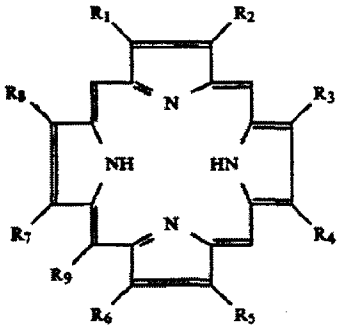

I

or the corresponding di- or tetrahydrotetrapyrroles,

'811, 1:50-62, thus excluding applicants' palladium-containing compound. This is a significant structural difference: the Pd in applicants' compound **4** increases both chemical and photochemical stability and confers different spectral properties upon the compound.

Although there is prophetic disclosure elsewhere in the '811 patent of metalating the amidated tetrapyrrole derivatives,[9] palladium is not specifically disclosed. And even if one were to credit such disclosure as adequate to broaden the '811 genus to include metalated, including palladium-containing, compounds – which applicants do not concede – the genus so described is simply too vast to permit one of ordinary skill in the art "at once [to] envisage" palladium 3^1-oxo-15-methoxycarbonylmethyl-rhodobacteriochlorin 13^1-(2-sulfoethyl) amide within the generic chemical formula. With wide latitude in selection of tetrapyrrole, *see* Table I; nine (9) positions at which the tetrapyrrole macrocycle may be independently substituted, *see* description of $R_1 - R_9$ at '811, 1:68-2:59; few restrictions on the structure of the amino acid moieties, '811, 4:52 – 5:27; and permissible variation in the number of amino acid moieties, '811, 1:44-46, the genus embraces a vast number of potential compounds, far exceeding the ability of any person of ordinary skill at once to envisage applicants' claimed compound. *In re Petering*, 301 F.2d 676, 133 USPQ 275 (CCPA 1962); *In re Meyer*, 599 F.2d 1026, 202 USPQ 175 (CCPA 1979). *See* MPEP §2131.02 (8th ed., rev. 6).

---

[9] "The final amide products can also be converted to metal complexes for example by reaction with metal salts. The magnesium or other non triplet state quenching metal complexes may be useful for the same purpose as the adduct product. Other metal complexes, as well as the magnesium complex, including, for example, iron and zinc, are useful to preclude contamination during processing of the adduct product by metals such as nickel, cobalt and copper, which are difficult to remove. Zinc and magnesium are readily removed from the final adduct product after processing is completed." '811, 9:21-32.

Pending claims 18 and 51 – 53 are drawn to compound **4**, palladium 3^1-oxo-15-methoxycarbonylmethyl-rhodobacteriochlorin 13^1-(2-sulfoethyl) amide, and various pharmaceutically acceptable salts thereof. The '811 patent does not disclose compound **4**, either specifically or by disclosure of a genus from which one might "at once envisage" the specific compound within the generic chemical formula. Claims 18 and 51 – 53 are thus novel over the '811 patent disclosure. Claim 19 is drawn to pharmaceutical compositions comprising the compound of claim 18, and claims 36, 37, and 54 – 68 are drawn to methods of using the compound of claim 18. Because the '811 patent does not disclose applicants' compound **4**, it cannot and does not disclose compositions that comprise the compound nor methods for its use; claims 19, 36-37 and 54 – 68 are not anticipated. Finally, claims 44 and 49 recite methods of synthesizing compound **4**, comprising, as a first step, reacting Pd-bacteriopheophorbide **a** with taurine. The '811 patent does not disclose Pd-bacteriopheophorbide a, nor reaction thereof with taurine. Currently pending claims 44 and 49 are thus novel thereover.

Rejections Under 35 U.S.C. § 103(a)

Claims 1-3 and 10-19 stand rejected under 35 U.S.C. § 103 as having been obvious over DE '876, WO '081, WO '232, and WO '833, each considered individually, with claims 36-38 and 42-50 rejected as having been obvious over WO '081, WO '232, and WO '833, considered separately. Applicants respectfully traverse.

As discussed in detail above, the claims have been focused by amendment herein to a single species of bacteriochlorophyll derivative that falls outside of the genera disclosed in these four references. This amendment thus vitiates the factual foundation underlying each of the stated rejections:

- "Scheer [DE '876] teaches a generic group of bacteriochlorophyll derivatives, which embraces Applicants' claimed compounds," Office Action, p. 5 (emphasis added);
- "Scher[ ]z [WO '081] teaches a generic group of bacteriochlorophyll derivatives, methods of preparing bacteriochlorophyll compounds and method of photodynamic therapy using said bacteriochlorophyll compounds, which embraces Applicants' claimed compounds," Office Action, p 6 (emphasis added);
- "Scheer [WO '232] teaches a generic group of bacteriochlorophyll derivatives, methods of preparing bacteriochlorophyll compounds and methods of photodynamic therapy using said bacteriochlorophyll compounds, which embraces Applicants' claimed compounds," Office Action, p. 7 (emphasis added);
- "Scher[]z [WO '833] teaches a generic group of bacteriochlorophyll derivatives, methods of preparing bacteriochlorophyll compounds and methods of photodynamic therapy using said bacteriochlorophyll compounds, which embraces Applicants' claimed compounds," Office Action, p. 8 (emphasis added).

With the factual foundation no longer sound, the rejections should be withdrawn.

However, in order to expedite allowance of the now-pending claims, applicants discuss below the nonobviousness of the claimed subject matter over the four references cited by the Examiner and the '811 patent cited by applicants. The discussion is exemplary, not exhaustive, of the reasons that applicants' now pending claims are nonobvious over the art of record.

Claims 18, 19 and 51 – 53 (compounds and compositions)

Claims 18 and 51 – 53 are drawn to a novel compound, palladium 3^1-oxo-15-methoxycarbonylmethyl-rhodobacteriochlorin 13^1-(2-sulfoethyl) amide. Each of the cited references discloses bacteriochlorophyll derivatives that share certain structural features with applicants' compound, while differing in others. The structural similarity is insufficient to create a *prima facie* case of obviousness.

"Obviousness based on structural similarity . . . can be proved by identification of some motivation that would have led one of ordinary skill in the art [first] to select and then [secondarily to] modify a known compound (*i.e.* a lead compound) in a particular way to achieve the claimed compound." *Eisai*, 533 F.3d 1353, 1356 (Fed. Cir. 2008). See also *Takeda Chemical Indus., Ltd. v. Alphapharm Pty., Ltd.*, 492 F.3d 1350, 1356 (Fed. Cir. 2007) ("[i]n addition to structural similarity between the compounds, a *prima facie* case of obviousness also requires a showing of 'adequate support in the prior art' for the change in structure" (quoting *In re Grabiak*, 769 F.2d 729, 731-32 (Fed.Cir.1985)); *Eli Lilly & Co. v. Zenith Goldline Pharms., Inc.*, 471 F.3d 1369 (Fed. Cir. 2006) (same; continued viability of this pre-*KSR* holding confirmed in *Eisai*, 533 F.3d at 1357). Any such "support" for selecting and modifying compounds must be found in the prior art; the relevant motivations are thus prior art motivations, *In re Dillon*, 919 F2d 688 (Fed. Cir. 1990) (*en banc*), uninfected by hindsight.

The effort to discern such contemporaneous motivation is much simplified here. Because all four of the references cited by the Examiner resulted from a continuing collaborative effort by the Scherz and Scheer labs to design improved bacteriochlorophyll derivatives for photodynamic therapy,[10] each

---

[10] The four references currently cited by the Examiner report work from the Scheer and the Scherz laboratories, with Drs. Scheer and Scherz listed as coinventors on three of the four references (as on the instant application). In each case, the compounds were intended for use in photodynamic therapy and related photosensitization methods. *See*, WO '081, p. 1, lines 10 – 11 ("The present invention relates to a new method of preparation of metalated bacteriochlorophyll derivatives for use in methods of *in vivo* photodynamic therapy"); WO '232, Abstract ("The compounds are for use in photodynamic therapy (PDT), for diagnosis of tumors, and for killing cells and infectious agents such as bacteria and virus, both in biological products and in living tissues"); DE '876, p. 2 ("The invention relates to modified bacteriochlorophylls, a method for their preparation and their use for preparing agents for the diagnosis or

successive reference can reasonably be understood to evidence the structural changes to the immediately preceding compounds that were then-thought to be most desirable to improve the compounds' properties for use in PDT. Since the progression of structural changes eventuates in the five-ring structures of WO '232, significantly divergent in structure from applicants' 4-ring compound **4**, it cannot be said that the references, either alone or in combination, motivate the structural modifications that would have been required to produce applicants' now-claimed compound. Applicants' compound **4** would not have been *prima facie* obvious, and applicants' now-pending composition of matter claims would not have been *prima facie* obvious over the references cited by the Examiner, alone or in combination.

Applicants offer some further comments, however, on the penultimate reference, WO '833, which describes the immediate synthetic precursor to applicants' compound **4**.

WO '833 discloses bacteriochlorophyll compounds derivatized at the 17 position with "a substituent capable of allowing an efficient plasma transfer" – that is, efficient blood-borne circulation following systemic administration – "and cell membrane penetration," for use in photodynamic therapy. WO '833, page 4, lines 18 – 22. The preferred substituent is hydroxyl, and the "most preferred embodiment" is Pd-Bpheid:

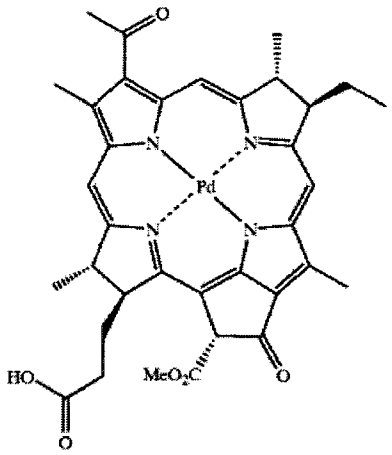

WO '833, p. 10, lines 5 – 20.

---

treatment of tumors"); WO '833, p. 1., lines 5-10 ("The present invention concerns palladium-substituted bacteriochlorophyll derivatives ... [for] use in the field of *in vivo* photodynamic therapy and diagnosis and *in vitro* photodynamic killing of viruses and microorganisms").

The references cited in the prior office action, U.S. Pat. Nos. 6,147,195 and 5,955,585, are likewise references from the Scherz laboratory.

Because the WO '833 reference itself identifies Pd-Bpheid as "most preferred", this compound is reasonably viewed as the lead compound to be selected for any further structural modification. Two structural modifications to this "most preferred" lead compound are required to arrive at applicants' compound **4**: the fifth, isocyclic, ring must be opened, and the resulting 13^1 carboxylic acid derivatized to a 2-sulfoethyl amide.

The WO '833 reference itself certainly provides no motivation to make these two changes, since Pd-Bpheid is already, and expressly, the most preferred embodiment. The required changes also would not have been motivated by the teachings of the later WO '232 reference, which is drawn exclusively to five-ring compounds.

However, the '811 patent by Bommer and colleagues discloses 4-ring compounds in which one or more carboxylic acid moieties on the tetrapyrrole is amidated with an amino acid substituent. Furthermore, "[w]hen the amino acid is primary, it must contain at least one sulfonic acid group, i.e., SO_3H." '811, 4:58-59. Nonetheless, and notwithstanding the disclosure of sulfonated amino acid derivatives of tetrapyrroles for use in PDT, the '811 patent would not have provided the requisite motivation to make the specific structural alterations to the WO '833 lead compound required to produce applicants' compound **4**, palladium 3^1-oxo-15-methoxycarbonylmethyl-rhodobacteriochlorin 13^1-(2-sulfoethyl) amide.

First, WO '833 clearly and explicitly teaches greatest preference for the five-ring compound, Pd-Bpheid. Nothing in the earlier '811 patent clearly dissuades such preference. To the extent that the '811 patent might reasonably be said to argue for further derivatization with sulfonated amino acids, the 5-ring "most preferred" Pd-Bpheid compound has two available carboxylic acid moieties, at positions 17 and 3; ring-opening is not required.[11]

Second, photodynamic therapy (PDT) was understood to require that the photosensitizing agent exert a direct photocytotoxic effect, and thus to require some degree of cellular uptake. Compounds were thus required to have sufficient water-solubility to permit systemic administration yet retain sufficient hydrophobicity to be able to enter cells. WO '833 explicitly extols the balance between those competing ends that was achieved by the compounds described therein, by virtue of derivatization at the 17 position with "a substituent capable of allowing an efficient plasma transfer" – that is, efficient blood-borne circulation following systemic administration – "***and*** cell membrane penetration." WO '833, page 4, lines 18 – 22 (emphasis added). Yet each of the structural modifications required to obtain compound **4**

---

[11] Indeed, the applicants themselves were intent on derivatizing the C-17 propionic acid moiety of Pd-Bpheid; the opening of the isocyclic ring and derivatization at C-13 were unintended, and serendipitous.

from the lead compound of WO '833 – isocyclic ring-opening, and the addition of anionic sulfonates – would have been expected to increase the hydrophilicity of Pd-Bpheid, the most preferred WO '883 compound; combining the two modifications would have been understood to pose a significant risk destroying the clinical efficacy of the compounds by reducing or eliminating their ability to enter cells.

Third, without the hindsight driven by knowledge of applicants' compound **4**, the '811 patent disclosure presents far less persuasive an argument for making *any* structural changes to the WO '883 "most preferred" compound than might at first appear.

One of ordinary skill reading the '811 patent would have noted, for example, that the inventors only ever synthesized chlorin derivatives, which differ from bacteriochlorins in the degree of ring saturation. Although Example 17 states prophetically that "by substituting bacteriochlorin e6 for chlorin e6 in Examples 1-8, the following compounds can also be prepared," including "[m]ono α-sulfo-β-alanyl bacteriochlorin e6," the person of ordinary skill would have viewed such prophecy with substantial skepticism. The referenced Examples, Examples 1 – 8, describe a reaction with a water soluble activator. Bacteriochlorins are water-insoluble; use of a water soluble activator would have been expected to lead to phase separation. If the prophesied reaction were even possible, yields would have been expected to be vanishingly low. Furthermore, it would have been deemed likely that any bacteriochlorin derivative produced in the reaction would oxidize, (re)creating the chlorin analogue. Furthermore, the reaction is not regioselective: as the '811 patent itself teaches, "mixtures of products can be formed including isomeric di- and even tri- or higher amide products, depending on the number of carboxyl groups and depending on the selected stoichiometry." '811, 9:59-63. And position matters. Applicants have found, for example, that taurine addition at C3 leads to Schiff base formation, change in spectral properties, loss of stability, and insufficient water solubility, while taurine addition at C17, the other available carboxylic acid moiety, creates a compound that is not water soluble. Nothing in the '811 patent points with particularity to the importance of the C13 position.[12]

In addition to structural similarity between the compounds, a *prima facie* case of obviousness requires a showing of adequate support in the prior art for the change in structure. The '811 patent simply provides no such support. Accordingly, applicants' compound **4** would not have been *prima facie* obvious over WO '833, taken in view of the '811 patent, and applicants' claims drawn to compound **4**, and compositions comprising compound 4, would not have been *prima facie* obvious thereover.

The same conclusion obtains if the '811 patent is considered the primary reference.

---

[12] Indeed, the applicants themselves were intent on derivatizing the C-17 propionic acid moiety of Pd-BPheid; the opening of the isocyclic ring and derivatization at C-13 were unintended, and serendipitous.

Without hindsight, there is little guidance for selecting one lead compound from amongst the enormous number of species within the scope of the '811 genus. To the extent that the patent itself expresses preferences, those preferences are clearly for a non-metalated chlorin derivative. Even if the '811 claims were properly viewed as defining preferred subgenera and preferred species, there are a number of such preferred compounds, of varying structure: trans-4-hydroxy-L-proline chlorin e_6; mono-N-methyl-DL-Aspartyl chlorin e_6; iminodiacetic acid chlorin e_6; iminodipropionic acid chlorin e_6; mono-N-methyl-L-serinyl chlorin e_6; α-sulfo-β-alanyl chlorin e_6; and mono-N-methyl-L-glutamyl chlorin e_6. All are non-metalated chlorin derivatives. The tetrapyrrole position that is amidated is not identified. Even if one of these were properly chosen as the lead compound, none of the references cited by the Examiner, and certainly not WO '833, motivates all of the required structural changes, including metalation with Pd, oxidation to the bacteriochlorin analogue, selection of the 13^1 position alone for amidation, and choice of taurine as the amino acid, yielding the 13^1 2-sulfoethyl amide.

Accordingly, applicants' compound **4** would not have been *prima facie* obvious over the '811 patent, taken in view of WO '833, and applicants' claims drawn to compound **4**, and compositions comprising compound 4, would not have been *prima facie* obvious over the combination of these two references.

Even if one assumes, *arguendo*, that a *prima facie* case of obviousness could viably be crafted from any of the references discussed above, in any combination, applicants' compound **4** exhibits unexpected, and unexpectedly superior, properties that are fully sufficient to rebut any such *prima facie* case.

As noted in applicants' specification, "[b]ecause of its low solubility in aqueous solutions, the clinical use of Pd-Bpheid requires the use of solubilizing agents such as Cremophor that may cause side effects at high doses." Spec., p. 4, lines 21 – 23. The pentacyclic compounds of WO '081, WO '232, and DE '876 were also found to be poorly soluble in water, and to necessitate use of detergents such as Cremophor. By contrast, applicants' compound **4** is remarkably water-soluble, which permits its formulation to high concentration simply by dissolution in distilled water or other standard IV diluents, without the need for further solubilizing agents. And once dissolved, the compound does not self-aggregate, either in the IV infusion set or in the blood. From a clinical perspective – and these compounds are intended for clinical use – the exceptional formulation characteristics of compound **4** alone confer significant superiority, significantly facilitating use and reducing side-effects.

As discussed at length in the section below, the highly water-soluble compound **4** also, unexpectedly, binds with significant affinity and specificity to serum albumin. Binding to serum albumin

was not foreseen: compound **4** fortuitously possesses an appropriate balance between electronegativity and hydrophobicity to drive noncovalent association with this serum protein. Remarkably, although the binding to serum albumin has been found to eliminate cellular uptake, long understood to be required for photodynamic therapy, compound **4** is profoundly potent in vascular-targeted PDT. This paradox implies that compound **4** has a unique mechanism of action, a mechanism that has now been found to overcome known shortcomings of existing PDT methods, including tumor recurrence from cells surviving in the tumor rim and neoangiogenic responses that are particularly disadvantageous in the treatment of macular degeneration.

Other properties – including retention of desirable spectral properties; ready distribution throughout the vasculature, bringing the photosensitizing agent into photoactive proximity to all possible tumor sites; and rapid elimination, reducing the possibility of lingering photosensitivity – contribute to making applicants' claimed compound far superior to all prior photosensitizing agents. Applicants' compound **4** newly makes practicable therapeutic approaches that had previously been only an unfulfilled promise.

Claim 36, 37, 54 – 68, 70 (methods of use)

As elaborated in detail above, applicants' compound **4**, palladium 3^1-oxo-15-methoxycarbonylmethyl-rhodobacteriochlorin 13^1-(2-sulfoethyl) amide, is novel and would have been nonobvious over the references applied by the Examiner and the '811 patent, made of record by applicants in the accompanying supplemental IDS. Because they require the use of this novel and nonobvious photosensitizer, applicants' claimed methods of effecting vascular-targeted photodynamic therapy, as presently recited in claims 36 and claims 54 – 67 (vascular-targeted photodynamic therapy of tumors), claim 37 (photodynamic therapy of age-related macular degeneration by vascular occlusion), claim 68 (vascular-targeted photodynamic therapy of benign prostatic hypertrophy), and claim 70 (which depends multiply from claims 36, 37 and 68), could not have been obvious. See *In re Ochiai*, 71 F.3d 1565 (Fed. Cir. 1995).

In addition, the *in vitro* properties of compound **4** provided no reasonable expectation that the compound would have significant *in vivo* therapeutic effect; to the contrary, the *in vitro* properties would have dissuaded persons of ordinary skill in the art from considering the compound as suitable for *in vivo* therapies. This too defeats any *prima facie* case of obviousness. *In re Dow Chemical Co.*, 837 F.2d 469, 473 (Fed. Cir. 1988) ("The consistent criterion for determination of obviousness is whether the prior art

would have suggested to one of ordinary skill in the art that this process should be carried out and would have a reasonable likelihood of success.").

Prior to the instant invention, photodynamic therapy (PDT) was understood to require that the photosensitizing agent exert a direct photocytotoxic effect – for classical PDT, on tumor cells; for vascular-targeted PDT, on vascular endothelial cells. Although other mechanisms were understood to contribute to the therapeutic effect, particularly in vascular-targeted PDT, it was nonetheless well accepted that at least some degree of cellular uptake and resulting intracellular oxidative damage were required. Accordingly, newly synthesized photosensitizing agents were usually assessed first for cytotoxic activity *in vitro*.

In WO '081, for example, Example 9 reports the "Phototoxicity *in vitro* of [Pd]-BChl-Ser", with Example 9b assessing the *in vitro* killing of melanoma cells:

> Monolayers of M2R cells were incubated with the indicated concentrations of [Pd]-BChl-Ser for 1h and subjected to photodynamic treatment as described above. Photocytotoxicity was assessed by [^{3}H] thymidine incorporation and percent survival of the treated cells and appropriate controls are described in Fig. 2. Survival of untreated cells was taken as 100%.
>
> It can be seen in Fig. 2 that the phototoxic effect was dose dependent with respect to [Pd]-BChl-Ser concentration with an approximate LD_{50} of 0.05 μM. The phototoxic effect was not seen in the dark controls.

WO '081, page 24, lines 10 – 19.

In WO '232, the *in vitro* phototoxicity of the M-Bchl derivatives on monolayers of M2R cells is reported in Example 13. The "results ... shown in Figs. 1 and 2" demonstrate that:

> [t]hree of the sensitizers shown in Figs. 1 and 2 were phototoxic to mouse M2R melanoma cells (Pd-Bpheid-et (LD_{90} = 0.02 μM) and tbb-Pd-Bpheid-me (LD_{90} = 1.1 μM), Pd-Bpheid-ser ((LD_{90} = 0. 1 μM). tbb-Pd-Bpheid-tbb and Pd-BPheid-*N*glc are ineffective under these conditions because they formed aggregates in the liposomes which are ineffective for PDT.

WO '232, page 26, lines 19 – 23.

Analogously, the *in vitro* cytotoxic activity of the vascular-targeted PDT agents described in WO '833 is reported in its Examples 8, 9, 10, and 11, and the *in vitro* cytotoxic activity of the agents disclosed in U.S. Pat. Nos. 5,955,585 and 6,147,195[13] is described in their respective Examples 12.

In keeping with this prior understanding, applicants tested compound **4** for direct *in vitro* phototoxicity.

As reported in applicants' specification in Example 14, compound **4** has detectable *in vitro* activity: "[a]s can be seen [in FIGS. 1A -1B], the phototoxicity of both pigments 4 and 8 is concentration- and light-dependent, without any dark toxicity in the stated range." Specification page 31, lines 19 – 22. However, the result is ***profoundly*** different under *in vitro* conditions that more closely approximate those expected *in vivo*: the phototoxicity of compound **4** is strongly dependent on the concentration of serum albumin in the medium.

Although compound **4** shows photocytotoxic activity under standard cell culture conditions, the cytotoxic activity is dramatically reduced – *i.e.*, percent cell survival dramatically increases – when serum albumin concentrations are raised to levels that approach those in blood:

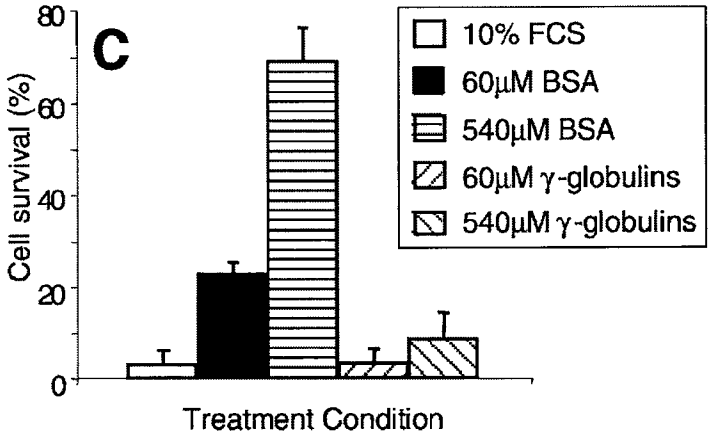

Mazor *et al.*[14], FIG. 4C. The reduction in phototoxicity is due to adsorption of the photosensitizer to serum albumin, markedly reducing cellular uptake, Mazor, p. 346, col. 1; with the photosensitizer

---

[13] Of record.

[14] Mazor *et al.*, "WST-11, A Novel Water-soluble Bacteriochlorophyll Derivative; Cellular Uptake, Pharmacokinetics, Biodistribution and Vascular-targeted Photodynamic Activity Using melanoma Tumors as a Model," *Photochemistry & Photobiology* 81:342-351 (2005) (attached hereto as Exhibit A). In this reference from the instant inventors' laboratory, compound **4** is referred to as "WST-11" (*see, e.g.*, the structure in reference FIG. 1A) (hereinafter, "Mazor").

excluded from the cells' interior, reactive oxygen species generated upon illumination cannot damage vital intracellular components.

This reduction in photocytotoxic activity at physiologic concentrations of serum albumin is *not* seen with Pd-Bpheid, the synthetic precursor to applicants' presently claimed compound **4**. Compare compound 3 (Pd-Bpheid), which remains highly cytotoxic even at 75% fetal calf serum, with compound 10 (applicants' compound **4**) in the figure below:

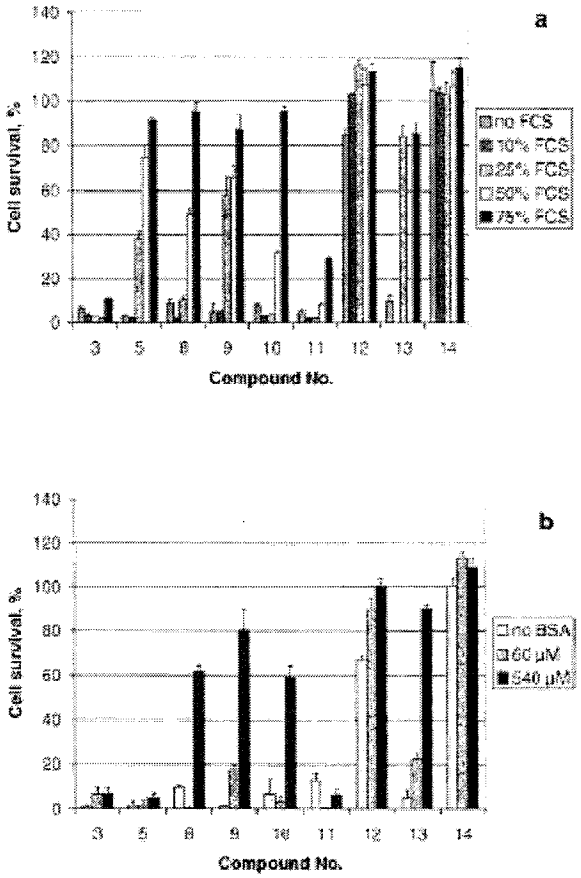

Figure 7. Phototoxicity dependence on the concentration of serum (a) and BSA (b). H5V cells were preincubated with 50 µM concentrations of the indicated pigments in cell culture medium for 3 min, illuminated for 10 min, then washed with fresh medium. The points are the mean ± SEM of triplicate determinations.

Brandis *et al.*,[15] Fig. 7.

---

[15] Brandis *et al.*, "Novel Water-soluble Bacteriochlorophyll Derivatives for Vascular-targeted Photodynamic Therapy: Synthesis, solubility, Phototoxicity and the Effect of Serum Proteins," *Photochemistry & Photobiology* 81:983-993 (2005) (attached hereto as Exhibit B) (hereinafter, "Brandis").

Given the prior understanding of the mechanism of PDT, including vascular-targeted PDT, these *in vitro* results would have dissuaded *in vivo* use, "because a direct insult of endothelial cells is considered important for successfully launching a tumor cure via VTP [vascular-targeted photodynamic therapy]." Brandis, p. 991, col. 2. The lack of any reasonable expectation of successful *in vivo* use precludes a *prima facie* case of obviousness of applicants' therapeutic method claims.

And yet, notwithstanding the lack of *in vitro* phototoxicity under physiologic conditions, "[r]emarkably, Mazor ... showed that the ... water-soluble Bchl-based sensitizer (WST11)[16], which was found to be practically nonphototoxic against individual cells in cultures in physiological serum albumin concentrations, is highly active as a VTP reagent" *in vivo*. Brandis, p. 984, col. 1.

> Mice bearing M2R melanoma xenografts were injected i.v. with WST11 (6 of 9 mg/kg body) and immediately illuminated at increasing light doses (30-45 J/cm^2).
>
> After VTP, all treated tumors developed necrosis within 24-48 h. Tumor flattening was observed for the next 14 days.... Increasing the WST11 dose to 9 mg/kg at a light dose of 30J/cm^2 improved the treatment outcome to 70% cure... at 90 days after treatment....These results are similar and even better than those obtained with Tookad®[17] on the same tumor model.

Mazor, p. 350, col. 1.

This paradoxical ability to kill tumors *in vivo* was a surprise, a compelling indicium of nonobviousness. It was particularly a surprise given that serum albumin is known to quench reactive oxygen species, which would have been thought disadvantageous in methods of photodynamic therapy. The binding of compound **4** to serum albumin would have been expected not only to reduce cellular uptake, and thus reduce cytotoxicity, but would also have been expected to lead to significant quenching of any reactive oxygen species generated extracellularly in the blood. Surprisingly, however, and paradoxically, it has now been found that the

> noncovalent complex with human serum albumin (HSA) ... functions as a photocatalytic oxidorreductase at biologically relevant concentrations enabling approximately 15 cycles of electron transfer from the associated HSA protein to molecular oxygen in the solution.

---

[16] Compound **4** herein.

[17] Pd-BPheid.

Ashur *et al.*,[18] Abstract.

The *in vivo* activity of compound **4** was so unexpected, and so inexplicable based on prior understanding of PDT mechanisms, as to demand an entirely new mechanistic theory.

> We therefore propose that the two studies collectively suggest that the antitumor activity of WST11 and probably of other similar candidates does not depend on direct photointoxication of individual endothelial cells but on the vascular tissue response to the VTP insult.

Brandis, Abstract.

Studies of this novel mechanism continue. It is currently thought that compound **4**, which is retained in the vascular lumen through noncovalent association with albumin, generates short-lived oxygen radicals (OH, $O2^-$) upon illumination. These radicals rapidly consume molecular oxygen in the vicinity, leading to endothelial cell release of NO, mostly from nitroso-thiols in circulating red blood cells, and a subsequent chain of physiologic and biochemical events that leads quickly to local vascular occlusion. Occlusion of the vessels feeding the tumor in turn leads to tumor necrosis.

This novel mechanism provides significant therapeutic advantages over prior PDT approaches using earlier photosensitizing agents. These advantages, like the mechanism itself, were wholly unforeseen. One such advantage is

> that, unlike Tookad®,[19] VTP with [compound] 10[20] has practically no effect on the vessels' permeability. Thus, the occlusion of tumor vessels, which was observed within minutes of illumination, was not accompanied by hemorrhagic necrosis, underscoring the advantage of such sensitizers for VTP applications where hemorrhagic necrosis may endanger the treated patient, such as in tumors situated near major vessels or in internal sensitive organs or in age-related macular degeneration, in which lateral photodamage may be considerable.

Brandis., p. 991, col. 2.

In addition, the situs of vascular damage differs, reducing the risk of tumor recurrence from cells that survive in the tumor rim. In classical antivascular therapies including vascular-targeted PDT that

---

[18] Ashur *et al.*, "Photocatalytic Generation of Oxygen Radicals by the Water-Soluble Bacteriochlorophyll Derivative WST-11, Noncovalently Bound to Serum Albumin," *J. Phys. Chem. A* 113:8027-8037 (2009) (attached hereto as Exhibit C) (hereinafter, "Ashur").

[19] Pd-BPheid, the preferred embodiment disclosed in WO '833 and a synthetic precursor to applicants' compound **4**, palladium 3^1-oxo-15-methoxycarbonylmethyl-rhodobacteriochlorin 13^1-(2-sulfoethyl) amide.

[20] Compound **4** herein.

aims at endothelial cells, the microcirculation is destroyed first, often sparing neoplastic cells at the tumor periphery. With vascular-targeted PDT using compound **4**, by contrast, damage starts in the feeding artery and veins, killing all tumor cells in the downstream watershed, including cells at the tumor rim. Another advantage is that efficacy does not require intracellular oxidation, and thus continued oxygen delivery to the tumor during photoactivation. Earlier agents had required through intermittent or pulsed illumination to allow activation of the PDT compound without occluding blood vessels that feed the tumor.

None of these advantages were expected; none could have been predicted. Applicants' claimed methods would have been nonobvious.

Claims 44 and 49 (methods of synthesis)

Claims 44 and 49 are drawn to a method of preparing compound **4** in a single step aminolysis reaction in which the isocyclic ring of Pd-Bpheid is cleaved and the 13^1 position concurrently derivatized with a 2-sulfoethyl amide substituent. Although the two reactants were known, nowhere is there a suggestion to undertake such reaction in pursuit of the novel and nonobvious compound **4**.

Claims 44 and 49 are nonobvious, and the rejections should be withdrawn.

CONCLUSION

Interview request

Claims 18 – 19, 36 – 37, 44, and 51 – 70 are believed to satisfy all of the criteria for patentability and are in condition for allowance. An early indication of the same is therefore kindly requested. However, the Examiner believes that any matters remain outstanding that preclude passing this application immediately to issuance, the Examiner is requested to contact the undersigned attorney to schedule a personal interview.

Fee authorization

No fees beyond those due (*i*) under 37 C.F.R. § 1.17(e) for continued examination and (*ii*) as specified on the accompanying transmittal for additional independent claims are believed to be due in connection with this Amendment. However, the Director is authorized to charge any additional fees that may required, or credit any overpayment, to Dechert LLP Deposit Account No. 50-2778 **(Order No. 378036-006 (107847))**.

Respectfully submitted,

Date: 23 JULY 2010

Daniel M. Becker
Reg. No. 38,376

Exhibit A: Mazor *et al.*, "WST-11, A Novel Water-soluble Bacteriochlorophyll Derivative; Cellular Uptake, Pharmacokinetics, Biodistribution and Vascular-targeted Photodynamic Activity Using melanoma Tumors as a Model," *Photochemistry & Photobiology* 81:342-351 (2005)

Exhibit B: Brandis *et al.*, "Novel Water-soluble Bacteriochlorophyll Derivatives for Vascular-targeted Photodynamic Therapy: Synthesis, solubility, Phototoxicity and the Effect of Serum Proteins," *Photochemistry & Photobiology* 81:983-993 (2005)

Exhibit C: Ashur *et al.*, "Photocatalytic Generation of Oxygen Radicals by the Water-Soluble Bacteriochlorophyll Derivative WST-11, Noncovalently Bound to Serum Albumin," *J. Phys. Chem. A* 113:8027-8037 (2009)

Exhibit A

Photochemistry and Photobiology, 2005, 81: 342–351

WST11, A Novel Water-soluble Bacteriochlorophyll Derivative; Cellular Uptake, Pharmacokinetics, Biodistribution and Vascular-targeted Photodynamic Activity Using Melanoma Tumors as a Model¶

Ohad Mazor[1,2], Alexander Brandis[2], Vicki Plaks[1], Eran Neumark[1], Varda Rosenbach-Belkin[2], Yoram Salomon[1] and Avigdor Scherz*[2]

[1]Department of Biological Regulation, The Weizmann Institute of Science, Rehovot, Israel
[2]Department of Plant Sciences, The Weizmann Institute of Science, Rehovot, Israel

Received 14 June 2004; accepted 17 December 2004

ABSTRACT

WST11 is a novel negatively charged water-soluble palladium-bacteriochlorophyll derivative that was developed for vascular-targeted photodynamic therapy (VTP) in our laboratory. The *in vitro* results suggest that WST11 cellular uptake, clearance and phototoxicity are mediated by serum albumin trafficking. *In vivo*, WST11 was found to clear rapidly from the circulation ($t_{1/2}$ = 1.65 min) after intravenous bolus injection in the mouse, whereas a longer clearance time ($t_{1/2}$ = 7.5 min) was noted in rats after 20 min of infusion. The biodistribution of WST11 in mouse tissues indicates hepatic clearance ($t_{1/2}$ = 20 min), with minor (kidney, lung and spleen) or no intermediary accumulation in other tissues. As soon as 1 h after injection, WST11 had nearly cleared from the body of the mouse, except for a temporal accumulation in the lungs from which it cleared within 40 min. On the basis of these results, we set the VTP protocol for a short illumination period (5 min), delivered immediately after WST11 injection. On subjecting M2R melanoma xenografts to WST11-VTP, we achieved 100% tumor flattening at all doses and a 70% cure with 9 mg/kg and a light exposure dose of 100 mW/cm^2. These results provide direct evidence that WST11 is an effective agent for VTP and provide guidelines for further development of new candidates.

INTRODUCTION

Photodynamic therapy (PDT) is a relatively new modality for treatment of solid tumors, which is based on administering a photosensitive agent followed by its *in situ* excitation at a matching wavelength. Through photogeneration of reactive oxygen species (ROS) at cytotoxic levels, PDT induces a series of destructive processes leading to irreversible cell or tissue damage followed by regression of early and advanced stage tumors (1–4).

The spectra, photophysics and photochemistry of native bacteriochlorophylls (Bchl) make them very efficient sensitizers, possessing optimal light-harvesting properties and with clear advantages as sensitizers in PDT (5). In particular, these molecules have a very high extinction coefficient at long wavelengths (λ_{max} = 760–780 nm, ε = (4–10) × 10^4 M^{-1} cm^{-1}) where light penetrates deeply into tissues, and they generate ROS at a high quantum yield (depending on the central metal and, to some extent, on peripheral substituting groups) (6,7).

Several second-generation sensitizers were derived from Bchl *a* in our laboratories at the Weizmann Institute (8–10) and further developed as PDT agents for clinical applications in collaboration with Steba-Biotech (Paris, France) and Negma-Lerads (Toussus-Le-Noble, France). Substitution of the central magnesium atom of Bchl for palladium and hydrolysis of the esterifying alcohol provided a highly stable and efficient sensitizer, palladium-bacteriopheophorbide (Pd-Bpheid, also known as Tookad® or WST09 (8, A. Scherz and coworkers, personal communication). This novel sensitizer was shown to be effective in the PDT of several solid tumors such as melanoma (11), rat glioma (12), human prostate xenografts (13,14), human HT29 colon carcinoma xenografts (15), normal canine prostate (16) and DS Sarcoma (17,18) in laboratory animal models. After bolus intravenous (i.v.) administration, 95% of the Tookad® clears from the circulation with a very short half lifetime ($t_{1/2}$ = 0.6 min, after bolus injection) (19) and the rest with $t_{1/2}$ ~11 min (A. Brandis, O. Mazor, S. Gross, N. Koudinova, E. Gladysh, R. Hami, N. Kammhuber, V. Rosenbach-Belkin, M. Greenwald, A. Bondon, G. Simonneaux, H. Scheer, Y. Salomon and A. Scherz, personal communication,19) with little or no extravasation into the surrounding tissues. After Tookad® perfusion, the majority of the drug clears from the circulation $t_{1/2}$ ~8 min. These properties are appropriate for vascular-targeted photodynamic therapy (VTP). In these studies, illumination is applied when the concentration of the drug in the circulation is sufficiently high. Under these conditions, ROS are photogenerated at high concentrations only within the blood vessels of the illuminated tissue. Oxygen depletion and ROS generation initiate blood stasis as well as rapid destruction of the blood vessels of the tumor, leading to hypoxia and secondary radical formation that culminates in necrosis and eradication of the

¶Posted on the website on 28 December 2004
*To whom correspondence should be addressed: Department of Plant Sciences, Weizmann Institute of Science, Herzel Street, Rehovot 76100, Israel. Fax: 972-8-9344181; e-mail: avigdor.scherz@weizmann.ac.il
Abbreviations: AVT, antivascular chemotherapy; Bchl, bacteriochlorophyll; BSA, bovine serum albumin; DDW, double-distilled water; FCS, fetal calf serum; ICP-MS, inductively coupled plasma mass spectroscopy; i.p., intraperitoneal; i.v., intravenous; PBS, phosphate-buffered saline; Pd-Bpheid, palladium-bacteriopheophorbide; PDT, photodynamic therapy; ROS, reactive oxygen species; SA, serum albumin; VTP, vascular-targeted photodynamic therapy.

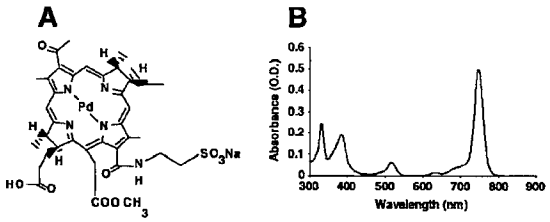

Figure 1. The chemical structure and absorption spectrum of WST11. (A) The chemical structure of WST11. (B) The absorption spectrum of WST11 (5 μM) in methanol.

tumors (A. Brandis, O. Mazor, S. Gross, N. Koudinova, E. Gladysh, R. Hami, N. Kammhuber, V. Rosenbach-Belkin, M. Greenwald, A. Bondon, G. Simonneaux, H. Scheer, Y. Salomon and A. Scherz, personal communication, 13), with negligible skin phototoxicity (N. Koudinova, unpublished). Phase I–II clinical trials with Tookad® have been completed (20) and Phase II trials are in progress in several clinical centers in Canada, Europe and Israel against recurrent localized prostate cancer in patients who failed radiation therapy.

Because of low solubility of Tookad® in aqueous solutions (octanol–water partitioning is 24:1), its clinical application requires the use of amphiphilic vehicles such as Cremophor® (8). A wealth of recent experimental data have indicated that Cremophor® is a biologically and pharmacologically active compound and its use as a drug formulation vehicle has been implicated in clinically important adverse effects, including acute hypersensitivity reactions and peripheral neuropathy (21). Such possible effects may limit the maximal allowed doses of Tookad® or its rate of administration (or both), particularly for the treatment of nonmalignant diseases. Furthermore, high hydrophilicity is usually associated with better retention in the circulation, as needed for vascular-targeted reagents. Therefore, it was desirable to prepare water-soluble Bchl derivatives with comparable photochemical properties and antivascular photodynamic activity.

In a recent study (A. Brandis, O. Mazor, E. Neumark, V. Rosenbach-Belkin, Y. Salomon and A. Scherz, personal communication, 22), we described the synthesis, solubility and optical spectroscopy of several new water-soluble derivatives of Bchl, substituted for Pd, Mn and Zn atoms. We also provided the affinity of the new derivatives to serum proteins and showed the effect of serum albumin (SA) on their photocytotoxicity in endothelial cell cultures. Modification of Pd-Bpheid with taurine (2-sulfoethylenamine) resulted in a taurinated dianionic salt of Pd-Bchl (under the code name WST11, Fig. 1) (A. Brandis, O. Mazor, E. Neumark, V. Rosenbach-Belkin, Y. Salomon and A. Scherz, personal communication, 22) with an octanol–water partitioning coefficient of 2:3. This compound dissolves readily in phosphate-buffered saline (PBS) or water in the form of small aggregates (A. Brandis, O. Mazor, E. Neumark, V. Rosenbach-Belkin, Y. Salomon and A. Scherz, personal communication, 23) at concentrations $\leq$50 mg/mL. In solutions containing serum, WST11 undergoes disaggregation to monomers by adsorbing mostly to the SA (>90% as 1:1, WST11–bovine serum albumin [BSA]) and high-density lipoprotein (<10%) (A. Brandis, O. Mazor, E. Neumark, V. Rosenbach-Belkin, Y. Salomon and A. Scherz, personal communication, 23).

Binding to SA increases the probability of sensitizers to remain confined to the tumor vasculature, as required for VTP (24). However, the apparent photoactivity of the SA-bound WST11 against endothelial cells was found to be substantially different from noncomplexed pigment (A. Brandis, O. Mazor, E. Neumark, V. Rosenbach-Belkin, Y. Salomon and A. Scherz, personal communication, 22). This could either reflect a reduction in the concentration of free sensitizers able to enter the cells by fluid-phase endocytosis or BSA-mediated trafficking of the bound sensitizers via specific SA receptors in these cells (25,26). The mode of endocytosis of WST11 into endothelial cells, its photocytotoxicity and the properties of its pharmacokinetics and biodistribution *in vivo* are probably key factors in determining its photodynamic efficacy and mode of action as an antivascular photosensitizer. Therefore, we set out to resolve these parameters to approach future developments and initiate appropriate treatment protocols for WST11-VTP.

The experiments presented in this study, combined with the assessment of WST11 phototoxicity under different SA concentrations (A. Brandis, O. Mazor, E. Neumark, V. Rosenbach-Belkin, Y. Salomon and A. Scherz, personal communication), provided evidence for SA-mediated cellular trafficking into endothelial cells. The temporal accumulation of WST11 in the lungs, along with its absence from the kidneys and the rapid hepatic clearance, provides additional indirect evidence for its interaction with SA. The pharmacokinetics, biodistribution and clearance rates of WST11 in mice and rats indicate a very short lifetime in the circulation with no significant extravasation into tissues. These findings suggest a rapid dissociation of the WST11-SA complex in target organs and corroborate the observed intermediate affinity of the sensitizer to the serum protein (A. Brandis, O. Mazor, E. Neumark, V. Rosenbach-Belkin, Y. Salomon and A. Scherz, in preparation, 22). Following our observations, the *in vivo* PDT protocol in animals was optimized to initiate illumination immediately after administrating the sensitizer. Under these conditions, WST11 was found to be a highly effective VTP reagent. Although, as reported in this study, this protocol was first tested with melanoma xenografts as a model (resulting in high cure rates), our data suggest that WST11 can be highly effective for VTP of other malignancies as well as nonmalignant diseases associated with abnormal vascularization such as age-related macular degeneration.

MATERIALS AND METHODS

Cell culture. M2R mouse melanoma and H5V mouse endothelial cells were cultured as monolayers in Dulbecco modified Eagle medium–F12 (Ham's F12 Nutrient Mix) containing 25 mM *N*-[2-hydroxyethyl]piperazine-*N'*-[2-ethanesulphonic acid], pH 7.4, 10% fetal calf serum (FCS), glutamine (2 mM), penicillin (0.06 mg/mL) and streptomycin (0.1 mg/mL) (hereafter referred to as the "culture medium"). Cells were grown at 37°C in an 8% CO_2-humidified atmosphere.

Preparation of pigments. WST11 (molecular weight 940, Fig. 1) was derived from Pd-Bpheid (WST09) by aminolysis with taurine (2-sulfoethylenamine; Aldrich; St. Louis, MO) as described earlier (A. Brandis, O. Mazor, E. Neumark, V. Rosenbach-Belkin, Y. Salomon and A. Scherz, personal communication) and kept dry in the dark under argon. Stock solutions of WST11 were prepared by dissolving the dry pigment directly in culture medium before use (for *in vitro* studies) or in PBS to the desired concentration for VTP in mice. Pigment purity and concentration were determined spectroscopically assuming $\varepsilon_0(\text{MeOH}) = 1.2 \times 10^5 M^{-1}\,\text{cm}^{-1}$ for WST11 using a Genesis-2 (Milton Roy; Rochester, NY) spectrophotometer.

Cellular pigment uptake. WST11, similar to other Pd-Bchl derivatives, presents extremely weak fluorescence complementary to its very high rate of intersystem crossing, as shown recently for Tookad® (Y. Vakrat and A. Scherz, personal communication). Therefore, the uptake of pigments by cells could not be determined by measuring fluorescence. Similarly, determination by optical absorption after extraction into methanol was found highly inaccurate at the lower concentration range. Because each WST11 molecule contains one Pd atom and its concentration can be determined to at least 1 ppb with inductively coupled plasma mass spectroscopy (ICP-MS; ELAN-6000, Perkin Elmer; Boston, MA), we chose

this mode of measurement as a viable alternative to determine the cellular content of Pd atoms under the selected experimental protocol. Importantly, the chelating of Pd^{2+} as a central metal within $Bchl^{2-}$ macrocycle was found extremely stable in the range of pH 1–9 (data not shown) and under physiological conditions. Validation of the ICP-MS determination was carried out independently by comparing the Pd concentration in blood extracts with the WST11 concentration determined by its optical absorption in methanol (data not shown). Thus, cells were preincubated with the pigments for the indicated times, washed three times in PBS and collected using a rubber policeman.

The cells were then centrifuged (2000 rpm, 5 min), resuspended in double-distilled water (DDW) and sonicated for 1 min. The protein in each sample was determined by Coomassie blue assay (27). For Pd analysis, the samples were prepared as described below.

In vitro *phototoxicity*. To determine the pigment phototoxicity under standard conditions, cells were cultured in 96 well plates and preincubated in culture medium with the indicated concentrations of WST11 in the dark for 2 h. To determine the cellular uptake of the pigment, the cells were preincubated with WST11 under different conditions as detailed in the individual experiments. Unbound sensitizer was then removed by washing the cells once with fresh warm culture medium, and the plates were illuminated at room temperature from the bottom for 10 min ($650 < \lambda < 800$ nm, 12 J/cm^2) using a 100 W halogen lamp (Osram; Munchen, Germany) equipped with a <650 nm cutoff and a 4 cm water filter. The culture plates were then placed in the culture incubator and cell survival was determined 24 h after illumination, using the neutral red cell survival assay (28). The reliability of the neutral red assay for the evaluation of Bchl-based photodynamic activity was confirmed by a comparative study using the MTT-thiazoyl blue assay. After subtraction of assay blanks, the net optical density (570 nm) was computed as the average value of triplicate determinations. Cell survival was calculated as the percentage of the dye that accumulated in the untreated controls. Experiments were conducted at least three times and representative experiments are shown. Three controls were used: (1) light control, cells illuminated in the absence of pigment; (2) dark control, cells treated with pigment but kept in the dark; and (3) untreated cells, cells kept in the dark.

Animals. Male CD1 nude mice (8 weeks old, ~30 g) or male WISTAR rats (6 months old, ~250 g) were housed with free access to food and water in the departmental animal facility. All experiments were conducted according to the guidelines of the institutional animal care and use committee of the Weizmann Institute of Science, Rehovot, Israel.

Anesthesia. Mice were anesthetized by an intraperitoneal (i.p.) injection of 80 μL ketamine (100 mg/mL; Rhone Merieux, Lyon, France) and a xylazine (2%; Vitamed, Benyamina, Israel) mixture (85:15, vol/vol). Rats were anesthetized by an i.p. injection of 300 μL ketamine and a diazepam mixture (1:1, vol/vol).

Tumor model. Cultured mouse M2R melanoma cell monolayers were scraped under saline with a rubber policeman and implanted subcutaneously on the backs of the mice (2×10^6 cells/mouse, 30 μL); tumors developed to the treatment size (6–8 mm in diameter) within 2–3 weeks.

Biodistribution. After i.v. injection of the WST11 (6 mg/kg), the mice were euthanatized at the indicated times and samples of the indicated organs or tissues were placed in preweighted vials and immediately frozen on dry ice. For examination, each sample was thawed and homogenized (1:10, wt/vol) in DDW. Aliquots of the homogenate (0.5 mL) were lyophilized in 1.5 mL test tubes. To each dry sample, HNO_3 (200 μL, 70%; TraceSelect, Fluka, Buchs, Switzerland) was added and the test tubes were incubated for 1 h at 90°C. The acid-digested samples were then transferred to test tubes containing 10 mL of DDW. Pd concentrations in these samples were determined by ICP-MS. Background Pd levels in tissues were determined on equivalent tissue samples obtained from untreated mice. Experimental values were corrected respectively and the results are given as WST11 micrograms pigment per gram wet tissue (mean ± SEM).

Pharmacokinetics. Anesthetized mice were i.v. injected with WST11 (6 mg/kg), and blood samples (~50 μL) were drawn from the tail vein at the indicated times, placed in preweighed 1.5 mL test tubes, weighted and lyophilized.

For infusion studies, rats were catheterized in the femur and tail veins. WST11 (10 mg/kg) was then infused for 20 min into the tail vein by a dedicated infusion pump, and blood samples (~100 μL) were drawn from the femur vein at the indicated times, placed in preweighed 1.5 mL test tubes, weighed and lyophilized. Samples from both experiments were then prepared for Pd determination as described above.

VTP protocol. The M2R tumor-bearing mice were anesthetized and WST11 (6 or 9 mg/kg) was injected i.v. via the tail vein. The tumors were immediately transcutaneously illuminated for 5 min using a 755 nm diode laser (CeramOptec, Germany) at the indicated light doses. After treatment, the mice were returned to the cage. The mice were considered cured if tumor free for 90 days after treatment. Mice were euthanatized when the tumor diameter reached 15 mm. The controls used were (1) dark control, the mice were i.v. injected with pigment and not illuminated; (2) light control, mice were illuminated without pigment injection; and (3) untreated control.

Statistical analyses. Triplicate determinations were performed in cell survival analyses and presented as the average ± SEM. All experiments were performed at least three times and representative examples are presented.

RESULTS AND DISCUSSION

Cellular uptake of WST11

To study the effect of temperature upon sensitizer uptake, endothelial H5V cells (Fig. 2A) and M2R melanoma cells (Fig. 2B) were incubated at 4°C or 37°C with 10 μ*M* WST11, washed at the indicated times and analyzed for Pd content. As shown, pigment association at 37°C increased rapidly during the first 5–10 min and then leveled off at ~50–60 min after the beginning of the incubation. In contrast, at 4°C, WST11 rapidly associated with the cells and leveled off at 10 min at lower concentrations.

The amount of cell-associated WST11 (Fig. 2A) arrives at a steady state in approximately 45 min. Pigment accumulation can be described by the following equation:

$$d[WST11]_{in}/dt = Y - k[WST11], \quad (1a)$$

where $d[WST11]_{in}/dt = 0$ after ~45 min of preincubation.

The solution of Eq. 1a is

$$[WST11]_{in} = Y/k(1 - e^{-kt}), \quad (1b)$$

where k (in min^{-1}) represents the rate constant for the sensitizer's efflux from the endothelial cells and Y represents the rate of the sensitizer's influx into the cells. This equation fits the experimental data regarding the temporal concentration of WST11 in the cells after incubation at 37°C with $k = 0.0946 \pm 0.0331$ min^{-1} (Fig. 2A, solid line). Notably, Eq. 1b can also be interpreted in terms of a Langmuir adsorption curve, as discussed below.

We next determined how the presence of serum affects WST11 uptake by M2R cells at low and high temperatures. Figure 2C shows that short incubation (10 min) of the cells with 10 μ*M* WST11 at 37°C in the presence of serum decreased Y/k by a factor of 3–5 compared with cells incubated without serum. In contrast, the presence of serum had only a slight effect on WST11 uptake at 4°C (Fig. 2C). On the basis of these experiments, we concluded that WST11 is taken up by the cells in two modes; the first is strongly affected by serum and is inhibited by low temperature, whereas the second is independent of serum and is maintained at low temperature. The temperature dependence of pigment uptake in the presence of serum suggests that active uptake takes place at 37°C, in agreement with endocytosis of other albumin-bound drugs, as described by others (29).

The association of WST11 at 4°C with both M2R and H5V cells in the presence or absence of serum was nonphototoxic on illumination, whereas 80% of cell death was induced after preincubation with WST11 at 37°C (Fig. 3). Notably, low temperatures were found to affect both active and passive pinocytosis of molecules of the WST11 size (as mentioned, WST11 forms small aggregates of 1–2 nm in diameter in the absence of serum) but not their adsorption to the cell membrane (29). Therefore, we propose

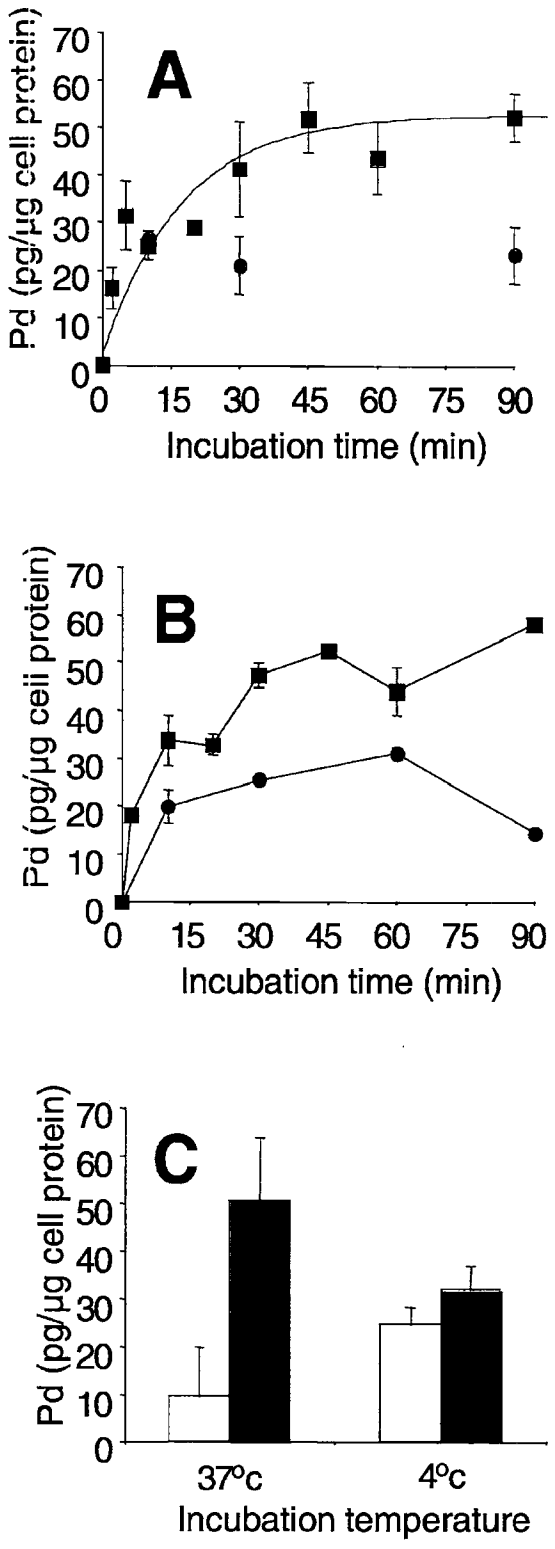

Figure 2. Cellular uptake of WST11. H5V (A) or M2R (B) cells were preincubated with 10 µ*M* WST11 at 37°C (squares) or 4°C (circles) for the indicated time periods, washed three times and collected. (C) M2R cells were preincubated for 10 min with 10 µ*M* WST11 at 37°C or 4°C in the absence (empty bars) or presence (filled bars) of 10% FCS, washed three times and collected. Pd concentrations were determined by ICP-MS. The points are the mean ± SEM of triplicate determinations. All other details were as described under Materials and Methods.

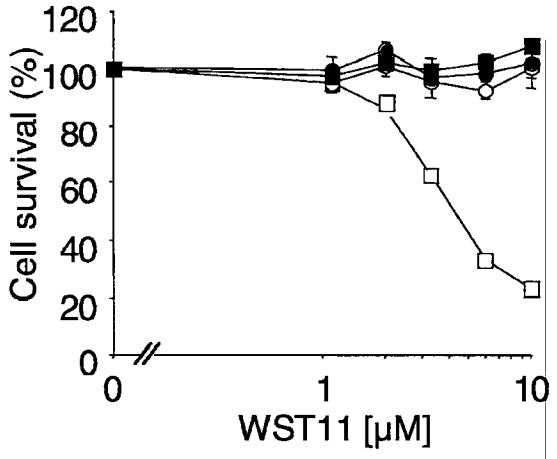

Figure 3. Inhibition of WST11 phototoxicity at low temperature. H5V cells were preincubated with the indicated increasing concentrations of WST11 at 37°C (squares) or 4°C (circles), washed and illuminated (open shapes) or kept in the dark (closed shapes). The points are the mean ± SEM of triplicate determinations.

that excitation of WST11 after preincubation at 4°C does not confer phototoxicity because the pigment localizes in sites that are not critically affected by ROS, possibly on the outer surface of the cell membrane. On the other hand, at 37°C, WST11 molecules reach appropriate targets for initiating phototoxic processes.

The phototoxicity of WST11 depends on the concentration of SA during preincubation

WST11 was shown to complex with BSA ($K_{assoc} \sim 10^4\ M^{-1}$), and similar binding was obtained with human serum and with purified human SA (A. Brandis, O. Mazor, E. Neumark, V. Rosenbach-Belkin, Y. Salomon and A. Scherz, personal communication). This complexation of WST11 should affect the cellular uptake, clearance rate and biodistribution of the pigment and consequently its phototoxicity and biological activity. Whereas unbound, free WST11 can undergo receptor-independent, fluid-phase pinocytosis, the SA-bound pigment may be subject to SA- or receptor-mediated trafficking (26). Notably, binding of other photosensitizers to SA but with significantly higher affinity constants (*e.g.* $2 \times 10^8\ M^{-1}$ for hydroxyethyl-vinyl-deuteropophyrin [30]) could be detrimental to its photocytotoxicity, as demonstrated for Chlorin e_6 derivative (Npe6) in P388 murine leukemia cells (31). The effect of serum proteins on the cellular uptake and photocytoxicity of PDT sensitizers is particularly important when considering treatment protocols for those that clear rapidly. Hence, we set out to study this effect with WST11.

The phototoxicity of WST11 was markedly attenuated if serum proteins were present during preincubation (Fig. 4A). The apparent LD_{50} of WST11 increased from ~1 µ*M* after 2 h of preincubation in the absence of serum to ~4 µ*M* in 10% FCS medium (10% FCS contains ~60 µ*M* BSA), with no dark toxicity in the tested concentration range. A similar shift was observed when WST11 was preincubated in the presence of increasing BSA concentrations (Fig.

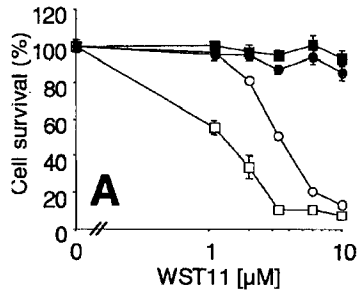

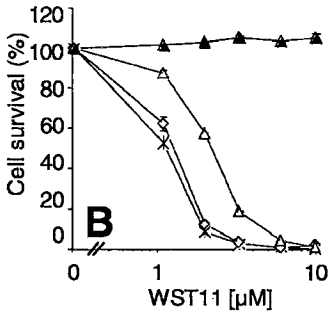

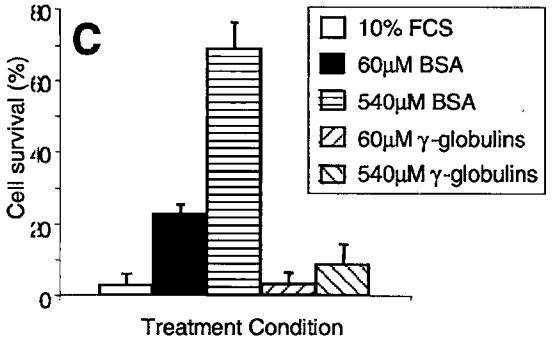

Figure 4. The effect of serum and BSA on WST11 phototoxicity. H5V cells were preincubated for 2 h with the indicated increasing concentrations of WST11 in (A) the absence (squares) or presence (circles) of 10% FCS or (B) in the absence or presence of BSA, 2 μ*M* (circles), 10 μ*M* (squares) or 60 μ*M* (triangles) or (C) in the presence of γ-globulins. Cells were then washed with fresh medium and illuminated (open shapes) or kept in the dark (closed shapes). Points are mean ± SEM of triplicate determinations.

4B). To confirm that the effect on the phototoxicity of WST11 is specific for BSA, cells were preincubated with WST11 in the presence of 60 or 540 μ*M* bovine γ-globulins, washed and illuminated. As shown in Fig. 4C, the presence of γ-globulins had only a minor effect on the WST11 phototoxicity. The preferred affinity of WST11 to BSA was further demonstrated in concentrated solutions of WST11 where the addition of BSA resulted in complete monomerization of the sensitizer, while no such effect was observed on adding γ-globulin (A. Brandis, O. Mazor, E. Neumark, V. Rosenbach-Belkin, Y. Salomon and A. Scherz, personal communication). Considering that phototoxicity can serve as a measure of pigment uptake, these findings suggest that binding to BSA (1) markedly reduces cellular uptake of WST11 as found for other photosensitizers because of reduction in free pigment concentrations (31,32) or (2) completely wipes out the phototoxicity of WST11 so that no photoxicity is conferred even if the pigment enters the cells, as suggested for the Npe6 in P388 leukemia cell suspension (31) (or both). Following this alternative, the percentage but not the rate of phototoxicity evolution should be affected by SA.

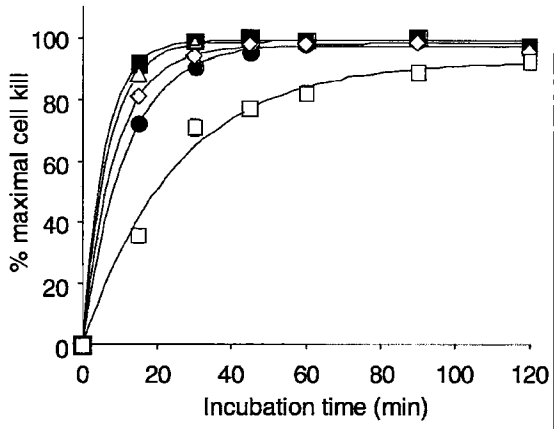

Figure 5. The effect of serum and BSA on WST11 uptake kinetics. H5V cells were preincubated for the indicated time periods with 10 μ*M* WST11, washed and illuminated. Preincubation conditions were the absence (filled squares) or presence of serum (filled circles) or BSA, 2 μ*M* (triangles), 10 μ*M* (diamonds) and 60 μ*M* (open squares). The results are presented as the percentage of maximal cell killing. The points are the mean ± SEM of triplicate determinations.

Figure 2C shows that the addition of BSA markedly reduced the total amount of WST11 taken up by H5V cells at 37°C. To study the effect of BSA on the uptake kinetics of WST11, we determined cell survival by monitoring increasing preincubation times with 10 μ*M* WST11 in the absence or presence of 10% FCS or BSA (2–60 μ*M*) (Fig. 5).

Clearly, the rate for the evolution of photocytotoxicity decreased with increasing concentrations of BSA. The fastest rate of cell killing was observed in the absence of added proteins, whereas in the presence of increasing BSA concentrations, this killing rate was attenuated progressively (Table 1). Complete cell killing was attained with 60 μ*M* BSA (the BSA concentration provided also by 10% FCS) only after 120 min of preincubation. This observation rules out alternative (2) as a possible mechanism.

The temporal evolution of phototoxicity can be simulated (Fig. 5, solid lines) by the equation

$$T(t)^* = 100\%(1 - e^{-k_2 t}), \qquad (2)$$

where T(t) represents the fraction (in percent) of photointoxicated cells at t min after starting preincubation and k_2 is the rate constant for the evolution of phototoxicity. Apparently, at increased concentrations of SA (either as part of FCS or when added in a purified

Table 1. Uptake parameters of WST11 in H5V cells under different medium conditions

Medium condition	k_2 (min^{-1})
10% FCS	0.088 ± 0.002
Without FCS	0.172 ± 0.011
2 μ*M* BSA	0.148 ± 0.007
10 μ*M* BSA	0.117 ± 0.005
60 μ*M* BSA	0.04 ± 0.005

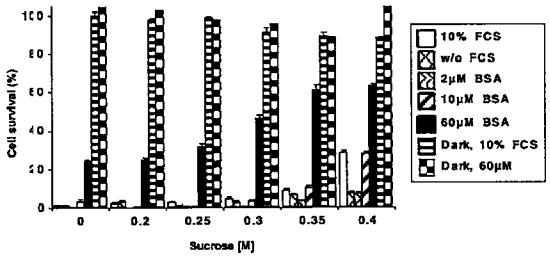

Figure 6. Inhibition of photocytotoxicity by sucrose. H5V cells were preincubated for 2 h with increasing concentrations of sucrose and 10 μ*M* WST11 in the presence of the indicated BSA or FCS concentrations, washed once with fresh medium and illuminated or kept in the dark. The bars are the mean ± SEM of triplicate determinations.

form) k_2 decreased and the phototoxicity of WST11 reached saturation at longer times. The simplest explanation for this phenomenon, considering the above-mentioned formation of a complex between WST11 and SA, is that cellular uptake of the photosensitizer follows Langmuir adsorption to a limited number of sites (eventually SA receptors), N, at the cell membrane. Consequently, Eq. 2 is the solution for Eq. 3

$$dx/dt = k_{ad}[WST11][N - f(SA)](1 - x), \qquad (3)$$

where k_{ad} is the adsorption rate constant of the SA-WST11 complex, [WST11] is the sensitizer concentration outside the cell, N is the total number of SA receptors, f(SA) is the fraction of receptors bound to noncomplex SA and x is the fraction of receptors free for binding SA-WST11. Thus, $k_2 = k_{ad}[WST11][N - f(SA)]$. Evidently, on increasing [SA] in the preincubation medium, f(SA) increases and k_2 decreases as observed (Table 1, Fig. 5). Thus, the formation of a complex with BSA affects both the overall concentration of free pigments and rate of WST11 uptake by H5V cells, probably in a receptor-mediated fashion. In fact, approaching physiological SA concentrations, there is practically very little uptake of WST11 within the first few minutes of incubation (A. Brandis, O. Mazor, E. Neumark, V. Rosenbach-Belkin, Y. Salomon and A. Scherz, personal communication).

The photocytotoxicity of WST11 becomes sucrose dependent in the presence of albumin

To verify the significance of the formation of the WST11-BSA complex to the photodynamic activity with WST11, we examined the phototoxicity of the sensitizer under conditions that should affect albumin endocytosis but not the cellular uptake of free WST11. Hypertonic conditions, encouraged by high sucrose concentrations, affect the endocytosis of SA (33–35), although it is traditionally considered as a marker for fluid-phase endocytosis (pinocytosis). Remarkably, when incubated in the presence of 0.2 *M* sucrose, the rate of [^{125}I]-tyramine cellobiose–labeled BSA accumulation in hepatocytes declined by ~50% compared with controls containing no sucrose (36).

Figure 6 shows the effect of increased sucrose concentration on the phototoxicity of WST11. In the absence of serum, the phototoxicity of WST11 was almost unaffected by sucrose (0–0.4 *M*). However, in the presence of BSA (≥10 μ*M*), the phototoxicity of WST11 significantly declined with increasing sucrose concentrations (25% cell survival at 0.4 *M* sucrose). At 60 μ*M* BSA and 0.4 *M* sucrose as in 10% FCS, cell survival increased to ~65%. Notably, the effect of sucrose on the temporal evolution of photocytotoxicity and its maximal value reported in this study appear similar to the previously reported effect of this agent on the kinetics of SA accumulation and its steady-state concentration in cells (35). This finding provides additional support to our hypothesis that in the presence of SA, the majority of WST11 enters the cells as WST11-BSA complexes and very little as free WST11, which was found to be sucrose independent.

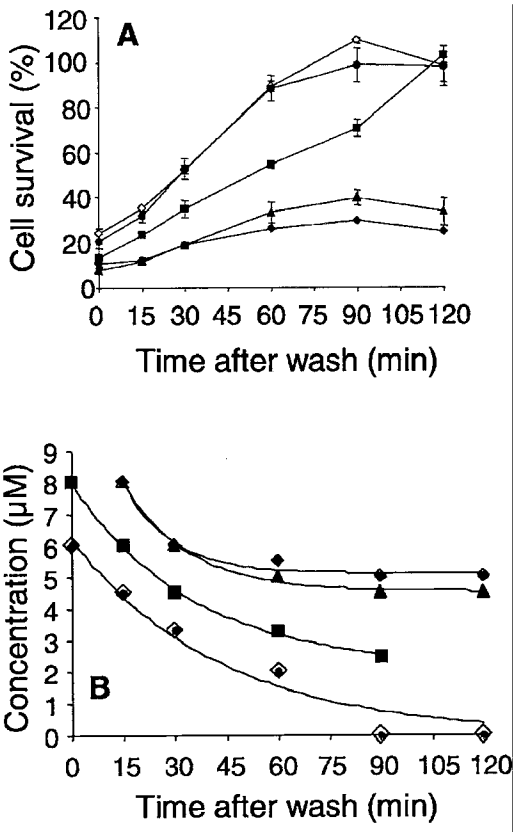

Figure 7. The effect of FCS and BSA on WST11 exocytosis rates. (A) H5V cells were preincubated for 2 h with 10 μ*M* WST11 in medium containing 10% FCS (comprising ~60 μ*M* BSA). Cells were then washed and further incubated under different medium conditions without WST11. Cells were illuminated thereafter at the indicated time points. The medium conditions were the absence (filled diamonds) or presence (open diamonds) of serum, 2 μ*M* (filled triangles), 10 μ*M* (filled squares) or 60 μ*M* (filled circles) of BSA. The points are the average of triplicates ± SEM. (B) Each experimental point of (A) was translated to effective WST11 concentrations on the basis of Fig. 3 as a calibration curve. The lines were fitted according to Eq. 3.

Exocytosis of WST11: effects of serum proteins and albumin

To further explore the role of serum proteins or SA in WST11 cell trafficking, we performed the following set of experiments: H5V cells were preincubated with 10 μ*M* WST11 in 10% FCS for 2 h, followed by replacing with a WST11-free medium but with different concentrations of BSA. Cells were then illuminated at different times after medium change and cell survival was determined. As shown in Fig. 7A, cell survival after medium replacement leveled off at values positively correlated with the BSA concentrations. In the presence of up to 2 μ*M* BSA, cell survival increased from 10% to 30% within 60 min without any further change. In the presence of higher BSA concentrations, cell survival reached 90% after 60 min (for 60 μ*M* BSA and 10% FCS) or 100% at 120 min (for 10 μ*M* BSA).

Table 2. Exocytosis parameters of WST11 in H5V cells under different medium conditions

Medium condition	k_3 (min^{-1})
10% FCS	0.023 ± 0.005
Without FCS	0.071 ± 0.019
2 μ*M* BSA	0.053 ± 0.007
10 μ*M* BSA	0.029 ± 0.003
60 μ*M* BSA	0.023 ± 0.005

To further illustrate this point, cell survival under each condition, as shown in Fig. 7A, was translated into the level of phototoxicity induced by effective concentrations of ambient WST11 in the preincubation step (Fig. 7B), taking the results of Fig. 3 as a calibration curve. The variation in the effective concentration of WST11 could be well fitted with a simple exponential equation,

$$[\text{WST11}] = a + b\exp(-k_3 t), \quad (4)$$

where k_3 stands for the rate of cell detoxification, "a" represents a fraction of WST11 that cannot be cleared from the preincubated cells and "b" stands for the cleared fraction. The exocytosis parameters are summarized in Table 2, and as can be seen, increasing the BSA concentrations decreased a while increasing b. The rate constant, k_3, appeared to remain practically constant at ≥10 μ*M* BSA, and it significantly increased at low or null BSA concentrations.

On the basis of these observations, we speculated that deactivation of WST11 during exocytosis involves binding to BSA molecules that undergo continuous endocytosis and exocytosis. Thus, the BSA molecules serve as a carrier for exocytosis of WST11 molecules from endothelial cells to the extracellular space where they dilute. Increasing the BSA concentration in the medium after incubation should enhance this mobilization, as shown in Fig. 7. Interestingly, binding to BSA appears essential for cellular detoxification after washing because phototoxicity seems to remain for a long time in the absence of external WST11 concentrations (Fig. 7). Moreover, the exocytosis rate in the absence of BSA is higher (Table 2), but this process can remove only a small fraction of the WST11 from the cell. The dependence of cell survival on BSA, as shown in this study, suggests the active involvement of this serum protein in the trafficking of WST11 both into and out of the treated cells. Taking that observation into consideration, we propose that under conditions where physiologically relevant BSA concentrations (≥60 μ*M*) are present the uptake and release of WST11 by H5V cells is mostly, if not completely, BSA mediated. However, on the basis of the equilibrium constant for BSA-WST11 association ($K \sim 10^4\ M^{-1}$), the incubating medium at 60 μ*M* BSA and 10 μ*M* WST11 should contain ~4 μ*M* of free WST11, a much higher concentration than LD_{50} in a BSA-free solution. This paradoxical finding may be explained by assuming that the BSA concentration is increased locally in the cell membrane compartments during internalization. Having WST11 exposed to increased BSA concentrations in the fluid phase of early endosomes should shift the equilibrium toward further association of WST11 with BSA molecules. Thus, we propose that although the external concentration of free WST11 is significant, it markedly decreases on entering the cells because of intracellular binding to BSA or other intracellular proteins. To gain phototoxicity, the SA-WST11 complexes probably have to enter the lysosomes where they most likely dissociate. Indeed, accumulation of other hydrophilic sensitizers in the lysosomes was reported previously (37–39).

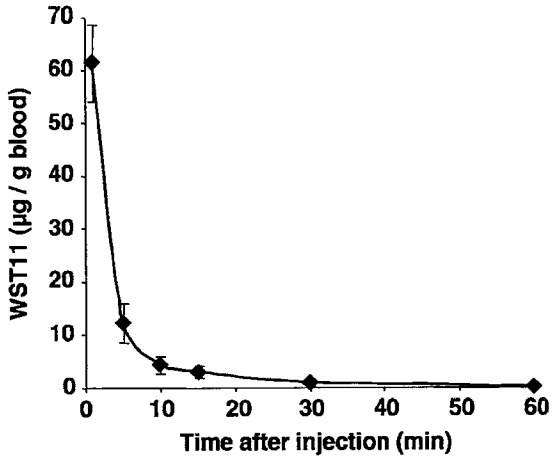

Figure 8. Clearance rate of WST11 in mouse blood after i.v. injection. WST11 (6 mg/kg) was i.v. injected into CD1 nude mice, and blood samples were taken from the tail vein at the indicated times. WST11 concentrations (dots) were determined (by ICP-MS of Pd) and given as micrograms WST11 per gram blood. Other details were as described in the Materials and Methods section. The values are the mean ± SEM of three mice. The solid line shows the theoretical fit using Eq. 5.

Our data suggest that exocytosis of WST11 from H5V cells includes at least two steps (36) involving $X_2 \rightarrow X_3 \rightarrow X_4$, where the first step comprises the conversion of a free phototoxic WST11 (X_2) into a nonphototoxic BSA-bound complex entrapped in plasmallema-derived vesicles (X_3). In the second step, these vesicles return to the plasmalemma membrane (X_4) and undergo extravasation.

In all, WST11 distribution in endothelial cells is proposed to be a four-step process: $X_1 \rightarrow X_2 \rightarrow X_3 \rightarrow X_4$, where X_1 and X_4 represent WST11-SA complexes available for endocytosis and exocytosis, respectively. This scheme is a variant of the three-step Poison jump process suggested by Niles and Malik (36) to describe a particulate dye distribution in endothelial cells, where new vesicles were found to enter state X_2 at a rate given by Eq. 2.

Pharmacokinetics of WST11 in mice

VTP with Tookad® and WST11 aims at shutting down the tumor blood supply (A. Brandis, O. Mazor, S. Gross, N. Koudinova, E. Gladysh, R. Hami, N. Kammhuber, V. Rosenbach-Belkin, M. Greenwald, A. Bondon, G. Simonneaux, H. Scheer, Y. Salomon and A. Scherz, personal communication, 11,40). In this protocol, the tumor is illuminated when the drug concentration in the blood is high, *i.e.* immediately after drug injection. To determine the clearance rate of WST11 from the circulation, the drug was bolus i.v. injected into nude mice (6 mg/kg) and blood samples were taken from the tail vein at various time points thereafter. Figure 8 shows the clearance of WST11 from the blood after injection. The kinetics is monoexponential

$$y = a + b\exp^{(-kt)}, \quad (5)$$

with $t_{1/2} = 1.65$ min. Approximately 90% of the injected pigment cleared within 5 min, reaching almost background levels 30 min after injection. The corresponding rate of elimination (K_{el}) was 0.42 min^{-1}, the volume of distribution (V_d) was 2.12 mL and the clearance rate was 0.89 mL/min.

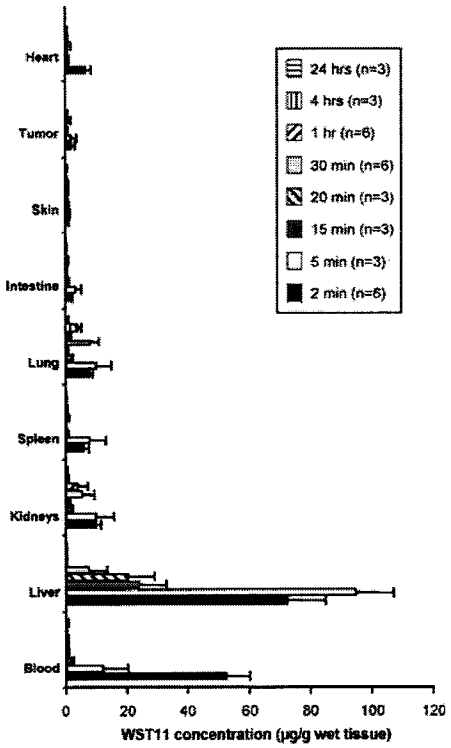

Figure 9. Biodistribution of WST11 in mice bearing melanoma xenografts. Mice were euthanatized at different times after i.v. injection of WST11 (6 mg/kg), and WST11 content in the respective tissue samples were determined (by ICP-MS of Pd) and presented as micrograms WST11 per gram wet tissue, as described in the Materials and Methods section. The values for each time point represent the mean ± SEM of three to six animals. Value for brain, testes, fat and muscle are not presented, yet found to be below 5µg/g wet tissue.

WST11 does not extravasate from the circulation and rapidly clears from the animal body

Figure 9 shows the biodistribution of WST11 in M2R melanoma–bearing mice after bolus i.v. administration (6 mg/kg body). The highest levels of WST11 in the blood were found immediately after injection (2 min) and in the liver, kidney, lung and spleen only 5 min after injection. Clearance of WST11 was completed in all these tissues by 60 min but in the lungs by 4 h with only background levels remaining 24 h after administration in any of the examined tissues. The clearance rate of WST11 from the lung ($t_{1/2}$ ~ 40 min) was markedly slower than from other tissues and significantly slower than from the liver (~20 min). The biodistribution and rate of clearance of WST11 from tissues may be related to water solubility and the negative charges introduced by the taurine side group and its complexation with SA (41). Taurine is a β-amino acid normally present in the intracellular fluid, and it is widely distributed in many tissues including the brain, retina and liver of mammals (42). It appears to be involved in brain and retinal development, osmoregulation, detoxification and xenobiotic conjugation. Conjugation of taurine to different molecules in the liver in the course of their detoxification increases their polarity and aqueous solubility, thereby facilitating their hepatic clearance (42). Thus, the rapid clearance of WST11 from the liver compared with that of Tookad® ($t_{1/2}$ = ~5 h in the liver) could be anticipated. The temporal accumulation of WST11 in the lungs is probably related to its association with SA and its transcellular trafficking through the caveoli of endothelial cells in this organ (43). The significant differences in structure between the polar WST11 and the hydrophobic Tookad® may therefore be reflected in their different biodistribution and pharmacokinetics. The rapid elimination of WST11 from the blood without accumulation in the skin assures the absence of coetaneous phototoxicity, as was found for Tookad® (A. Brandis, O. Mazor, S. Gross, N. Koudinova, E. Gladysh, R. Hami, N. Kammhuber, V. Rosenbach-Belkin, M. Greenwald, A. Bondon, G. Simonneaux, H. Scheer, Y. Salomon and A. Scherz, personal communication).

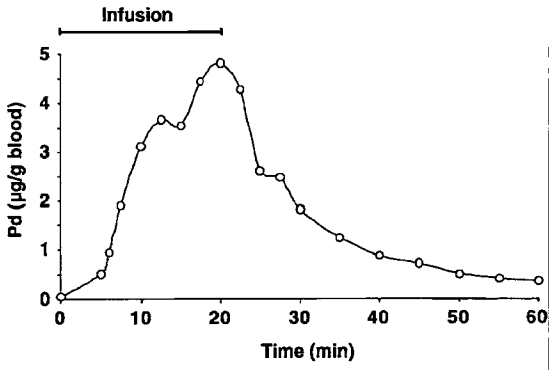

Figure 10. Blood levels of WST11 during and after infusion. WISTAR rats were infused for 20 min with WST11 (10 mg/kg), and blood was drawn at the indicated time points. WST11 concentrations were determined by ICP-MS for Pd. The graph is a representative example of one rat (out of three).

Infusion of WST11 can extend its presence in the circulation

As shown previously, WST11 clears rapidly from the circulation, leaving only a short time-window for illumination where pigment levels in the blood are photodynamically effective. This may pose some technical difficulties in the PDT protocol in large animals and humans where manipulations of surgical gear may not be so fast. Thus, extension of the effective time-window may be achieved by sensitizer infusion without increasing the total drug dose delivered. Theoretically, by infusion, drug levels will reach their maximum in the blood within 4.3 $t_{1/2}$ and will remain so during a constant infusion rate (41). On termination of infusion, the drug is expected to clear with its inherent clearance rate. Changing the rate of infusion or the injected dose will affect the maximal circulating levels reached without changing the time needed to attain a maximal level (38).

To test the feasibility of this approach, we infused WST11 to rats for 20 min and its circulating levels were monitored by blood sampling at the indicated time points (Fig. 10) followed by determination with ICP-MS. Figure 10 shows that the WST11 concentration in the blood increased initially for ~20 min and started to level off without reaching a steady-state concentration by the end of the infusion. Immediately after the infusion was stopped, WST11 cleared according to a monophasic behavior according to Eq. 8. The calculated $t_{1/2}$ of WST11 after infusion was found to be 7.12 ± 0.37 min (n = 3). Thus, 40 min after the end of infusion, the circulating concentrations of WST11 reached the background level. Evidently, during infusion, small aggregates of WST11 dissociated and bound to albumin (at ~60 µ*M* WST11 and ~600 µ*M* BSA, >90% of the pigment should become SA-bound, assuming an equilibrium constant of 10^4 M^{-1}). Thus, the clearance rate constant after bolus injection probably reflects the pharmacokinetics of small WST11 aggregates, and on infusion, the clearance rate re-

presents the pharmacokinetics of albumin-bound molecules. At $3 \times t_{1/2}$ (~21 min), one expects the WST11 to arrive at a steady-state concentration in the plasma. Note that the clearance rates of WST11 from the mouse and rat blood are expected to differ (because of a slower circulation rate, metabolism, *etc.*) (41).

PDT of melanoma xenografts with WST11

In light of the pharmacokinetic results described, the VTP protocol was set for 5 min of illumination starting immediately after the i.v. injection of the pigment. To determine the optimal conditions for the VTP protocol, we varied the drug and light doses over the indicated ranges (Fig. 11). Mice bearing M2R melanoma xenografts were injected i.v. with WST11 (6 or 9 mg/kg body) and immediately illuminated at increasing light doses (30–45 J/cm^2).

After VTP, all treated tumors developed necrosis within 24–48 h. Tumor flattening was observed for the next 14 days. The best results with 6 mg/kg WST11 were obtained with a light dose of 45 J/cm^2 (6/10 mice cured and monitored for up to 90 days). At lower light doses (39 and 30 J/cm^2), the cure rates declined to 2/8 and 6/14 mice, respectively. Increasing the WST11 dose to 9 mg/kg at a light dose of 30 J/cm^2 improved the treatment outcome to 70% cure (7/10 mice) at 90 days after treatment. The tumor growth rate in the light, dark and untreated controls was similar, and no skin toxicity was observed at 30 min after i.v. injection (data not shown). These results are similar and even better than those obtained with Tookad® on the same tumor model (60% cure, 10 mg/kg, 90 J/cm^2) (11). Tumor recurrence, if observed, occurred in ~25% of the treated animals mainly at the tumor rim. A similar phenomenon but to a much higher extent was observed in tumor models treated by antivascular chemotherapy (AVT) reagents and was proposed to reflect accelerated neoangiogenesis at the tumor rim (44). Notably, although tumor regrowth in the AVT was observed with the majority of treated animals, most of the VTP-treated animals were cured and, on increasing the light fluence or the applied drug dose (or both) the cure rate even increased. Furthermore, in other tumor models such as human colon carcinoma, we observed tumor regrowth in only 9% of the treated animals (A. Scherz and coworkers in preparation). Thus, with respect to local tumor treatment, VTP with WST11 appears to have a clear advantage over treatment with AVT reagents.

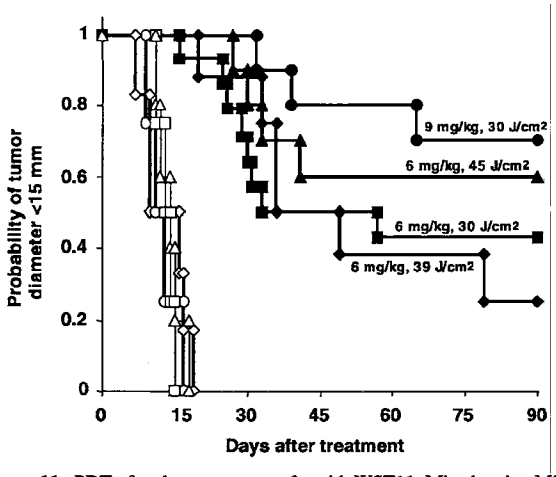

Figure 11. PDT of melanoma xenografts with WST11. Mice bearing M2R melanoma xenografts were i.v. injected with WST11 (6 mg/kg) and illuminated for 5 min with a light dose of 30 J/cm^2 (n = 14, filled squares), 39 J/cm^2 (n = 8, filled diamonds) or 45 J/cm^2 (n = 10, filled triangles). Mice that were injected with 9 mg/kg of WST11 were illuminated for 5 min with 30 J/cm^2 (n = 10, filled circles). Control groups: untreated (n = 4, open squares), the dark control received 6 mg/kg (n = 4, open circles) or 9 mg/kg (n = 5, open triangles) of WST11 and the light control, 45 J/cm^2 (n = 6, open diamonds).

CONCLUSIONS

The results of this study show that WST11 is an effective and safe sensitizer for VTP of relatively large solid tumors. In preliminary experiments, we have demonstrated a shutdown of the tumor vasculature by WST11-VTP already within the course of illumination (O. Mazor, in preparation). The significance of sensitizer binding to SA for conferring VTP warrants additional comments. Such binding may have two effects: (1) because of the long half-life of SA (19 days for humans and 3–4 days for smaller animals such as rabbits) (45), it may significantly extend the drug's lifetime in the circulation and thereby its bioavailability; and (2) complexation with SA should bring the drug to SA target organs such as liver, spleen, kidneys and lungs. Hence, liver and hepatic temporal accumulation and clearance (for smaller molecules) characterize drugs that adsorb to SA (46). The overall clearance of the drug and its biodistribution depend on the affinity to SA relative to tissue and cellular factors in the target organs. Most reported photosensitizers that were found in complexes with SA had a significantly higher affinity to the serum protein than WST11. Such high affinities pose a problem for PDT or VTP because of the prolonged residence in the circulation, and the potential accompanying slow extravasation to surrounding tissues should subject the patient to prolonged skin toxicity. This may account for the 6 weeks of potential toxicity of HPD-treated patients ($\sim 3 \cdot t_{1/2}$ of SA in humans). Hence, the moderate affinity of WST11 ($10^4\ M^{-1}$) is an important advantage because it assures SA-mediated trafficking in the body but allows for rapid dissociation and subsequent clearance in the liver and kidneys as found, for example, for warfarin and other drugs (47).

Taken together, the characteristics of WST11 make it a promising VTP sensitizer for vascular-associated diseases such as cancer and age-related macular degeneration (48).

Acknowledgements—This study is in partial fulfillment of the Ph.D. thesis of O.M. at the Feinberg Graduate School, The Weizmann Institute of Science. Y.S. is the incumbent of the Tillie and Charles Lubin Professorial Chair in Biochemical Endocrinology. A.S. is the incumbent of the Robert and Yaddele Sklare Professorial Chair in Biochemistry. The authors wish to thank Mrs. Ester Shai for her helpful assistance and Dr. P.-H. Brun from Negma-Lerads for continuous fruitful discussions. This study was supported by grants from the Yeda Research and Development Co. Ltd. (Israel) and Steba-Biotech.

REFERENCES

1. Ackroyd, R., C. Kelty, N. Brown and M. Reed (2001) The history of photodetection and photodynamic therapy. *Photochem. Photobiol.* **74**, 656–669.
2. MacDonald, I. J. and T. J. Dougherty (2001) Basic principles of photodynamic therapy. *J. Porphyrins Phtalocyanines* **5**, 105–129.
3. Handerson, B. W. and T. J. Dougherty (1992) How does photodynamic work? *Photochem. Photobiol.* **55**, 145–157.
4. Kessel, D. and T. J. Dougherty (1999) Agents used in photodynamic therapy. *Rev. Contemp. Pharmacother.* **10**, 19–24.
5. Pandey, R. K., D. A. Bellnier, K. M. Smith and T. J. Dougherty (1991) Chlorin and porphyrin derivatives as potential photosensitizers in photodynamic therapy. *Photochem. Photobiol.* **53**, 65–72.
6. Vakrat, Y., L. Weiner, A. Brandis, O. Mazor, R. Hami, S. Gross, S. Schreiber, Y. Salomon and A. Scherz (1999) Bacteriochlorophyll

derivatives: phototoxicity, hydrophobicity & oxygen radicals production. *Free Radic. Biol. Med.* **27**, s129.
7. Noy, D., L. Fiedor, G. Hartwich, H. Scheer and A. Scherz (1998) Metal-substituted bacteriochlorophylls. 2. Changes in redox potentials and electronic transition energies are dominated by intramolecular electrostatic interactions. *J. Am. Chem. Soc.* **120**, 3684–3693.
8. Scherz, A., Y. Salomon, A. Brandis and H. Scheer (2003) Palladium-substituted bacteriochlorophyll derivatives and use thereof. US Pat 6,569,846.
9. Scherz, A., L. Feodor and Y. Salomon (1997) Chlorophyll and bacteriochlorophyll derivatives, their preparation and pharmacological compositions comprising them. US patent 5,650,292.
10. Rosenbach-Belkin, V., L. Chen, L. Fiedor, I. Tregub, F. Pavlotsky, V. Brumfeld, Y. Salomon and A. Scherz (1996) Serine conjugates of chlorophyll and bacteriochlorophyll: phototoxicity in vitro and tissue distribution in mice bearing melanoma. *Photochem. Photobiol.* **64**, 174–181.
11. Gross, S., A. Gilead, A. Scherz, M. Neeman and Y. Salomon (2003) Monitoring photodynamic therapy of solid tumors online by BOLD-contrast MRI. *Nat. Med.* **9**, 1327–1331.
12. Schreiber, S., S. Gross, A. Brandis, A. Harmelin, V. Rosenbach-Belkin, A. Scherz and Y. Salomon (2002) Local photodynamic therapy (PDT) of rat C6 glioma xenografts with Pd-bacteriopheophorbide leads to decreased metastases and increase of animal cure compared with surgery. *Int. J. Cancer* **99**, 279–285.
13. Koudinova, N. V., J. H. Pinthus, A. Brandis, O. Brenner, P. Bendel, J. Ramon, Z. Eshhar, A. Scherz and Y. Salomon (2003) Photodynamic therapy with Pd-bacteriopheophorbide (TOOKAD): successful in vivo treatment of human prostatic small cell carcinoma xenografts. *Int. J. Cancer* **104**, 782–789.
14. Plaks, V., N. Koudinova, U. Nevo, J. H. Pinthus, H. Kanety, Z. Eshhar, J. Ramon, A. Scherz, M. Neeman and Y. Salomon (2004) Photodynamic therapy of established prostatic adenocarcinoma with TOOKAD: a biphasic apparent diffusion coefficient change as potential early MRI response marker. *Neoplasia* **6**, 224–233.
15. Preise, D., O. Mazor, N. Koudinova, M. Liscovitch, A. Scherz and Y. Salomon (2003) Bypass of tumor drug resistance by antivascular therapy. *Neoplasia* **5**, 1–6.
16. Chen, Q., Z. Huang, D. Luck, J. Beckers, P. H. Brun, B. C. Wilson, A. Scherz, Y. Salomon and F. W. Hetzel (2002) Preclinical studies in normal canine prostate of a novel palladium-bacteriopheophorbide (WST09) photosensitizer for photodynamic therapy of prostate cancers. *Photochem. Photobiol.* **76**, 438–445.
17. Kelleher, D. K., O. Thews, A. Scherz, Y. Salomon and P. Vaupel (2004) Perfusion, oxygenation status and growth of experimental tumors upon photodynamic therapy with Pd-bacteriopheophorbide. *Int. J. Oncol.* **24**, 1505–1511.
18. Kelleher, D. K., O. Thews, A. Scherz, Y. Salomon and P. Vaupel (2003) Combined hyperthermia and chlorophyll-based photodynamic therapy: tumour growth and metabolic microenvironment. *Br. J. Cancer* **89**, 2333–2339.
19. Mazor, O. (2004) Synthesis and Phototoxicity of Novel Sulfonated Bacteriochlorophyll Derivatives. Ph.D. thesis, Weizmann Institute of Science, Rehovot, Israel.
20. Gertner, M. R., A. Bogaards, R. A. Weersink, S. A. McCluskey, M. A. Haider, C. K. K. Yue, J. Savard, S. Simpson, P. H. Brun, P. Cohen, A. Scherz, Y. Salomon, A. G. Aprikian, M. M. Elhilali, B. C. Wilson and J. Trachtenberg (2003) Initial results of a 23 phase I/II trial of WST09-mediated photodynamic therapy (WST09-PDT) for recurrent prostate cancer following failed external beam radiation therapy (EBRT). In Society of Urologic Oncology, 4th Annual Meeting, Bethesda, Maryland.
21. ten Tije, A. J., J. Verweij, W. J. Loos and A. Sparreboom (2003) Pharmacological effects of formulation vehicles: implications for cancer chemotherapy. *Clin. Pharmacokinet.* **42**, 665–685.
22. Scherz, A., A. Brandis, O. Mazor, Y. Salomon and H. Scheer (2002) Preparation of water soluble anionic bacteriochlorophyll derivatives for use as cancer photodynamic therapy and diagnostic agents. PCT Int. Appl. (2004), 56 pp. WO 2004045492 A2 20040603.
23. Brandis, A., O. Mazor, Y. Salomon and A. Scherz (2003) Analyses of the sensitizer's affinity to serum proteins. 9th Int. Photodyn. Assoc., Book of Abstracts, P-019, p. 43, Miyazaki, Japan, May 20–23.
24. Krammer, B. (2001) Vascular effects of photodynamic therapy. *Anticancer Res.* **21**, 4271–4277.
25. Schnitzer, J. E., P. Oh and D. P. McIntosh (1996) Role of GTP hydrolysis in fission of caveolae directly from plasma membranes. *Science* **274**, 239–242.
26. Tiruppathi, C., W. Song, M. Bergenfeldt, P. Sass and A. B. Malik (1997) Gp60 activation mediates albumin transcytosis in endothelial cells by tyrosine kinase-dependent pathway. *J. Biol. Chem.* **272**, 25968–25975.
27. Bradford, M. M. (1976) A rapid and sensitive method for the quantitation of microgram quantities of protein utilizing the principle of protein-dye binding. *Anal. Biochem.* **7**, 248–254.
28. Zhang, S. Z., M. M. Lipsky, B. F. Trump and I. C. Hsu (1990) Neutral red (NR) assay for cell viability and xenobiotic-induced cytotoxicity in primary cultures of human and rat hepatocytes. *Cell Biol. Toxicol.* **6**, 219–234.
29. Mukherjee, S., R. N. Ghosh and F. R. Maxfield (1997) Endocytosis. *Physiol. Rev.* **77**, 759–803.
30. Cohen, S. and R. Margalit (1990) Binding of porphyrin to human serum albumin. Structure-activity relationships. *Biochem. J.* **270**, 325–330.
31. Sheyhedin, I., K. Aizawa, M. Araake, H. Kumasaka, T. Okunaka and H. Kato (1998) The effect of serum on cellular uptake and phototoxicity of mono-L-aspartyl chlorin e_6 (NPe6) in vitro. *Photochem. Photobiol.* **68**, 110–114.
32. Bohmer, R. M. and G. Morstyn (1985) Uptake of hematoporphyrin derivative by normal and malignant cells: effect of serum, pH, temperature, and cell size. *Cancer Res.* **45**, 5328–5334.
33. Hansen, S. H., K. Sandvig and B. van Deurs (1993) Clathrin and HA2 adaptors: effects of potassium depletion, hypertonic medium, and cytosol acidification. *J. Cell Biol.* **121**, 61–72.
34. Oka, J. A., M. D. Christensen and P. H. Weigel (1989) Hyperosmolarity inhibits galactosyl receptor-mediated but not fluid phase endocytosis in isolated rat hepatocytes. *J. Biol. Chem.* **264**, 12016–12024.
35. Synnes, M., K. Prydz, T. Lovdal, A. Brech and T. Berg (1999) Fluid phase endocytosis and galactosyl receptor-mediated endocytosis employ different early endosomes. *Biochim. Biophys. Acta* **1421**, 317–328.
36. Niles, W. D. and A. B. Malik (1999) Endocytosis and exocytosis events regulate vesicle traffic in endothelial cells. *J. Membr. Biol.* **167**, 85–101.
37. Ball, D. J., S. Mayhew, S. R. Wood, J. Griffiths, D. I. Vernon and S. B. Brown (1999) A comparative study of the cellular uptake and photodynamic efficacy of three novel zinc phthalocyanines of differing charge. *Photochem. Photobiol.* **69**, 390–396.
38. Berg, K. and J. Moan (1997) Lysosomes and microtubules as targets for photochemotherapy of cancer. *Photochem. Photobiol.* **65**, 403–409.
39. Siboni, G., H. Weitman, D. Freeman, Y. Mazur, Z. Malik and B. Ehrenberg (2002) The correlation between hydrophilicity of hypericins and helianthrone: internalization mechanisms, subcellular distribution and photodynamic action in colon carcinoma cells. *Photochem. Photobiol. Sci.* **1**, 483–491.
40. Zilberstein, J., S. Schreiber, M. C. Bloemers, P. Bendel, M. Neeman, E. Schechtman, F. Kohen, A. Scherz and Y. Salomon (2001) Antivascular treatment of solid melanoma tumors with bacteriochlorophyll-serine-based photodynamic therapy. *Photochem. Photobiol.* **73**, 257–266.
41. Shargel, A. and A. B. C. Yu (1999) *Applied Biopharmaceutics and Pharmacokinetics*. Appleton & Lange, McGraw-Hill.
42. Huxtable, R. J. (1992) Physiological actions of taurine. *Physiol. Rev.* **72**, 101–163.
43. John, T. A., S. M. Vogel, R. D. Minshall, K. Ridge, C. Tiruppathi and A. B. Malik (2001) Evidence for the role of alveolar epithelial gp60 in active transalveolar albumin transport in the rat lung. *J. Physiol.* **533**, 547–559.
44. Thorpe, P. E. (2004) Vascular targeting agents as cancer therapeutics. *Clin. Cancer Res.* **10**, 415–427.
45. McCurdy, T. R., S. Gataiance, L. J. Eltringham-Smith and W. P. Sheffield (2004) A covalently linked recombinant albumin dimer is more rapidly cleared in vivo than are wild-type and mutant C34A albumin. *J. Lab. Clin. Med.* **143**, 115–124.
46. Takakura, Y., R. I. Mahato and M. Hashida (1998) Extravasation of macromolecules. *Adv. Drug Delivery Rev.* **34**, 93–108.
47. Wosilait, W. D., M. P. Ryan and K. H. Byington (1981) Competition between serum albumin and soluble fraction of liver for binding of warfarin and other drugs. *Res. Commun. Chem. Pathol. Pharmacol.* **32**, 113–121.
48. Behar-Cohen, F. F., M. Berdugo, R. A. Bejjani, F. Valamanesh, M. Savoldelli, L. Jonet, A. Scherz and Y. Salomon (2003) Toxicological evaluation of a new water-soluble photo-sensitizer for PDT, in the rabbit eye. *Investig. Ophthalmol. Vis. Sci.* **44**, E4947.

Exhibit B

Photochemistry and Photobiology, 2005, 81: 983–993

Novel Water-soluble Bacteriochlorophyll Derivatives for Vascular-targeted Photodynamic Therapy: Synthesis, Solubility, Phototoxicity and the Effect of Serum Proteins¶

Alexander Brandis[1], Ohad Mazor[1,2], Eran Neumark[2], Varda Rosenbach-Belkin[1], Yoram Salomon[2] and Avigdor Scherz*[1]

[1]Department of Plant Sciences, The Weizmann Institute of Science, Rehovot, Israel
[2]Department of Biological Regulation, The Weizmann Institute of Science, Rehovot, Israel

Received 1 December 2004; accepted 18 April 2005

ABSTRACT

New negatively charged water-soluble bacteriochlorophyll (Bchl) derivatives were developed in our laboratory for vascular-targeted photodynamic therapy (VTP). Here we focused on the synthesis, characterization and interaction of the new candidates with serum proteins and particularly on the effect of serum albumin on the photocytotoxicity of WST11, a representative compound of the new derivatives. Using several approaches, we found that aminolysis of the isocyclic ring with negatively charged residues markedly increases the hydrophilicity of the Bchl sensitizers, decreases their self-association constant and selectively increases their affinity to serum albumin, compared with other serum proteins. The photocytotoxicity of the new candidates in endothelial cell culture largely depends on the concentration of the serum albumin. Importantly, after incubation with physiological concentrations of serum albumin (500–600 μM), WST11 was found to be poorly photocytotoxic (>80% endothelial cell survival in cell cultures). However, in a recent publication (Mazor, O. *et al.* [2005] *Photochem. Photobiol.* 81, 342–351) we showed that VTP of M2R melanoma xenografts with a similar WST11 concentration resulted in ~100% tumor flattening and >70% cure rate. We therefore propose that the two studies collectively suggest that the antitumor activity of WST11 and probably of other similar candidates does not depend on direct photointoxication of individual endothelial cells but on the vascular tissue response to the VTP insult.

INTRODUCTION

The role of vascular shutdown in the induction of tumor necrosis is now well established and it has provided the motivation for several new avenues of cancer treatment (1–3). Novel methods of antivascular therapy are rapidly being developed for the treatment of solid tumors and nonmalignant diseases associated with abnormal vascularization. The methodology of antivascular therapy is based either on destroying existing blood vessels, preventing the formation of *de novo* neovascularization or inhibiting blood flow (4). All these interventions result in oxygen and nutrient deprivation in the treated tissues, which is expected to cause complete starvation and total necrosis of the malignant cells. Similar treatment modalities are currently aimed at age-related macular degeneration (AMD) (5) and look promising for the treatment of obesity (6).

The antivascular effect of photodynamic therapy (PDT) with some reagents has been recognized for quite some time and has been utilized in several clinical protocols (7). PDT is a relatively new treatment modality whereby nontoxic drugs (sensitizers) and nonhazardous light (VIS/NIR) combine to generate cytotoxic reactive oxygen species (ROS) at a selected treatment site. Numerous experiments have indicated that tumor regression and cure after most PDT treatment protocols involve the occlusion and/or perforation of blood vessels (8–12), in addition to the direct killing of tumor cells. This effect is more pronounced in treatment protocols that involve short light/drug intervals and/or more hydrophilic sensitizers (13). Differences between the response of the tumor and the normal tissue vasculature may provide the key in selecting the best treatment (14–22).

In looking for a more effective and selective vascular-targeted PDT (VTP), we have synthesized new bacteriochlorophyll (Bchl) derivatives (23). These new derivatives present minimal extravasation from the circulation (24,25) and therefore should confine ROS generation to the vascular compartment of the illuminated tissue. Chen *et al.* (26) recently reviewed several of these compounds. Their illumination at the highest concentration in the blood (shortly after bolus administration or after approaching a steady-state concentration following perfusion [27]) resulted in a very rapid occlusion of tumor blood vessels and a markedly slower occlusion of normal blood vessels (19,28). Pd-bacteriopheophorbide (Pd-Bpheid, Tookad®) is the first of these drugs to enter clinical trials (Phase II) for treating local recurrent prostate cancer after failed radiation. However, vascular destruction with Tookad®, as with several other PDT reagents, was shown to involve hemorrhagic necrosis (29), which may induce nondesirable effects when applied to certain tumor sites such as the brain and lungs. Moreover, hemorrhagic necrosis may induce local inflammation and the subsequent proliferation of neovessels, which may retard the

¶Posted on the website on 19 April 2005

*To whom correspondence should be addressed: Prof. Avigdor Scherz, Dept. of Plant Sciences, Weizmann Institute of Science, Rehovot 76100 Israel. Fax: 972-8-9344181; e-mail: avigdor.scherz@weizmann.ac.il

Abbreviations: Bchl, bacteriochlorophyll; FCS, fetal calf serum; Pd-Bpheid, palladium-bacteriopheophorbide; PDT, photodynamic therapy; ROS, reactive oxygen species.

therapeutic effect (4). Thus, VTP, which causes vascular shutdown while minimizing the direct destruction of endothelial cells and the subsequent infarction of the blood vessels, is desirable under some circumstances.

To explore this possibility and its practical implications, we decided to synthesize a number of hydrophilic Bchl derivatives that cause minimal photodamage to endothelial cells under physiologically relevant conditions *in vitro* but still maintain high VTP efficacy *in vivo*. The synthesis of hydrophilic Bchl derivatives was performed via aminolysis of the Bchl isocyclic ring. This reaction was shown to be simple and regioselective when used for the synthesis of chlorophyll (Chl) amide derivatives at the C-13[1] position (30–37). The obtained compounds appeared to be highly water-soluble as well as potent antivascular sensitizers. Here we describe the synthesis, solubility and affinity of serum proteins and the spectral properties of the new compounds in aqueous solutions as well as their photocytotoxicity against endothelial cell lines with different concentrations of serum proteins. In a previous manuscript (38), we reported on the biological activity of WST11, a representative of this new group of photosensitizers, selected for clinical trials (24,38). The previous report describes the cellular trafficking, biodistribution, pharmacokinetics and PDT of M2R melanoma xenografts. Remarkably, Mazor *et al.* (38) showed that the representative water-soluble Bchl-based sensitizer (WST11), which was found to be practically nonphototoxic against individual cells in cultures in physiological serum albumin concentrations, is highly active as a VTP reagent. In a view of these observations, we think that WST11 and other similar compounds of that family, which are relatively nonphototoxic to the endothelial cells but possess potent antitumor activity, are good candidates for VTP, particularly when hemorrhagic necrosis is undesirable.

MATERIALS AND METHODS

Materials. 3-Amino-1-propane sulfonic acid (homotaurine, Aldrich, Milwaukee, WI), 2-aminoethane sulfonic acid (Taurine, Sigma, St. Louis, MO), *N*-hydroxysulfosuccinimide (sulfo-NHS, Pierce, Rockford, IL), 1-(3-dimethylaminopropyl)-3-ethylcarbodiimide (EDC, Fluka, Buchs SG, Switzerland).

Methods. Thin-layer chromatography (TLC) was performed on silica plates (Kieselgel-60, Merck, Darmstadt, Germany). System A: chloroform-methanol (80:20, v/v); system B: chloroform-methanol-water (65:30:0.4, v/v).

Column adsorption chromatography was performed with silica (70/200 mesh, Kieselgel-60, Merck).

^{1}H Nuclear magnetic resonance (NMR) spectra were recorded on Avance DPX 250 and 400 instruments (Bruker, Rheinstetten, Germany) and reported in parts per million (δ) downfield from tetramethylsilane with residual solvent peaks as the internal standards.

Optical absorption spectra were routinely recorded with Genesis-2 (Milton Roy, Berkshire, England). More accurate measurements, *e.g.* for performing factor analysis as described below, were performed with a Cary-5E instrument (Varian, Palo Alto, CA) by using 0.1, 2 and 10 mm path length quartz cells.

Circular dichroism spectra were recorded by an Aviv-202 CD spectrometer (Aviv Instruments, Inc., Lakewood, NJ) by using rectangular quartz cells with a 5 and 10 mm path length.

For determining the extinction coefficients of the Pd-, Cu-, Zn- and Mn-containing derivatives, the metal concentration determined by the previously described ICP-AES methodology (SpectroFlame, Spectro, Kleve, Germany) was correlated with the optical density of the examined solution at the particular wavelength (39), assuming one metal ion per macrocycle.

The hydrophobicity values of the compounds were expressed in terms of their partition coefficient (P) between *n*-octanol:water and determined as recently described (40).

Electrospray ionization mass spectra (ESI-MS) were recorded on a platform LCZ spectrometer (Micromass, Manchester, England).

High-performance liquid chromatography (HPLC) was carried out using a LC-900 instrument (JASCO, Tokyo, Japan) equipped with a MD-915 diode-array detector. Column: ODS-A 250 × 20 S10P-μm column (YMC, Kyoto, Japan).

The partition of photosensitizers among serum proteins was estimated by the following steps.

(1) Preparation of photosensitizer-serum protein complexes. Two hundred microliters of Tookad® (a micellar solution of **3** in aqueous medium at 2.5 mg/mL stabilized with Cremophor EL®, provided by Negma-Lerads, Magny-Les-Hameaux, France; batch no. 56D05002, lot no. 02120) and 180 μL of aqueous solution of **10** (4 m*M*) were incubated with fetal calf serum (FCS, 0.6 mL; Kibbutz Beit Haemek, Israel) at 37°C in the dark for 10 min. The mixtures were loaded onto PD-10 columns containing Sephadex G-25 M (Pharmacia, Biotech, Piscataway, NJ) and eluted by using phosphate-buffered saline (PBS) (pH 7.4, containing 4.7 m*M* ethylenediaminetetraacetic acid [EDTA]) or TBE (89 m*M* Tris-borate, pH 8.3, 2 m*M* EDTA) buffer, both stabilized with 0.2% sodium azide. The fast-running colored zone containing sensitizer-protein complexes was collected for further analysis. The sensitizer's recovery was estimated spectrophotometrically (Genesis-2, Milton Roy) in 93% methanol/TBE buffer (for **3**) and 50% methanol/TBE buffer (for **10**).

(2) Size-exclusion chromatography. Size-exclusion chromatography was performed by using a Superose 6 HR 10/30 (Pharmacia, Biotech) column, connected to a HPLC system. Elution was performed with PBS or a TBE buffer at a flow rate of 0.4 mL/min (41,42). After primary equilibration of the column (two column volumes with the buffer), the sample (250 μL) was injected. Fetal high-density lipoprotein (HDL), obtained from serum ultracentrifugation (43) and bovine serum albumin (BSA) (Sigma, catalogue no. A 2153) was used for calibration (see Fig. 6a). The elution profile was monitored by using a diode-array detector at a 220–900 nm spectral range.

Determining the sensitizer-BSA association was carried out by the interaction of BSA with increasing amounts of **10**. Concentrations in PBS (0.5 mL) after mixing: BSA, 10 μ*M*; compound **10**, 2, 5, 10, 20 and 50 μ*M*. The mixtures were briefly vortexed, incubated for 5 min at 37°C and 0.5 h at room temperature, loaded onto PD-10 (Sephadex G-25) columns and prewashed with 25-mL portions of TBE buffer. The associates were eluted with 6-mL portions of TBE buffer. The obtained eluates were frozen and lyophilized overnight. The dry residues were extracted with methanol (2 mL for each sample). The extracts were centrifuged in 2-mL microtubes to remove insoluble material and the amounts of sensitizer were determined spectophotometrically.

Factor analyses were performed following Noy *et al.* (44). Samples containing different concentrations of tested sensitizers (1 μ*M*–3 m*M*) or BSA (0–1 m*M*) were prepared.

Synthesis. Bacteriochlorophyll a (Bchl a) (1) was extracted and purified from lyophilized cells of *Rhodovolum sulfidophilum* as previously described (23).

Bacteriopheophorbide a (Bpheid, **2**) and *palladium bacteriopheophorbide a* (Pd-Bpheid, **3**, Tookad®) were prepared as described (45 and 23, respectively).

Palladium bacteriochlorin 13^1-(3-sulfopropyl)amide dipotassium salt (5). Homotaurine (30 mg) dissolved in 1 mL of 1 *M* K_2HPO_4 (pH adjusted with HCl to 8.2) was added to a solution of Pd-Bpheid (**3**) (20 mg) in dimethyl sulfoxide (DMSO) (3 mL) while stirring and argon was bubbled into the solution. Then, the reaction mixture was completely dried after a 40 min evaporation at 1–2 millibar and 35°C (Rotavapor R-134, Büche, Switzerland). The solids were redissolved in 7 mL of MeOH, and the colored solution was filtered through cotton wool to remove buffer salts and excess taurine. Next, the methanol was evaporated and the product **5**, redissolved in water, was purified by HPLC, applying 5% methanol in 5 m*M* phosphate buffer at pH 8.0 as solvent A and methanol as solvent B using gradient elution: B, 45% (0 min), 70% (14 min), 100% (16–18 min), 45% (24 min), with a flow rate of 12 mL/min from 0 to 14 min and thereafter at 6 mL/min. The product **5** was eluted and collected in ~9–11 min. The main impurities, collected after 4–7 min (*ca* 3–5%), corresponded to Schiff base by-product(s). The peaks at 22–25 min (*ca* 1–2%) possibly corresponded to the isoform of the main product **5** and the untreated Pd-Bpheid residues. The purified product **5** was dried under reduced pressure, then redissolved in methanol (3 mL) and filtered from insoluble material. Finally, the solvent was evaporated again and the solid compound **5** was stored under argon atmosphere in the dark at –20°C. Yield: 23 mg (87%). ESI-MS (–): 889 (M^--K-H), 873 (M^--2K-H+Na), 851 (M^--2K), 819 (M^--2K-H-OMe) *m/z*. ^{1}H NMR in methanol-d_4, δ: 9.36 (5-H, s), 8.74 (10-H, s),

8.54 (20-H, s), 5.30 and 4.93 (15^1-CH_2, dd), 4.2–4.4 (7,8,17,18-H, m), 3.85 (15^3-Me, s), 3.50 (2^1-Me, s), 3.16 (12^1-Me, s), 3.05 (3^2-Me, s), 1.90–2.40, 1.56–1.74 (17^1, 17^2-CH_2, m), 2.14 (8^1-CH_2, m), 1.90 (7^1-Me, d), 1.59 (18^1-Me, d), 1.08 (8^2-Me, t), 3.57, 3.03 and 2.77 (CH_2s of homotaurine). UV-VIS in methanol ($\varepsilon \times 10^5$ $M^{-1}cm^{-1}$): 747 (1.21), 516 (0.16), 384 (0.50), 330 (0.61) nm.

Palladium bacteriopheophorbide a 17^3-(3-sulfo-1-oxy-succinimide)ester sodium salt (6). Fifty milligrams of Pd-Bpheid (**3**), 80 mg of *N*-hydroxysulfosuccinimide (sulfo-NHS) and 65 mg of 1-(3-dimethylamino-propyl)-3-ethylcarbodiimide (EDC) were mixed in 7 mL of dry DMSO overnight at room temperature under argon atmosphere. Next, the solvent was evaporated under reduced pressure. The dry residue was redissolved in chloroform (50 mL), filtered from the insoluble material and evaporated. The conversion was ~95% (TLC). The product **6** did not undergo further chromatographic purification. ESI-MS (–): 890 (M^--Na) *m/z*. ^{1}NMR in chloroform-*d*, δ: 9.19 (5-H, s), 8.49 (10-H, s), 8.46 (20-H, s), 5.82 (13^2-H, s), 4.04–4.38 (7,8,17,18-H, m), 3.85 (13^4-Me, s), 3.47 (2^1-Me, s), 3.37 (12^1-Me, s), 3.09 (3^2-Me, s), 1.77 (7^1-Me, d), 1.70 (18^1-Me, d), 1.10 (8^2-Me, t), 4.05 (CH_2 of sNHS), 3.45 (CH of sNHS).

Palladium bacteriopheophorbide a 17^3-(3-sulfopropyl) amide potassium salt (7). Activated ester **6** (10 mg) in DMSO (1 mL) was mixed with homotaurine (20 mg) in 0.1 *M* K-phosphate buffer, pH 8.0 (1 mL) overnight. Next, the reaction mixture was evaporated. Finally the residue was redissolved in chloroform-methanol (19:1) and the product **7** was purified by chromatography on silica using chloroform-methanol (4:1, v/v) as an eluent. Yield: 8 mg (83%). ESI-MS (–): 834 (M-K) *m/z*. ^{1}NMR in chloroform-*d*/methanol-d_4 (4:1, vol.), δ: 9.16 (5-H, s), 8.71 (10-H, s), 8.60 (20-H, s), 6.05 (13^2-H, s), 4.51, 4.39, 4.11, 3.98 (7,8,17,18-H, all m), 3.92 (13^4-Me, s), 3.48 (2^1-Me, s), 3.36 (12^1-Me, s), 3.09 (3^2-Me, s), 2.02-2.42 (17^1 and 17^2-CH_2, m), 2.15 (8^1-CH_2, q), 1.81 (7^1-Me, d), 1.72 (18^1-Me, d), 1.05 (8^2-Me, t), 3.04, 2.68 and 2.32 (CH_2 of homotaurine, m).

Palladium bacteriochlorin 13^1,17^3-di(3-sulfopropyl)amide dipotassium salt (8). Ten milligrams of compound **6** or **7** were dissolved in 3 mL of DMSO, mixed with 100 mg of homotaurine in 1 mL of 0.5 *M* K-phosphate buffer, pH 8.2, and incubated overnight at room temperature. The solvent was then evacuated under reduced pressure and the product **8** was purified on HPLC as described above for **5**. Yield: 9 mg (81%). ESI-MS (–):1011 (M^--K), 994 (M^--2K+Na), 972 (M^--2K), 775 (M^--2K-CO_2Me-homotaurine $NHCH_2CH_2CH_2SO_3$), 486 ([M-2K]/2) *m/z*. ^{1}NMR in methanol-d_4, δ: 9.35 (5-H, s), 8.75 (10-H, s), 8.60 (20-H, s), 5.28 and 4.98 (15^1-CH_2, dd), 4.38, 4.32, 4.22, 4.15 (7,8,17,18-H, all m), 3.85 (15^3-Me, s), 3.51 (2^1-Me, s), 3.18 (12^1-Me, s), 3.10 (3^2-Me, s 2.12-2.41 (17^1-CH_2, m), 2.15–2.34 (8^1-CH_2, m), 1.76–2.02 (17^2-CH_2, m), 1.89 (7^1-Me, d), 1.61 (18^1-Me, d), 1.07 (8^2-Me, t), 3.82, 3.70, 3.20, 3.10, 2.78, 2.32, 1.90 (CH_2 of homotaurine at C-13^1 and C-17^3). UV-VIS in methanol ($\varepsilon \times 10^5$ M^{-1} cm^{-1}): 747 (1.26), 516 (0.17), 384 (0.51), 330 (0.63) nm.

Palladium 3^1-(3-sulfopropylimino)bacteriochlorin 13^1,17^3-di(3-sulfopropyl)amide tripotassium salt (9). Compound **9** was separated as a minor by-product (*ca.* 3%) during synthesis of **8** and separated by HPLC. HPLC was used in a second cycle of purification of **5**, but with 10–15% gradient of B in a 0–14 min interval. ESI-MS (–): 1171 (M^--K+H), 1153 (M^--2K-H+Na), 1131 (M^--2K), 566 ([M^--K]/2), 364 ([M^--3K]/3) *m/z*. ^{1}NMR in methanol-d_4, δ: 8.71 (1H), 8.63 (1.5H), 8.23 (0.5H) (5-, 10- and 20-H, all-m), 5.30 and 4.88 (15^1-CH_2, dd), 4.43 and 4.25 (7,8,17,18-H, m), 3.85 (15^3-Me, s), 3.31 (2^1-Me, s), 3.22 (12^1-Me, s), 3.17 (3^2-Me, m), 1.89–2.44 (17^1 and 17^2-CH_2, m), 2.25 (8^1-CH_2, m), 1.91 (7^1-Me, s), 1.64 (18^1-Me, s), 1.08 (8^2-Me, t), 4.12, 3.56, 3.22, 3.16, 2.80 and 2.68 (CH_2 of homotaurine). UV-VIS in methanol ($\varepsilon \times 10^4$ M^{-1} cm^{-1}): 729 (9.00), 502 (0.90), 380 (5.44), 328 (5.13).

Palladium bacteriochlorin 13^1-(2-sulfoethyl)amide dipotassium salt (10, WST11). Taurine (1.3 g) dissolved in 40 mL of 1 *M* K_2HPO_4 (pH adjusted to 8.2 with HCl) was added to Pd-Bpheid **3** (935 mg) in DMSO (120 mL) while stirring under bubbled argon. Purification was carried out as described for **5**. Yield: 1.07 g (89%). ESI-MS (–): 875 (M^--K-H), 859 (M^--2K-H+Na), 837 (M^--2K), 805 (M^--2K-H-OMe), 719 *m/z*. ^{1}H NMR in methanol-d_4, δ: 9.38 (5-H, s), 8.78 (10-H, s), 8.59 (20-H, s), 5.31 and 4.95 (15^1-CH_2, dd), 4.2-4.4 (7,8,17,18-H, m), 3.88 (15^3-Me, s), 3.52 (2^1-Me, s), 3.19 (12^1-Me, s), 3.09 (3^2-Me, s), 1.92-2.41, 1.60-1.75 (17^1, 17^2-CH_2, m), 2.19 (8^1-CH_2, m), 1.93 (7^1-Me, d), 1.61 (18^1-Me, d), 1.09 (8^2-Me, t), 3.62, 3.05 (CH_2 of taurine). UV-VIS in methanol ($\varepsilon \times 10^5$ M^{-1} cm^{-1}): 747 (1.20), 516 (0.16), 384 (0.49), 330 (0.60) nm.

Bacteriochlorin 13^1-(2-sulfoethyl)amide dipotassium salt (11). Taurine (160 mg) dissolved in 5 mL of 1 *M* K_2HPO_4 (pH adjusted to 8.2 as above) was added to Bpheid **2** (120 mg) dissolved in 15 mL of DMSO. The reaction and purification continued as described for **5**. Yield: 138 mg (87%). ESI-MS (–): 734 (M^--2K) *m/z*. NMR in methanol-d_4, δ: 9.31 (5-H, s), 8.88 (10-H, s), 8.69 (20-H, s), 5.45 and 5.25 (15^1-CH_2, dd), 4.35 (7,18-H, m), 4.06 (8,17-H, m), 4.20 and 3.61 (2-CH_2, m of taurine), 3.83 (15^3-Me, s), 3.63 (2^1-Me, s), 3.52 (3-CH_2, m of taurine), 3.33 (12^1-Me, s), 3.23 (3^2-Me, s), 2.47 and 2.16 (17^1-CH_2, m), 2.32 and 2.16 (8^1-CH_2, m), 2.12 and 1.65 (17^2-CH_2, m), 1.91 (7^1-Me, d), 1.66 (18^1-Me, d), 1.07 (8^2-Me, t). UV-VIS in methanol ($\varepsilon \times 10^4$ M^{-1} cm^{-1}): 747 (6.30), 519 (1.89), 354 (7.43) nm.

Copper (II) bacteriochlorin 13^1-(2-sulfoethyl)amide dipotassium salt (12). Bacteriochlorin amide **11** (50 mg) and copper (II) acetate (35 mg) were dissolved in 40 mL of methanol and left under bubbled argon for 10 min. Then, palmitoyl ascorbate (500 mg) was added and the solution was stirred for 30 min. The progress of the reaction was monitored by the spectral shifts of the Q_x and Q_y transitions to 537 and 768 nm, respectively. Next, the reaction mixture was evaporated, redissolved in acetone and filtered to discard excess salt. The acetone was evaporated and the product **12** was purified by HPLC, as described for **5**, using a gradient elution: B, 42% (0 min), 55% (14 min), 100% (16–18 min), 42% (24 min), with a flow rate of 12 mL/min from 0 to 14 min, then 6 mL/min. The purified compound was dried under reduced pressure, redissolved in methanol and separated by filtration from insoluble material. Yield: 46 mg (85%). ESI-MS (–): 795 (M^--2K) *m/z*. UV-VIS in methanol ($\varepsilon \times 10^4$ M^{-1} cm^{-1}): 768 (7.60), 537 (1.67), 387 (5.40) and 342 (6.00) nm.

Zinc bacteriochlorin 13^1-(2-sulfoethyl)amide dipotassium salt (13). Zinc was incorporated into **11** as previously described (47, 48) with some modifications. Thus, a mixture of bacteriochlorin amide **11** (30 mg) and zinc acetate (100 mg) was heated in 5 mL of acetic acid under argon atmosphere at 110°C for about 1 h. The product that accumulated was monitored following the shift of the Q_x transition to 558 nm. Then the reaction mixture was cooled and evaporated. The final purification was carried out by HPLC as for compound **5**. The solvent was evaporated again and the solid compound was collected and stored under argon in the dark at –20°C. Yield: 24 mg (74%). ESI-MS (–): 834 (M^--K), 818 (M^--2K+Na), 796 (M^--2K+H) *m/z*. UV-VIS in methanol ($\varepsilon \times 10^4$ M^{-1} cm^{-1}): 762 (5.51), 558 (1.43), 390 (3.42) and 355 (4.63) nm.

Manganese (III) bacteriochlorin 13^1-(2-sulfoethyl)amide dipotassium salt (14). Manganese insertion into compound **11** was carried out via transmetalation as previously described (47–49) with some modifications. Thus, bacteriochlorin amide **11** (50 mg) in 10 mL of dimethylformamide (DMF) was heated with cadmium acetate (220 mg) under argon atmosphere at 110°C for about 15 min (Cd-complex formation was monitored in acetone by the shift of the Q_x transition from 519 to 585 nm). Then, the reaction mixture was cooled and evaporated. The dry residue was redissolved in 15 mL of acetone and stirred with manganese (II) chloride to form the Mn(III) product **14**. The product formed was monitored in acetone by the shift of the Q_x and Q_y transition from 585 to 600 nm and from 768 to 828 nm, respectively (49). The acetone was evaporated and the product was purified by HPLC using gradient elution by acetonitrile in water: 10% (0 min), 15% (14 min), 100% (16–18 min), 10% (24 min) at a flow rate of 8 mL/min. The purified pigment was then dried under reduced pressure, redissolved in methanol and separated from the insoluble material by filtration. Next, the solvent was evaporated again and the solid compound was stored under argon in the dark at –20°C. Yield: 42 mg (76%). ESI-MS (+): 832 (M^+-2K+2Na) *m/z*. UV-VIS in methanol ($\varepsilon \times 10^4$ M^{-1} cm^{-1}): 825 (4.61), 588 (1.47), 372 (3.75) and 327 (3.78) nm.

H5V mouse endothelial cells were cultured as monolayers in Dulbecco's modified Eagle's medium (DMEM)/F12 containing 25 m*M* 4-(2-hydroxyl)-1-piperazineethanesulfonic acid (HEPES), pH 7.4, 10% fetal bovine serum (FBS), glutamine (2 m*M*), penicillin (0.06 mg/mL) and streptomycin (0.1 mg/mL) (hereafter referred to as the "Culture Medium"). Cells were grown at 37°C in an 8% CO_2-humidified atmosphere.

The photocytotoxicity of the different sensitizers against H5V cells in cultures was determined after preincubation with increasing concentrations of the compounds in the dark for the times and conditions indicated for the individual experiments. Compounds **3** and **7** were primarily dissolved in DMSO (1% of the final volume); all other compounds were dissolved directly in the culture medium. Unbound sensitizer was removed by washing the cells once with culture medium and the plates were illuminated at room temperature from the bottom (650 nm $< \lambda <$ 800 nm, 12 J/cm^2). The light source used was a 100W Halogen lamp (Osram, Munich, Germany) equipped with a 4-cm water filter. The cultures were placed in the culture incubator and cell survival was determined 24 h after illumination by a Neutral Red viability assay that was validated against the 3-(4,5-

Table 1. Partition values of different Bchl derivatives described in this manuscript, between *n*-octanol and water

Compound	Octanol/water partition (P)	log P
3	96:4	1.38
5	40:60	−0.18
7	74:26	0.45
8	12:88	−0.86
9	23:77	−0.52
10	39:61	−0.19
11	59:41	0.16
12	40:60	−0.18
13	48:52	−0.03
14	5:95	−1.28

dimtheylthiazol-2-yl)-2,5-diphenyl tetrazolium bromide (MTT) viability assay as previously described (17,50). Three kinds of controls were used: (1) ligh: control, cells illuminated in the absence of sensitizers; (2) dark control, cells treated with sensitizer but kept in the dark; and (3) untreated cells that were kept in the dark.

RESULTS

Polarity and solubility

The low solubility and the subsequent aggregation of Bchl derivatives in aqueous solutions pose major problems in their application as VTP reagents. On increasing the polarity of the new derivatives, we expected to see a significant increase in their hydrophilicity and a marked reduction in the aggregation constants. The first parameter was quantified by means of their partitioning coefficient. Table 1 presents the partition coefficients (P) of the new sensitizers in *n*-octanol:water solutions. It appears that cleavage of the isocyclic ring has a profound effect on the molecule's polarity and solubility. Thus, all products of aminolysis presented relatively high polarity (Table 1) that was also reflected in their good solubility in polar organic solvents such as alcohols (methanol, ethanol), DMF and DMSO and their very poor solubility in less polar solvents such as chloroform, acetone and acetonitrile (data not shown). The high polarity of the open ring sensitizers allows for good solubility in water (or PBS) (up to 40 mg/mL with no precipitation after centrifugation at 17 000 *g*). The increased solubility of **5** or **10** compared with **7** is evidence of the greater significance of the isocyclic ring cleavage compared with the addition of charged peripheral groups for enhancing the polarity/solubility of the Bchl derivatives. Nevertheless, up to ~4 mg/mL of **7** could be introduced into aqueous solutions (*e.g.* PBS) with no precipitation of aggregates upon centrifugation. Because of its amphiphilic nature, **7** could also be introduced into solvents of low polarity like chloroform after dissolving in alcohol (methanol, ethanol) and mixing to make a final alcohol concentration of 3–5%. The addition of a second and even third sulfonic group (**8** and **9**) to the aminolysis products had some effect on P (somewhat enhanced water solubility), whereas metal replacement had a smaller effect as long as the metal redox state was not changed. However, the replacement of Pd(II) by Mn(III) strongly affected P (Table 1). In contrast, changing the length (and thereby the hydrophobicity) of the alkenyl linkage (**5** and **10**) had only a minor effect on P.

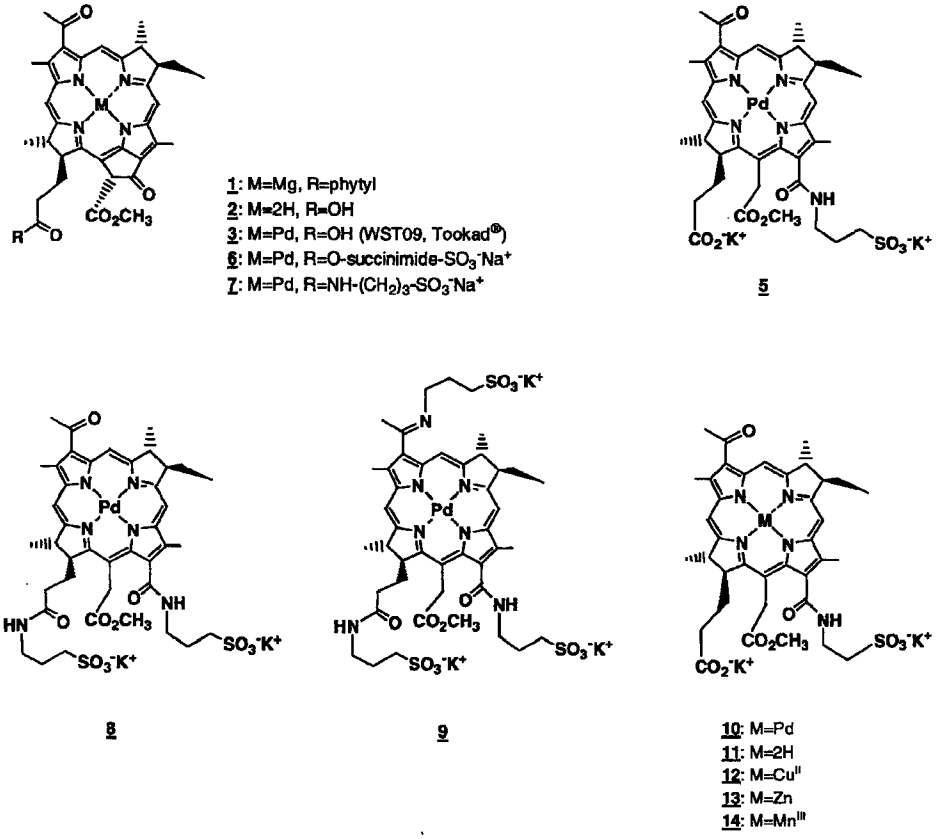

Scheme.

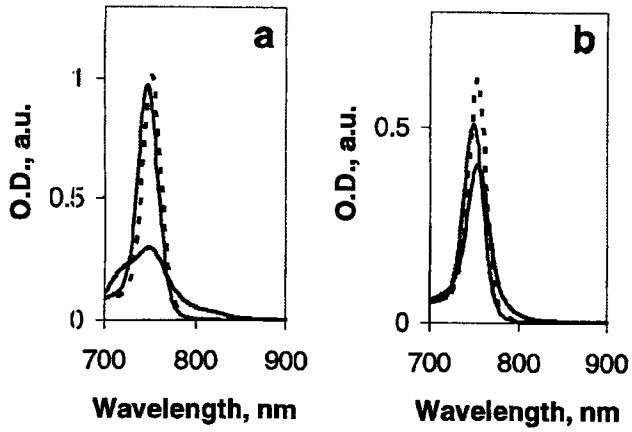

Figure 1. Absorption spectra of Bchl derivatives **10** (a) and **13** (b) (40 μ*M* solutions) in PBS (black), 1% TX-100/PBS (dashed) and methanol (gray). Spectra were recorded with a 2-mm quartz cuvette using a Cary-5E spectrophotometer.

Notably, despite their relatively high solubility, all open-ring products formed small aggregates (estimated to be two to eight molecules; see below and also F. Martinic, Negma-Lerads, private communication) in the aqueous solutions that underwent dissociation upon dilution, micelle incorporation or introduction of physiologic concentrations of serum albumin.

To quantify the aggregation tendency of the different compounds, we first explored the effect of concentration and detergents on their optical absorption and circular dichroism (CD) in serum-free aqueous solutions. Then, we investigated the effect of whole serum on the aggregated state. Next, we examined the affinity of representative compounds to specific serum proteins using size-exclusion chromatography. Finally, we quantified these interactions for BSA by monitoring the effect of BSA on the optical absorption and CD of the selected compound. By employing factor analysis to the resulting spectra, we derived the percentage of monomers, dimers and larger aggregates at a specific total concentration of the selected compound.

Aggregate formation in serum-free solutions

Figure 1 describes the optical absorption of aminolysis products **8**, **10**–**14** at 40 μ*M* in PBS (black lines) and in methanol (gray lines). The Q_y bands of compounds **8**, **10** and **12** were markedly broadened and attenuated in PBS compared with methanol (Fig. 1a illustrates the absorption spectra of **10**), those of **11** and **13** were less attenuated and slightly broadened (Fig. 1b illustrates the absorption spectra of **13**), whereas the Q_y line shape of **14** hardly changed. Remarkably, the decrease in the extinction coefficients of **8**, **10** and **12** in PBS was accompanied by an overall decrease of the Q_y integrated optical absorption (700–900 nm), suggesting both shading and intensity borrowing by higher electronic transitions because of strong excitonic coupling in the aggregated states, as previously found for Bchl *a* and Chl *a* (51–53).

The effect of concentration. The effect of concentration on the optical absorption and CD spectra of the aminolysis products in PBS is illustrated for **10** in Fig. 2a,b, respectively. The presented spectra were recorded using quartz cuvettes with different path lengths (l) and then multiplied by ($l_x/l_{40} \cdot 40/X$), where X stands for the recorded concentration. Notably, on increasing the concentration, the monomeric Q_y transition at ~750 nm split into new

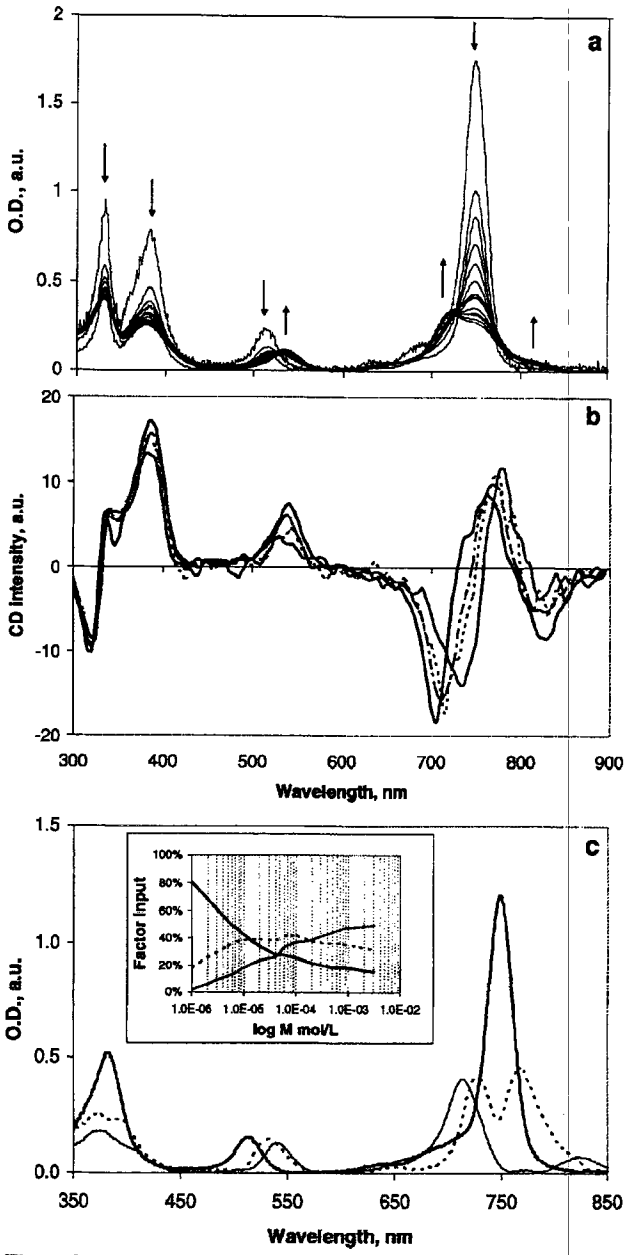

Figure 2. The effect of concentration on the spectra of compound **10**. a: The optical absorption of **10** at 0.1 μ*M* to 3 m*M*. Spectra were recorded using different optical path-lengths (l) and then multiplied by ($l_x/l_{40} \cdot 40/X$), where X stands for the recorded concentration (μ*M*); arrows indicate changes upon increasing the concentration of **10**. b: The circular dichroism spectra of selected concentrations of **10** in PBS solution (the spectra normalized as described above): 10 μ*M* (gray line), 80 μ*M* (dotted line), 200 μ*M* (dashed–dotted line) and 3 m*M* (solid line). c: Principal components of the optical absorption resolved by factor analysis: Solid line, monomer; dashed line, dimer; gray line, larger aggregate (probably hexamer or octamer). Inset: The dependence of the principal components on the concentration of **10**.

electronic transitions at higher and lower energies, as expected upon the formation of excitonically coupled aggregates.

Using the previously described factor analysis technique (44), we found three spectroscopic components that accounted for the spectroscopic evolution throughout the entire concentration range (Fig. 2c). The first component (solid line) has a spectrum similar to that of **10** in methanol, with a slightly broadened Q_y transition (at

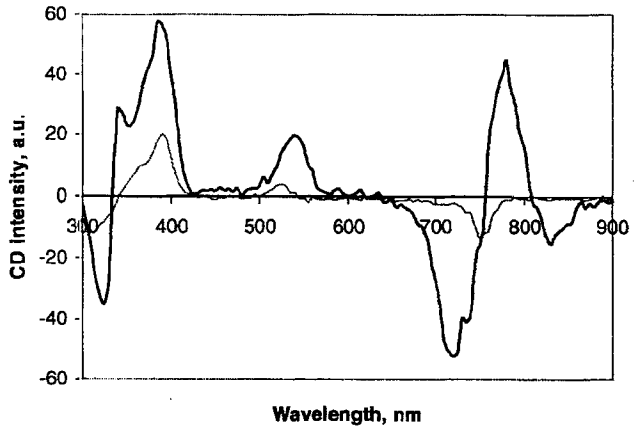

Figure 3. CD spectra of compound **10** (40 μ*M*, in 5- and 10-mm quartz cuvettes using an Aviv-202 CD spectrometer) in PBS (black line) and 1% TX-100/PBS (gray line).

750 nm). Hence, this spectrum is assigned to monomers. In the second component (dotted line), the Q_y transition splits into two new excitonic transitions at 726 and 765 nm. In the third component (gray line), the energy difference between the upper and lower excitonic transitions (712 and 822 nm, respectively) is markedly increased. Assuming that the exciton splitting reflects the extent of coupling among the individual transition dipoles (51–56), the concentration dependence of the **10** in the spectra clearly indicates the formation of two forms of aggregates: small ones, probably dimers (Fig. 2c, dashed line) with strong excitonic splitting ($\Delta\nu$ ~750 cm^{-1}) among two major transition dipoles and at increasing concentrations of **10** and larger ones consisting of at least hexamers (Fig. 2c, gray line), with increased splitting (1900 cm^{-1}) but similar coupling among the Q_y transition dipoles.

The CD spectra (Fig. 2b) provide complementary evidence to the factor analyses' assignments being dominated by different excitonically coupled components, at the intermediate (negative and positive bands at 735 and 780 nm, respectively) and high (negative, positive, and negative bands at 705, 765 and 825 nm, respectively) concentration ranges. The contribution of the monomeric species (weak negative band at 750 nm, identified by recording solutions of **10** in PBS/Triton X-100 [TX-100]) (Fig. 3) becomes apparent at a very low concentration. Importantly, the CD spectra of the two lowest concentrations are not shown because of too low signal/noise values.

The relative contributions of the principal components (Fig. 2c, inset) provided the means for calculating the monomer/dimer equilibrium at low concentrations of **10**, where the higher oligomer contribution is negligible (inset, left side, Fig. 2c):

$$2 \cdot \mathbf{10} \Longleftrightarrow (\mathbf{10})_2$$

$$K_{\text{dimerization}} = [(\mathbf{10})_2]/[\mathbf{10}]^2$$

Substituting $0.8 \cdot 10^{-6}$ and $0.2 \cdot 10^{-6}$ for [**10**] and [$(\mathbf{10})_2$], respectively (based on the contributions of the principal components presented in the inset, Fig. 2c), we obtain

$$K_{\text{dimerization}} = 3 \cdot 10^5\ M^{-1}.$$

The effect of detergents. In our previous studies of Bchl and Chl aggregation in different solvents, we found that the addition of TX-100 to aqueous solutions of Bchl/Chl induced disaggregation into monomers trapped in the formed TX-100 micelles (51–56). Following this observation, we tested the effect of adding TX-100, above the critical micelle concentration (53, 55), to the presently examined derivatives of Bchl (Fig. 1, dashed lines). Indeed, the line shape and peak position of the Q_y transition of all tested compounds (~825 for Mn derivative **14** and ~750–760 nm for the other compounds) in PBS/TX-100 appeared similar to the monomeric spectra in methanol, with a single negative Cotton effect at the peak of the Q_y transition, as illustrated for **10** (Fig. 3). Notably, the Mn complex **14** appeared practically monomeric in aqueous solution, both in the absence or presence of TX-100 micelles. The metal-free **11** and Zn complex **13** form loose aggregates (probably dimers) with relatively small excitonic splitting (Fig. 1b), whereas in Pd compounds **8** and **10** and in Cu complex **12**, these small aggregates appeared to assemble into larger ones with strong interactions among their transition dipoles (Fig. 1a).

Aggregate formation in serum/PBS solutions: the effect of serum proteins

The opening of the isocyclic ring by aminolysis appeared to have a dramatic effect on the hydrophobicity of the compounds, as reflected by their aggregation in aqueous solutions (Fig. 1). Consequently, these compounds should become more amenable to solvation by serum proteins. Thus, when FCS was added to **3** (Tookad®) or **7**, the compounds with intact isocyclic rings, the Q_y transition remained broad and redshifted to 800–830 nm, as expected for high-aggregate content (Fig. 4a,b, respectively). In contrast, upon adding FCS or BSA to **10**, as with all other products of aminolysis in aqueous solutions, the line shape of the Q_y transitions became monomeric, similar to that observed in organic solvent (Fig. 4c).

Considering **3** and **10** as representatives of hydrophobic and hydrophilic Bchl derivatives, respectively, we set out to resolve their interactions with specific serum proteins.

Binding compounds 3 and 10 to lipoproteins and serum albumin, respectively

Figure 5a–c describes the elution profiles of the major proteins in FCS, the protein-associated **3** (Tookad®) and the protein-associated **10** (WST11), respectively, after being mixed with FCS as described in Materials and Methods. Remarkably, a significant portion of **3** was eluted with the void volume, probably in the form of very large aggregates (having a maximum absorption at 825 nm). The protein-associated **3** (optical absorption at 760 nm) mainly comprised HDL (>90%) and a minor fraction was found associated with the serum albumin component (Fig. 5b). Considering the relative concentrations of serum albumin and HDL in the plasma, the affinity of **3** to serum albumin should be negligible compared with HDL. In contrast, **10** mostly adsorbed to serum albumin (Fig. 5c), with a minor fraction being eluted with the lipoproteins.

To determine the association constant of **10** and BSA, we resolved the concentrations of the protein complex [**10**-BSA] and the corresponding monomer concentrations [**10**] using two experimental approaches: (1) chromatographically, by measuring the [**10**-BSA] values after chromatographic separation of the protein-associated compound in different mixtures of **10** and BSA and (2) spectroscopically, by deriving the monomeric optical absorption using factor analysis, in solutions of **10** with different concentrations of BSA.

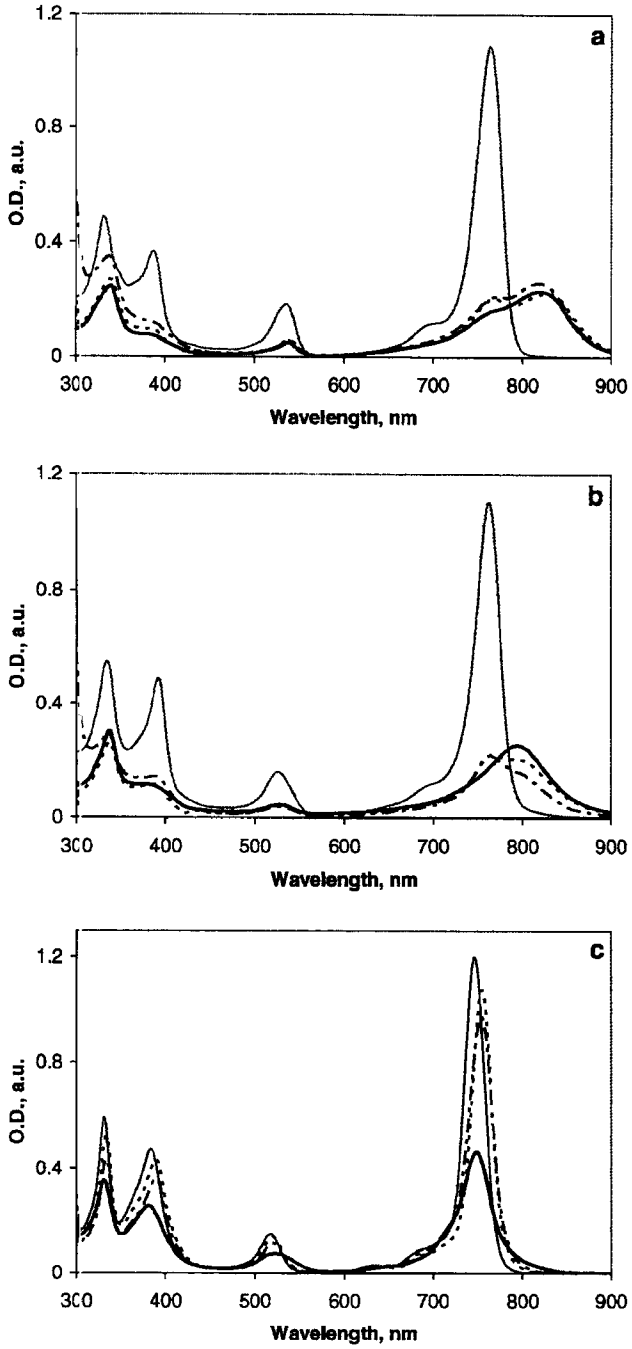

Figure 4. The effect of diluting different Bchl derivative in PBS by solutions of FCS or BSA to make a final sensitizer's concentration of 10 μ*M*, on their optical absorption (recorded in 10-mm quartz cuvettes). a: Compound **3** (obtained by dilution of 2.5 mg/mL Tookad® solution stabilized with Cremophor EL®). b: Compound **7** (initially dissolved in PBS). c: Compound **10** (initially dissolved in PBS). Solid black line, spectra in PBS; dotted line, in 90% FCS/PBS; dashed–dotted line, in 540 μ*M* BSA/PBS; solid gray line, in organic solvent (chloroform for **3**, chloroform/methanol [90:10] for **7** and methanol for **10**).

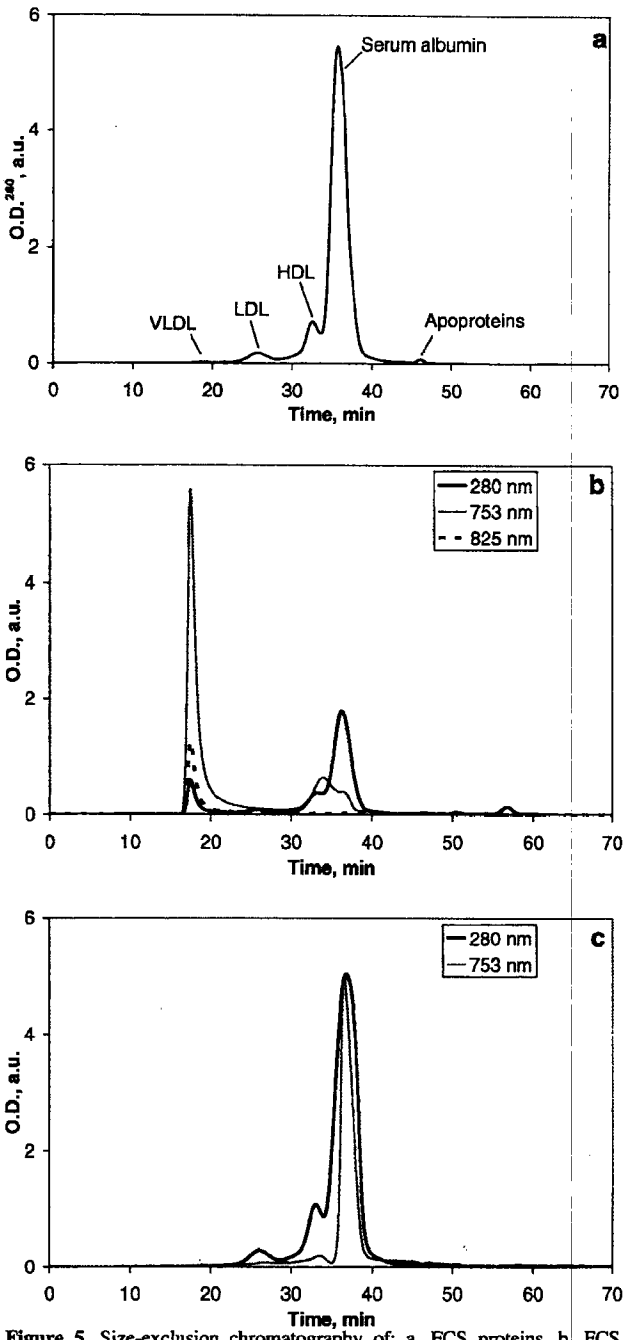

Figure 5. Size-exclusion chromatography of: a, FCS proteins. b, FCS protein-associated **3** (Tookad®) and c, FCS protein-associated **10** (WST11). The chromatogram profiles in b and c are normalized for better viewing.

Chromatographic determination of [10-BSA]. Table 2 presents the concentrations of **10** and BSA after mixing 10 μ*M* BSA with different concentrations of **10** in PBS followed by flash separation with size exclusion.

Assuming a simple, second-order equation:

$$\mathbf{10} + \mathrm{BSA} \Longleftrightarrow \mathbf{10} - \mathrm{BSA};$$

$$K_{\mathrm{assoc}} = \frac{[\mathbf{10}\cdot BSA]}{[\mathbf{10}]\cdot[BSA]}.$$

The average value of K_{assoc} amounts to $\sim 10^4\ M^{-1}$.

Determination of [10-BSA] values at different concentrations of BSA and 40 μM 10 using factor analysis of the corresponding optical absorption spectra. Figure 6a,b illustrates the optical absorption and CD spectra, respectively, of 40 μ*M* **10** in the presence of different BSA concentrations. Using factor analysis for the optical absorption spectra as previously described, we were

Table 2. The concentration of free ([**10**]) and BSA-bound ([**10**-BSA]) WST11 after mixing 50 μ*M* WST11 with 10 μ*M* BSA

Experiment no.	[**10**] × 10^{-6} *M*	[BSA] × 10^{-6} *M*	[**10**-BSA] × 10^{-6} *M*	$K_{assoc} \times 10^3$
1	1.87	9.87	0.13	7.0
2	4.53	9.53	0.47	10.9
5	9.00	9.00	1.00	12.3
3	18.67	8.67	1.33	8.2
4	47.10	7.10	2.90	8.7

able to resolve the concentrations of three principal components (Fig. 6a, inset) that appear similar to monomeric (solid line), dimeric (dashed line) and higher-order aggregates (gray line). The line shape of these components is also similar to those resolved for different concentrations of **10** in the absence of BSA. Using the relative contribution of the different components and the overall concentration of **10**, we arrived at an association constant of $K_{assoc} = 1 \cdot 10^4\ M^{-1}$, assuming that **10**-BSA comprises only bound monomers. Thus both methods, chromatographic and spectroscopic, provided similar results. The construction of a physical model that includes the detailed equilibrium constants between the different aggregates is in progress. Using the obtained association constant between BSA and **10**, one expects that at physiologic concentrations of BSA (~0.6 m*M*) about 2 μ*M* **10** (5%) remains nonbound to BSA.

Photocytotoxicity of the new compounds in the absence and presence of serum proteins

The phototoxicity of compounds **3** and **7–14** was tested on cultured H5V mouse endothelial cells by two experimental procedures. In the first procedure, after our previous experiments (21,50,57), cells were preincubated in the presence of 10% FCS with increasing concentrations of the test compounds for 2 h, then washed and illuminated or kept in the dark. The second procedure attempted to simulate the conditions of *in vivo* VTP, where illumination is applied immediately after intravenous administration of the test compound (sensitizer) in the presence of physiologic concentrations of serum proteins and decreasing concentrations of the sensitizer in the plasma (because of rapid clearance [25,38]). Within the illumination time (5–10 min, immediately after administrating bolus sensitizer) the plasma concentrations of all currently tested sensitizers decreased to less than 5% of their initial values (*e.g.* 38,58). Hence, the average sensitizer concentration during illumination is ~$[C_0]/2$, where $[C_0]$ is the initial concentration of the sensitizer in the plasma, usually in the range of 100 μ*M* (in the blood). Following these constraints, in testing the second procedure in the present study, we applied a 10-min illumination after a 3-min incubation of the different compounds (50 μ*M*) with endothelial cells in the presence of 0–75% FCS or 0–540 μ*M* BSA without washing.

The results of the first procedure are presented in Table 3. The phototoxicities of compounds **8** and **10** were concentration- and light-dependent, without substantial dark toxicity in the tested range. The LD_{50} of the nonmetalated compound **11** and the Pd-containing sensitizers **3**, **5**, **7–10** were almost the same (~1–5 μ*M*), whereas the complexes with Cu, Zn and Mn (**12–14**) were photodynamically inactive (the Zn complex was found inoperative due to its oxidation into chlorin during 2 h incubation).

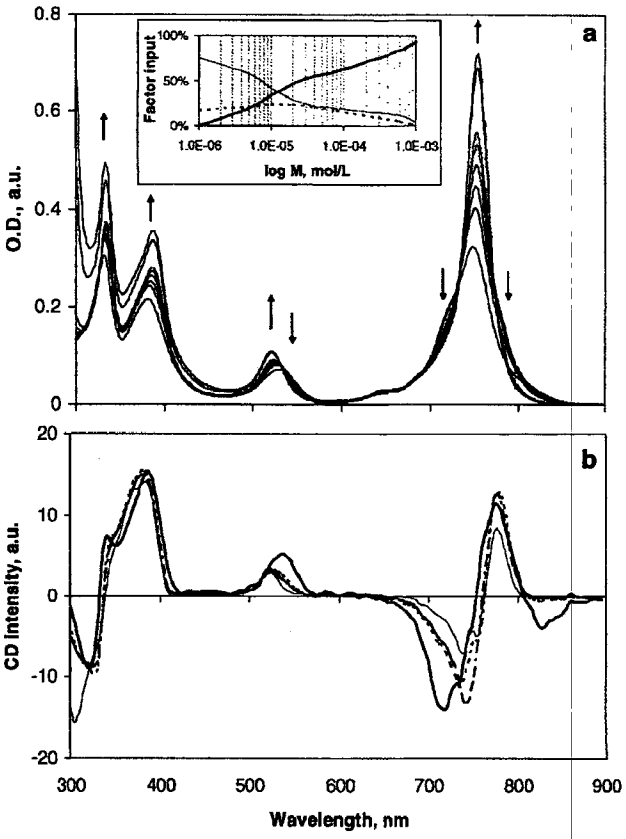

Figure 6. Aggregation forms of **10** in PBS at a constant pigment concentration (40 μ*M*) and increasing concentrations of BSA (0–1 m*M*). a: Absorption spectra (spectra were recorded and normalized as described in the legend for Fig. 2a); arrows indicate changes upon an increase in BSA concentration. Inset: Dependence of the principal components of the optical absorption on the concentration of BSA as resolved by factor analysis of the optical absorption. Solid line, monomer; dashed line, dimer; gray line, oligomer. b: CD spectra (spectra were recorded and normalized as described in the legend for Fig. 2a): no BSA, solid black line; 40 μ*M*, dotted line; 80 μ*M*, dashed–dotted line; 1 m*M*, gray solid line.

The results of the second procedure are displayed in Fig. 7. Evidently, the photocytotoxicity of the palladium-containing compounds **7–10** and the zinc complex **13** declined markedly, whereas that of **3** (Tookad®) and the metal-free **11** remained the same (Fig. 7a). Derivatives with copper **12** and manganese **14** were photoinactive at all serum concentrations examined. Similar results were obtained when BSA was used instead of whole serum (Fig. 7b).

Based on the synthetic simplicity and the near resemblance of physicochemical properties of Pd complexes **5**, **8** and **10**, the latter taurinated* compound was chosen as the main representative of water-soluble Bchl derivatives for further biological examination (24,38). This compound was found to be stable in solutions (in contrast to the zinc derivative **13**; data not shown) as well as during prolonged storage (months), when kept as a solid in the dark at –20°C.

*Taurine (2-amino-1-ethane sulfonic acid), a close homologue of homotaurine, is a widely available biochemical product. Taurine is not poisonous; on the contrary, it is a conditionally essential nutrient, important for mammalian development, especially for cerebellum and retina cells (59); for the biological and therapeutic potential of taurine, see reviews (60–62).

Table 3. Sensitizers' phototoxicity. H5V cells were preincubated with compounds **3** and **7–14** in medium containing 10% FCS for 2 h, then washed with fresh medium and illuminated. Points are the mean ± SEM of triplicate determinations

Compound no.	LD_{50} (μM)
3	1.0
5	2.1
7	3.1
8	1.5
9	5.2
10	0.8
11	1.8
12	n.d.*
13	n.d.
14	n.d.

*n.d., nondetected.

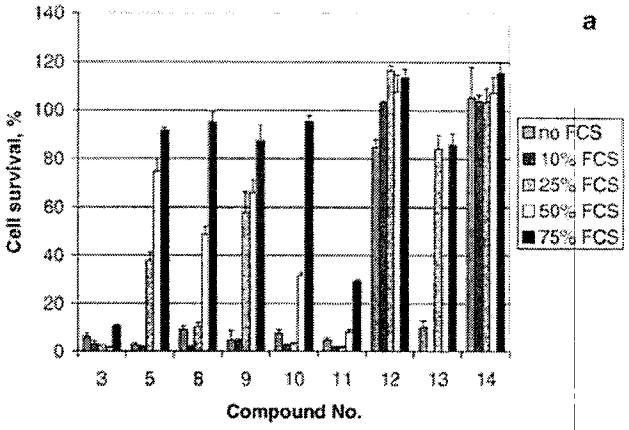

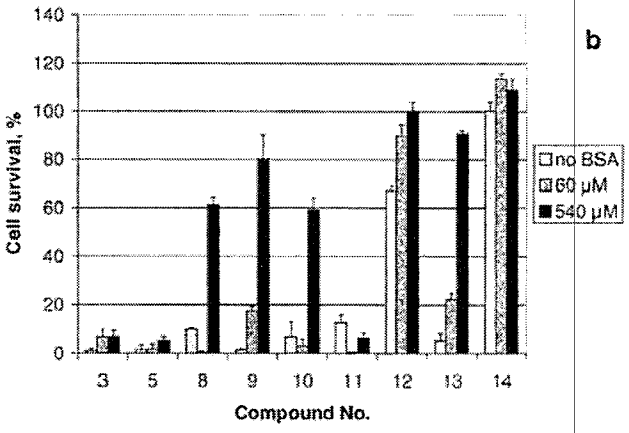

Figure 7. Phototoxicity dependence on the concentration of serum (a) and BSA (b). H5V cells were preincubated with 50 μM concentrations of the indicated pigments in cell culture medium for 3 min, illuminated for 10 min, then washed with fresh medium. The points are the mean ± SEM of triplicate determinations.

DISCUSSION AND CONCLUSIONS

Preclinical and clinical trials with antiangiogenic agents have been at the cutting edge of tumor therapy for quite some time. However, systemic application of antiangiogenic agents, which prevents the development of new blood vessels and thereby inhibits tumor growth, was found most effective in regions of neovascularization such as the tumor periphery, but not in areas of existing tumors with a supply of mature vessels or in tumor regions that share vascularization with adjacent normal tissues (63,64). Vascular targeting agents (VTA) provide an interesting alternative, but such agents were found more active in the interior of relatively large tumors, possibly because of the high interstitial pressure in these regions, which contributes to vascular collapse (64). Furthermore, VTA often generate a characteristic pattern of widespread central necrosis in experimental tumors, which can extend to as much as 95% of the tumor volume. However, a thin frame of tumor cells at the tumor's rim may survive, resulting in tumor regrowth. Thus, despite very promising experimental results, both antiangiogenic and antivascular targeting agents have so far failed in completely eradicating tumors. VTA and therapies designed for direct tumor cell killing (conventional chemotherapeutic drugs, radiation or PDT based on cell-selective uptake) are awaiting further development (64–66).

Recent promising results with VTP therapy based on a Bchl derivative to achieve complete tumor eradication showed high cure rates with various tumor types (20,58,67). In the present study we focused on the synthesis and characterization of new Bchl-type candidates for VTP. Here we showed that aminolysis of the isocyclic ring with negatively charged residues markedly increases the hydrophilicity of the Bchl sensitizers, decreases their self-association constant and selectively increases their affinity to serum albumin, compared with other serum proteins. To that end, we suggest several simple analytical procedures that can be applied to other sensitizers as well. The remarkable polarity and solubility of compound **14**, compared with the other products of Bpheid aminolysis, probably reflects the high dipole moment of this molecule. As we have recently shown (49), the Mn(III)Bpheid derivatives are axially biligated with hydroxyl anion and hydroperoxide in the absence of other strong ligands.

The enhanced hydrophilicity and increased affinity of some of the new sensitizers to serum albumin seem advantageous for VTP. This is mainly because serum albumin stays in the circulation and can also bring the sensitizers to the vasculature of important target organs, such as the liver and lungs, as recently shown for the biodistribution of compound **10** (38). However, the concomitant reduction in the photocytotoxicity toward endothelial cells appears at first to be a drawback for this treatment modality because a direct insult of endothelial cells is considered important for successfully launching a tumor cure via VTP (12). Strikingly, in several studies that were recently performed in our laboratory (24,38; Mazor *et al.*, unpublished data), we showed that such sensitizers are highly efficacious VTP agents that deliver high cure rates for a variety of tumor types. However, these experiments showed that, unlike Tookad®, VTP with **10** has practically no effect on the vessels' permeability. Thus, the occlusion of tumor vessels, which was observed within minutes of illumination, was not accompanied by hemorrhagic necrosis, underscoring the advantage of such sensitizers for VTP applications where hemorrhagic necrosis may endanger the treated patient, such as in tumors situated near major vessels or in internal sensitive organs or in age-related macular degeneration, in which lateral photodamage may be considerable.

Acknowledgements—This study was supported by grants from the Yeda Research and Development Co., Ltd. (Israel) and Steba-Biotech (France).

We are grateful to Dr. Vlad Brumfeld for his assistance in circular dichroism spectroscopy and to Dr. Roie Yerushalmi for factor analysis. A.S. is the incumbent of the Robert and Yadelle Sklare Professorial Chair in Biochemistry. Y.S. is the incumbent of the Tillie and Charles Lubin Professorial Chair in Biochemical Endocrinology.

REFERENCES

1. Folkman, J. (1995) Angiogenesis in cancer, vascular, rheumatoid and other disease. *Nat. Med.* **1**, 27–31.
2. Schnitzer, J. E. (1998) Vascular targeting as a strategy for cancer therapy. *N. Engl. J. Med.* **339**, 472–474.
3. Paris, F., Z. Fuks, A. Kang, P. Capodieci, G. Juan, D. Ehleiter, A. Haimovitz-Friedman, C. Cordon-Cardo and R. Kolesnick (2001) Endothelial apoptosis as the primary lesion initiating intestinal radiation damage in mice. *Science* **293**(5528), 293–297.
4. Mokuma, G. (2002) Tumor vasculature directed drug targeting: applying new technologies and knowledge to the development of clinically relevant therapies. *Pharm. Res.* **19**, 1251–1258.
5. Miller, J. W. (2003) Photodynamic therapy for choroidal neovascularization. *Graefe's Arch. Clin. Exp. Ophthalmol.* **241**, 258–262.
6. Rupnick, M. A., D. Panigrahy, C. Y. Zhang, S. M. Dallabrida, B. B. Lowell, R. Langer and M. J. Folkman (2002) Adipose tissue mass can be regulated through the vasculature. *Proc. Natl. Acad. Sci. USA* **99**, 10730–10735.
7. Reno, R. Z. and J. W. Miller (2001) Photosensitizer delivery for photodynamic therapy of choroidal neovascularization. *Adv. Drug Deliv. Rev.* **52**, 63–78.
8. Boyle, R. W. and D. Dolphin (1996) Structure and biodistribution relationships of photodynamic sensitizers. *Photochem. Photobiol.* **64**, 469–485.
9. Dougherty, T. J., C. J. Gomer, B. W. Henderson, G. Jori, D. Kessel, M. Korbelik, J. Moan and Q. Peng (1998) Photodynamic therapy. *J. Natl. Cancer Inst.* **90**, 889–905.
10. Pandey, R. K. and G. Zheng (2000) Porphyrins as photosensitizers in photodynamic therapy. In *The Porphyrin Handbook*, Vol. 6 (Edited by K. M. Kadish, K. M. Smith and R. Guilard), pp. 157–230. Academic Press, San Diego.
11. Macdonald, I. J. and T. J. Dougherty (2001) Basic principles of photodynamic therapy. *J. Porphyrins Phthalocyanines* **5**, 105–129.
12. Abels, C. (2004) Targeting of the vascular system of solid tumours by photodynamic therapy (PDT). *Photochem. Photobiol. Sci.* **3**, 765–771.
13. Krammer, B. (2001) Vascular effects of photodynamic therapy. *Anticancer Res.* **21**, 4271–4277.
14. Ferrario, A., D. Kessel and C. J. Gomer (1992) Metabolic properties and photosensitizing responsiveness of mono-L-aspartyl chlorin-e6 in a mouse-tumor model. *Cancer Res.* **52**, 2890–2893.
15. Roberts, W. G. and T. Hasan (1992) Role of neovasculature and vascular-permeability on the tumor retention of photodynamic agents. *Cancer Res.* **52**, 924–930.
16. McMahon, K. S., T. J. Wieman, P. H. Moore and V. H. Fingar (1994) Effects of photodynamic therapy using mono-L-aspartyl chlorin E(6) on vessel constriction, vessel leakage, and tumor response. *Cancer Res.* **54**, 5374–5379.
17. Zilberstein, J., S. Schreiber, M. C. W. M. Bloemers, P. Bendel, M. Neeman, E. Schechtman, F. Kohen, A. Scherz and Y. Salomon (2001) Antivascular treatment of solid melanoma tumors with bacteriochlorophyll-serine-based photodynamic therapy. *Photochem. Photobiol.* **73**, 257–266.
18. Dolmans, D. E. J. G. J., A. Kadambi, J. S. Hill, K. R. Flores, J. N. Gerber, J. P. Walker, I. H. M. Borel Rinkes, R. K. Jain and D. Fukumura (2002) Targeting tumor vasculature and cancer cells in orthotopic breast tumor by fractionated photosensitizer dosing photodynamic therapy. *Cancer Res.* **62**, 4289–4294.
19. Gross, S., A. Gilead, O. Mazor, A. Brandis, S. Schreiber, Y. Machluf, M. Neeman, A. Scherz and Y. Salomon (2003) Selective vascular and tumor responses to photodynamic therapy (PDT) with Pd bacteriopheophorbide (TOOKAD): online and offline analyses. *Proc. Am. Assoc. Cancer Res.* **44**, 27.
20. Koudinova, N. V., J. H. Pinthus, A. Brandis, O. Brenner, P. Bendel, J. Ramon, Z. Eshhar, A. Scherz and Y. Salomon (2003) Photodynamic therapy with Pd-bacteriopheophorbide (TOOKAD): successful *in vivo* treatment of human prostatic small cell carcinoma xenografts. *Int. J. Cancer* **104**, 782–789.
21. Preise, D., O. Mazor, N. Koudinova, M. Liskovich, A. Scherz and Y. Salomon (2003) Bypass of tumor drug resistance by antivascular therapy. *Neoplasia* **5**, 475–480.
22. Kelleher, D. K., O. Thews, A. Scherz, Y. Salomon and P. Vaupel (2004) Perfusion, oxygenation status and growth of experimental tumors upon photodynamic therapy with Pd-bacteriopheophorbide. *Int. J. Oncol.* **24**, 1505–1511.
23. Scherz, A., Y. Salomon, A. Brandis and H. Scheer (2003) Palladium-substituted Bacteriochlorophyll Derivatives and Use Thereof. U.S. Patent 6 569 846.
24. Mazor, O. (2004) Synthesis and Phototoxicity of Novel Sulfonated Bacteriochlorophyll Derivatives. Ph.D. thesis, Weizmann Institute of Science, Rehovot, Israel.
25. Brun, P. H., J. L. DeGroot, E. F. G. Dickson, M. Farahari and R. H. Pottier (2004) Determination of the in vivo pharmacokinetics of palladium-bacteriopheophorbide (WST09) in EMT6 tumour-bearing Balb/c mice using graphite furnace atomic absorption spectroscopy. *Photochem. Photobiol. Sci.* **3**, 1006–1010.
26. Chen, Y., G. Li and R. K. Pandey (2004) Synthesis of bacteriochlorins and their potential utility in photodynamic therapy (PDT). *Curr. Org. Chem.* **8**, 1105–1134.
27. Shargel, L. and A. B. C. Yu (1999) *Applied Biopharmaceutics and Pharmacokinetics*. Appleton & Lange, McGraw-Hill, New York.
28. Borle, F., A. Radu, C. Fontolliet, H. van den Bergh, P. Monnier and G. Wagnieres (2003) Selectivity of the photosensitiser Tookad® for photodynamic therapy evaluated in the Syrian golden hamster cheek pouch tumour model. *Br. J. Cancer* **89**, 2320.
29. Chen, Q., Z. Huang, D. Luck, J. Beckers, P.-H. Brun, B. C. Wilson, A. Scherz, Y. Salomon and F. Hetzel (2002) Preclinical studies in normal canine prostate of a novel palladium-bacteriopheophorbide (WST09) photosensitizer for photodynamic therapy of prostate cancer. *Photochem. Photobiol.* **76**, 438–445.
30. Weller, A. and R. Livingstone (1954) The reaction of chlorophyll in amines. *J. Am. Chem. Soc.* **76**, 1575–1578.
31. Pennington, F. C., S. D. Boyd, H. Horton, S. W. Taylor, D. G. Wulf, J. J. Katz and H. H. Strain (1967) Reactions of chlorophylls a and b with amines. Isocyclic ring rupture and formation of substituted chlorin-6-amides. *J. Am. Chem. Soc.* **89**, 3871–3875.
32. Ando, T., K. Irie, K. Koshimizu, T. Shingu, N. Takeda, T. Takemura, S. Nakajima and I. Sakata (1991) New photosensitizers for photodynamic therapy: syntheses of chlorin e6 dimer and trimer. *Agric. Biol. Chem.* **55**, 2441–2443.
33. Ando, T., I. Kazuhiro, K. Koshimizu, S. Nakajima, T. Takemura and I. Sakata (1992) A convenient synthesis of chlorin e6 dimer and trimer. In *Photodynamic Therapy and Biomedical Lasers* (Edited by P. Spinelli, M. Dal Fante and R. Marchesini), pp. 769–773. Elsevier Science Publishers B.V., Amsterdam.
34. Gurinovich, G. P., T. E. Zorina, S. B. Melnov, N. I. Melnova, I. F. Gurinovich, L. A. Grubina, M. V. Sarzhevskaya and S. N. Cherenkevich (1992) Photodynamic activity of chlorin e_6 and chlorin e_6 ethylenediamide *in vitro* and *in vivo*. *J. Photochem. Photobiol. B Biol.* **13**, 51–57.
35. Ma, L. F. and D. Dolphin (1996) Nucleophilic reaction of 1,8-diazabicyclo[5.4.0]undec-7-ene and 1,5-diazabicyclo[4.3.0]non-5-ene with methyl pheophorbide *a*. Unexpected products. *Tetrahedron* **52**, 849–860.
36. Zhang, L. and D. Y. Xu (1999) Synthesis of chlorin e(6)-6-amide derivatives. *Chin. J. Org. Chem.* **19**, 424–430.
37. Belykh, D. V., L. P. Karmanova, L. V. Spirikhin and A. V. Kutchin (2002) Synthesis of chlorin e_6 amide derivatives. *Mendeleev Commun.* 77–78.
38. Mazor, O., A. Brandis, V. Plaks, V. Rosenbach-Belkin, Y. Salomon and A. Scherz (2005) WST11, a novel water-soluble bacteriochlorophyll derivative; cellular uptake, pharmacokinetics, biodistribution, and vascular targeted photodynamic activity against melanoma tumors. *Photochem. Photobiol.* **81**, 342–351.
39. Gross, S., A. Brandis, L. Chen, V. Rosenbach-Belkin, S. Roehrs, A. Scherz and Y. Salomon (1997) Protein-A-mediated targeting of bacteriochlorophyll-IgG to *Staphylococcus aureus*: a model for enhanced site-specific photocytotoxicity. *Photochem. Photobiol.* **66**, 872–878.
40. Kessel, D. (1989) Determinants of photosensitization by mono-L-aspartyl chlorin e6. *Photochem. Photobiol.* **49**, 447–452.

41. Westerlund, J. and Z. Yao (1995) Elution of lipoprotein fractions containing apolipoproteins E and A-I in size exclusion on Superose 6 columns is sensitive to mobile phase pH and ionic strength. *J. Chromatogr. A* **718**, 59–66.
42. Ordovas, J. M. and D. Osgood (1998) Preparative isolation of plasma lipoproteins using fast protein liquid chromatography. In *Lipoprotein Protocols*, Vol. 110 (Edited by J. Ordovas), pp. 105–111. Humana Press, Inc., Totowa, NJ.
43. Havel, R. J., H. A. Eder and J. H. Bragdon (1955) The distribution and chemical composition of ultracentrifugally separated lipoprotein in human sera. *J. Clin. Investig.* **34**, 1345–1353.
44. Noy, D., R. Yerushalmi, V. Brumfeld, I. Ashur, H. Scheer, K. Baldridge and A. Scherz (2000) Optical absorption and computational studies of [Ni]-bacteriochlorophyll-a. New insight into charge distribution between metal and ligands. *J. Am. Chem. Soc.* **122**, 3937–3944.
45. Wasielewski, M. R. and W. A. Svec (1980) Synthesis of covalently linked dimeric derivatives of chlorophyll a, pyrochlorophyll a, chlorophyll b, and bacteriochlorophyll a. *J. Org. Chem.* **45**, 1969–1974.
46. Scherz, A., L. Fiedor and Y. Salomon (1998) Chlorophyll and Bacteriochlorophyll Derivatives, Their Preparation and Pharmaceutical Compositions Comprising Them. U.S. Patent 5 726 169.
47. Scherz, A., Y. Salomon, H. Scheer, G. Hartwich and A. Brandis (2001) Synthetic Metal-substituted Bacteriochlorophyll Derivatives and Use Thereof. U.S. Patent 6 333 319.
48. Hartwich, G., L. Fiedor, I. Simonin, E. Cmiel, W. Schafer, D. Noy, A. Scherz and H. Scheer (1998) Metal-substituted bacteriochlorophylls. 1. Preparation and influence of metal and coordination on spectra. *J. Am. Chem. Soc.* **120**, 3675–3683.
49. Ashur, I., A. Brandis, M. Greenwald, Y. Vakrat-Haglili, V. Rosenbach-Belkin, H. Scheer and A. Scherz (2003) Control of redox transitions and oxygen species binding in Mn centers by biologically significant ligands; model studies with [Mn]-bacteriochlorophyll a. *J. Am. Chem. Soc.* **125**, 8852–8861.
50. Rosenbach-Belkin, V., L. Chen, L. Fiedor, I. Tregub, F. Pavlotsky, V. Brumfeld, Y. Salomon and A. Scherz (1996) Serine conjugates of chlorophyll and bacteriochlorophyll: photocytotoxicity *in vitro* and tissue distribution in mice bearing melanoma tumors. *Photochem. Photobiol.* **64**, 174–181.
51. Scherz, A. and W. W. Parson (1984) Oligomers of bacteriochlorophyll and bacteriopheophytin with spectroscopic properties resembling those found in photosynthetic bacteria. *Biochim. Biophys. Acta* **766**, 653–665.
52. Scherz, A. and V. Rosenbach-Belkin (1988) The spectral properties of chlorophyll and bacteriochlorophyll dimers; a comparative study. In *NATO ASI Series, Series A: Life Sciences*, Vol. 149 (Photosynth. Bact. React. Cent.), pp. 295–306.
53. Fisher, J. R. E., V. Rosenbach-Belkin and A. Scherz (1990) Cooperative polymerization of photosynthetic pigments in formamide-water solution. *Biophys. J.* **58**, 461–470.
54. Scherz, A. and W. W. Parson (1984) Exciton interactions in dimers of bacteriochlorophyll and related molecules. *Biochim. Biophys. Acta* **766**, 666–678.
55. Scherz, A. and V. Rosenbach-Belkin (1989) Comparative study of optical absorption and circular dichroism of bacteriochlorophyll oligomers in Triton X-100, the antenna pigment B850, and the primary donor P-860 of photosynthetic bacteria indicates that all are similar dimers of bacteriochlorophyll a. *Proc. Natl. Acad. Sci. USA* **86**, 1505–1509.
56. Rosenbach-Belkin, V., J. R. E. Fisher and A. Scherz (1991) Effect of nonexcitonic interactions among the paired molecules on the Qy transition of bacteriochlorophyll dimers. Applications to the primary electron donors P-860 and P-960 in bacterial reaction centers. *J. Am. Chem. Soc.* **113**, 676–678.
57. Plaks, V., Y. Posen, O. Mazor, A. Brandis, A. Scherz and Y. Salomon (2004) Homologous adaptation to oxidative stress induced by the photosensitized Pd-bacteriochlorophyll derivative (WST11) in cultured endothelial cells. *J. Biol. Chem.* **279**, 45713–45720.
58. Schreiber, S., S. Gross, A. Brandis, A. Harmelin, V. Rosenbach-Belkin, A. Scherz and Y. Salomon (2002) Local photodynamic therapy (PDT) of rat C6 glioma xenografts with Pd-bacteriopheophorbide leads to decreased metastases and increase of animal cure compared with surgery. *Int. J. Cancer* **99**, 279–285.
59. # 9421 (1996) Taurine. In *The Merck Index: An Encyclopedia of Chemicals, Drugs, and Biologicals*, 12th edition (Edited by S. Budavari, M. J. O'Neil, A. Smith, P. E. Heckelman and J. F. Kinneary), p. 1554. Merck, Whitehouse Station, NJ.
60. Redmond, H. P., P. P. Stapleton, P. Neary and D. Bouchier-Hayes (1998) Immunonutrition: the role of taurine. *Nutrition* **14**, 599–604.
61. Saransaari, P. and S. S. Oja (2000) Taurine and neural cell damage. *Amino Acids* **19**, 509–526.
62. Schaffer, S. W., J. B. Lombardini and J. Azuma (2000) Interactions between the actions of taurine and angiotensin II. *Amino Acids* **18**, 305–318.
63. Hu, P., J. Yan, J. Sharifi, T. Bai, L. A. Khawli and A. L. Epstein (2003) Comparison of three different targeted tissue factor fusion proteins for inducing tumor vessel thrombosis. *Cancer Res.* **63**, 5046–5053.
64. Thorpe, P. E. (2004) Vascular targeting agents as cancer therapeutics. *Clin. Cancer Res.* **10**, 415–427.
65. Nilsson, F., H. Kosmehl, L. Zardi and D. Neri (2001) Targeted delivery of tissue factor to the ED-B domain of fibronectin, a marker of angiogenesis, mediates the infarction of solid tumors in mice. *Cancer Res.* **61**, 711–716.
66. Jain, R. K. (2003) Molecular regulation of vessel maturation. *Nat. Med.* **9**, 685–693.
67. Huang, Z., Q. Chen, N. Trncic, S. M. LaRue, P. H. Brun, B. C. Wilson, H. Shapiro and F. W. Hetzel (2004) Effects of Pd-bacteriopheophorbide (TOOKAD)-mediated photodynamic therapy on canine prostate pretreated with ionizing radiation. *Radiat. Res.* **161**, 723–731.

Exhibit C

Photocatalytic Generation of Oxygen Radicals by the Water-Soluble Bacteriochlorophyll Derivative WST11, Noncovalently Bound to Serum Albumin

Idan Ashur,[†] Ruth Goldschmidt,[†] Iddo Pinkas,[†] Yoram Salomon,[‡] Grzegorz Szewczyk,[§] Tadeusz Sarna,[§] and Avigdor Scherz*,[†]

Department of Plant Sciences, The Weizmann Institute of Science, Rehovot, Israel, Department of Biological Regulation, The Weizmann Institute of Science, Rehovot, Israel, and Department of Biophysics, Jagiellonian University, Krakow, Poland

Received: January 20, 2009; Revised Manuscript Received: May 5, 2009

Light-induced radical generation is the hallmark of fundamental processes and many applications including photosynthesis and photodynamic therapy (PDT). In this manuscript, we present two novel observations made upon monitoring light-induced generation of reactive oxygen species (ROS) in aqueous solutions by WST11, a water-soluble derivative of the photosynthetic pigment Bacteriochlorophyll *a* (Bchl). Using a host of complementary experimental techniques including time-resolved spectroscopy at the subpicosecond to the millisecond range, ESR spectroscopy, electrochemistry, spectroelectrochemistry, oximetry, and protein mass spectroscopy, we first show that in aqueous solutions WST11 generates only superoxide ($O_2^{-\bullet}$) and hydroxyl ($OH^{\bullet}$) radicals with no detectable traces of singlet oxygen. Second, we show that WST11 makes a noncovalent complex with human serum albumin (HSA) and that this complex functions as a photocatalytic oxidoreductase at biologically relevant concentrations enabling approximately 15 cycles of electron transfer from the associated HSA protein to molecular oxygen in the solution. These findings rule out the paradigm that porphyrin and chlorophyll based PDT is mainly mediated by formation of singlet oxygen, particularly in vascular targeted photodynamic therapy (VTP) with sensitizers that undergo photoactivation during circulation in the plasma, like [Pd]-Bacteriopheophorbide (WST09, Tookad). At the same time, our findings open the way for new design paradigms of novel sensitizers, since $O_2^{-\bullet}$ and $OH^{\bullet}$ radicals are well-recognized precursors of important pathophysiological processes that can be activated for achieving tumor eradication. Moreover, the finding that promiscuous protein scaffolds become sinks for holes and electrons when holding light-activated pigments provides a new insight to the evolution and action mechanism of natural light activated oxidoreductases (such as photosynthetic reaction centers) and new guidelines for the preparation of synthetic-light converting machineries.

Introduction

Photoexcitation of pigment molecules followed by energy transfer and radical generation promotes both constructive and destructive biological processes. The first group includes fundamental biological machineries such as photosynthesis and vision, while photoinhibition and plants senescence are two examples of the second group. The photocatalytic centers involved in the constructive processes usually comprise protein scaffolds which hold the pigment molecules in a manner that assures unidirectional and well-controlled transfer of energy or electrons from donors to acceptors. The protein involvement in these processes has been thoroughly studied but remained controversial to date.[1,2] Light-induced destructive processes are usually the result of conformational changes or even disintegration of the pigment/protein complexes resulting in noncontrolled energy or electron transfer from the photoactive pigments into acceptor molecules that become highly active and impair vital cellular or tissue activities. An example is provided by the formation of reactive oxygen species (ROS) through energy or electron transfer from a host of photoexcited pigment molecules (sensitizers) into colliding or nearby molecular oxygen. This phenomenon was found responsible for photoinhibition[3] and several pathologies (e.g., porphyria)[4] and has been translated into a cancer treatment modality termed photodynamic therapy (PDT).[5] In PDT, pigments that can generate ROS at high yield upon illumination in the VIS−NIR wavelength range are delivered to a cancerous tissue and locally illuminated. The formed ROS initiate a cascade of events that result in reduction or oxidation of vital components (e.g., proteins and lipids) in the cellular compartment of the cancerous tissue and thereby cause cell death and tumor eradication. Numerous studies have suggested that the PDT toxicity in the cells is mainly mediated by singlet oxygen which dominates the ROS profile (type II mechanism).[6−9] In the type II mechanism, the photosensitizer in the excited triplet state can interact with ground state oxygen molecules, generating singlet oxygen through an energy transfer process.[10,11] An alternative route is the type I mechanism in which the photosensitizer in the excited triplet state can interact directly with the substrate and/or solvent through electron or proton transfer processes. This leads to generation of charged or neutral radicals, which quickly react with oxygen molecules to produce ROS such as superoxide ($O_2^{-\bullet}$) and hydroxyl ($OH^{\bullet}$) radicals and hydrogen peroxide (H_2O_2). Evidence for the

* Corresponding author. Tel.: +972-8-9342336. Fax: +972-8-9344181. E-mail: avigdor.scherz@weizmann.ac.il.
[†] Department of Plant Sciences, The Weizmann Institute of Science.
[‡] Department of Biological Regulation, The Weizmann Institute of Science.
[§] Jagiellonian University.

10.1021/jp900580e CCC: $40.75
Published on Web 06/22/2009

SCHEME 1: Water-Soluble [Pd]-Bacteriopheophorbide Derivative, WST11

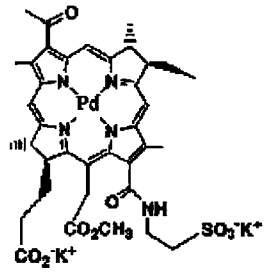

occurrence of the type I mechanism is limited and less conclusive.[10,11]

A new approach to PDT termed vascular-targeted PDT (VTP) aims to induce instantaneous collapse of the tumor vasculature. The consequent deprivation of nutrients and oxygen results in cell death and tumor eradication. So far, VTP has been applied using hydrophobic sensitizers that preferentially reside in the endothelial cells of the tumor vasculature during illumination and generate singlet oxygen.[12,13] Recently we developed a different approach to VTP using a novel class of amphiphilic photosensitizers comprising different derivatives of Bacteriochlorophyll *a* (Bchl).[14−17] These sensitizers stay in the circulation until clearance with minimal or even no uptake by the endothelial cells during illumination. Hence, ROS generation is confined to the aqueous plasma, resulting in instantaneous clot formation, vascular arrest, and high rates of tumor control, both in the preclinical[14,16−18] and clinical[19−22] arenas. We have previously hypothesized that under these conditions the ROS generation profile can be markedly different from the one assumed for the cellular environment[23] because the high dielectric nature of aqueous solutions may help promote electron transfer. Indeed, Vakrat-Haglili et al.[24] showed a dramatic increase in the content of $O_2^{-\bullet}$ and $OH^{\bullet}$ radicals when [Pd]-Bacteriopheophorbide (WST09, Tookad) was photoexcited in aqueous compared to organic solutions. However, the significant concentration of singlet oxygen still present in the aqueous solutions prevented a clear conclusion concerning the role played by the oxygen radicals in mediating the VTP effect. This important issue can now be resolved using the water-soluble [Pd]-Bacteriopheophorbide derivative (WST11, Stakel, Scheme 1)[14,16] that was recently synthesized by our lab in collaboration with Steba laboratories, France.

This compound has entered phase I/II clinical trials for AMD management[17] and localized prostate cancer. Unlike WST09, WST11 needs no micelles when being introduced to aqueous solutions. It stays in the plasma until clearance,[25] most probably as a noncovalent complex with human serum albumin (HSA),[14] and does not seem to primarily interact with endothelial cells.[17] Therefore, WST11 provides the means for studying the impact of ROS generation in the aqueous vascular lumen. Following this presumption, we set out to explore the generation of ROS by WST11 upon photoexcitation in stepwise reconstituted blood solutions, starting in buffered aqueous solutions and then adding different serum proteins, plasma, blood cells, etc. The present paper focuses on the effect of HSA on the ROS generation profile by photoexcited WST11 in aqueous solutions. Collectively, our data introduce a novel concept, suggesting that a noncovalent WST11−HSA complex acts as a light-activated oxido-reductase that catalyzes electron transfer from the protein matrix to the dissolved oxygen molecules, thereby amplifying the production of $O_2^{-\bullet}$ and $OH^{\bullet}$ radicals. Using optical absorption and fluorescence spectroscopy at the different time domains, spectroelectrochemistry, spin-trap ESR technique, dissolved oxygen concentration measurements, and gel electrophoresis techniques, we (1) followed the physical and chemical response of WST11 to photoexcitation in the presence of HSA and quenchers; (2) identified and quantified the evolved ROS; (3) monitored the rate and yield of oxygen consumption in response to photoexcitation of WST11 in the absence and presence of HSA; and (4) monitored induced chemical modifications of the HSA molecules subsequent to the ROS generation. We showed that in pure aqueous solutions (H_2O and D_2O) WST11 rapidly degrades through oxidative processes. The ROS profile comprises comparable amounts of $O_2^{-\bullet}$ and $OH^{\bullet}$ radicals (spin-trapped by DMPO and DEPMPO) but no detectable singlet oxygen. In the presence of HSA, the photochemical degradation of WST11 is profoundly retarded. Only $OH^{\bullet}$ radicals can be detected, and their total concentration increases by more than 2-fold compared with that observed in the absence of HSA. The rate and yield of oxygen consumption increases by more than an order of magnitude per single molecule of WST11. Upon adding the metal chelator desferrioxamine (DFO) to both HSA-free and HSA-containing solutions, a strong ESR signal of the trapped $O_2^{-\bullet}$ radical replaces that of the $OH^{\bullet}$ radical, suggesting that $O_2^{-\bullet}$ is the primarily formed ROS and the precursor of the $OH^{\bullet}$ radicals. Finally, upon the complete degradation of the WST11 reservoir, each HSA molecule appears to undergo peroxidation and, possibly, covalent binding to photodegradation products of the WST11 molecules.

Altogether, our findings establish the foundation for resolving the in vivo activity of WST11−VTP and may provide a new insight to the role played by the protein scaffold in light-induced electron transfer. In a photosystem II reaction center (PSII RC), a photoexcited pair of chlorophyll (Chl) molecules (termed P680) that are noncovalently bound to the protein scaffold transfers an electron through a chain of redox centers to a quinone molecule at the other side of the photosynthetic membrane. By oxidizing a nearby tyrosine (Tyr) residue, P680 is rapidly regenerated. Although the exceptionally high midpoint potential of the $P680/P680^+$ redox couple (+1.25 V) matches nicely that of the Tyr/Tyr^+ redox couple (+1.21 V),[26] the energetic barrier should be greatly reduced by an accompanied proton translocation from the $Tyr^{+\bullet}$ residue to form the more stable tyrosyl radical ($Tyr^{\bullet}$). This is possible in a protein scaffold having a nearby protonated side chain within a hydrogen bonding distance of the oxidizable Tyr.[27] Following these insights, Kalman et al.[28] were able to demonstrate $P860^+$ reduction in RC of purple bacteria by Tyr residues that replaced Arginine L135 and Arginine M164 although the $P860^+/P860$ midpoint potential is only +0.50 V. Thus, it appears that the protein milieu overcomes the midpoint potentials difference in a fashion that involves particular arrangement and interactions of amino acid residues. However, data shown in our present study suggest that a promiscuous protein scaffold can function as a nonspecific supplier of electrons when bound to Bchls and thereby facilitate their regeneration after oxidation. This finding may provide new guidelines for deciphering the evolution of photocatalytic protein−pigment complexes and constructing artificial systems for light energy conversion.

Materials and Methods

Different concentrations of WST11 solutions (Steba Biotech, stored as dry powder) were prepared in D-Phosphate Buffer Saline solution (PBS × 10, pH 7.4, Gibco) as specified for each experiment. 5,5-Dimethyl-1-pyrroline *N*-oxide (DMPO, GC

grade >97%), 2,2,6,6-tetramethyl-1-piperidone-*N*-oxyl (95%, 4-oxo-TEMP), desferrioxamine mesylate salt (95% TLC powder), and Albumin from Human Serum (essentially fatty acid free, lyophilized powder) were purchased from Sigma-Aldrich. 5-Diethoxyphosphoryl-5-methyl-1-pyrroline *N*-oxide (DEPMPO, 99.9% HPLC) was purchased from Calbiochem.

Electron-Spin Resonance Spectroscopy (ESR). Standard ESR measurements were carried out using a Magnettech ESR Miniscope MS 100 spectrometer, equipped with a Microwave X-band Bridge. The spectrometer operates at 9.3−9.55 GHz and 20 mW microwave power. The light source for the experiments was a Spectra Physics model 3900 Ti:sapphire laser (Spectra-Physics, Mountain View, California, USA), 1 W, pumped by 5 W of a 532 nm Spectra Physics Millenia Pro 10 W CW Nd:VO_4 laser. For the purpose of our experiments, the laser operated at 755 nm, and the input power was adjusted to 20 mW using neutral density optical filters. The sample was illuminated by an optical fiber that was located inside the ESR cavity and directed at the sample. This allowed simultaneous illumination and ESR detection. The produced $O_2^{-\bullet}$ and $OH^{\bullet}$ radicals were detected as the spin adducts DMPO−OOH and DMPO−OH, respectively. To verify if the DMPO−OH (or part of it) originates from DMPO−OOH degradation, we added 10% DMSO as a quencher of the $OH^{\bullet}$ radical.[29]

Optical Absorption Measurements. ***Steady-State and Submicro to the Millisecond Time Domain Measurements.*** Steady-state optical absorption spectra were recorded by a Thermo Scientific-Evolution 300 UV−visible spectrophotometer. Submicro to the millisecond time domain absorption measurements and luminescence measurements were performed as previously described.[24]

Time-Resolved Measurements at the Femtosecond to Picosecond Time Domain. The femtosecond laser system consists of several commercially available components. The system is driven by a mode-locked Ti:sapphire oscillator (Spectra Physics Tsunami) pumped by a CW diode pumped Nd:YVO4 laser (Millennia X). The oscillator produces a train of <100 fs pulses (bandwidth ~10 nm fwhm), with a peak wavelength at around 815 nm, typically of 850 mW, corresponding to ~10 nJ per pulse. The weak oscillator pulses are amplified by a chirped pulse regenerative amplifier (CPA) (Spectra Physics Spitfire). The pulses are first stretched to about 200 ps, then regeneratively amplified in a Ti:sapphire cavity, pumped by a pulsed Nd:YLF laser (Spectra Physics Evolution-15 operating at 1 kHz). After the pulse has been amplified and recompressed, its energy is about 1.0 mJ in a train of 1 kHz pulses. An independent pump pulse is obtained by pumping an optical parametric amplifier (Spectra Physics OPA-800CF) that produces 120 fs pulses tunable from 300 nm to 3 μm.

The output power of the OPA ranges from a few microjoules to tens of microjoules (depending on the chosen wavelength) at 1 kHz. The pump beam is mechanically chopped at half the amplifier repetition rate. The chopper (C-995 TTI) is synchronized to the Spitfire amplifier. Normally a few thousand pulse pairs are averaged to produce a transient absorption spectrum with a noise level below 0.3 mOD.

A small portion of the remaining amplified pulse is used to generate a white light continuum as a probe pulse. To this end, the Ti:sapphire beam is focused onto a 3 mm thick sapphire disk by a 10 cm focal length lens, and the numerical aperture of the beam is controlled by an iris placed in front of the lens, which helps to obtain a stable and smooth white light continuum (Riedle, E., private communication). The resulting beam is passed through a short pass filter to remove the remains of the fundamental beam from the white light continuum.

The pump and probe pulses are crossed in the sample at a small angle, while maintaining a magic angle between the pump and probe polarizations. The remains of the pump pulse are removed by an iris, and the probe light is imaged onto an optical fiber that brings it into an imaging interface that focuses the light onto the entrance slit of a Jobin Yivon Triax 180 spectrograph. The light is normally dispersed by a 300 1/mm grating onto a fast CCD camera (Andor Newton DU-970N-UV, operating at 1000 spectra per second using "crop mode"). The whole setup is controlled by a PC running National Instruments LabView. The time domain is scanned by delaying the pump pulse relative to the probe pulse using a hollow retroreflector mounted on a motorized translation stage (Aerotech, ALS130).

Gel Electrophoresis. Sodium dodecyl sulfate polyacrylamide gel−electrophoresis (SDS−PAGE) was performed using 1% polyacrylamide separating gel and 10% polyacrylamide stacking gel. Samples were diluted in a sample buffer, and the reference was the dual-color (Bio-Rad).

ESI−MS. Prior to mass spectrometry analysis, the samples were filtered in PD-10 columns (Sephadex G-25) and desalted using Porous R1 resin (ABI, Framingham, USA). The resin was equilibrated with 10 μL of 5% formic acid. An amount of 5 μL of the sample was applied to the R1 desalting column and washed with 5 μL of 5% formic acid three times. The samples were eluted by 50% methanol (MeOH) and 5% formic acid.

Human serum albumin mass spectra were acquired on an API 300 triple quadrupole mass spectrometer (ABI, Sciex, Concord, Ontario) using a nanoelectrospray ion source (Protana A/S, Denmark).

Molecular weight was determined by Analyst 1.4 software through the deconvolution of the multiply charged ions obtained after scanning the first quadrupole (Q1), operating in the positive mode. The typical ion source parameters are as follows: ion spray voltage 1.5kV, declustering potential (DP) 80 V, focusing potential (FP) 380 V, entrance potential (EP) 10 V, deflector −100 V, channel electron multiplier (CEM) 2700 V.

Electrochemical and Spectroelectrochemical Measurements. ***Cyclic Voltammetry (CV) Measurements.*** Cyclic voltammetry (CV) of WST11 (1.4×10^{-4} M) in acetonitrile (AN) was measured by using a three-electrode configuration at 25 °C. The working electrode was an Au electrode (1.6 mm diameter, BAS), and the counter electrode was a platinum wire. Potentials were measured vs Ag/Ag^+ reference electrode (BAS, 0.1 M $AgNO_3$, 0.6 V vs NHE). Supporting electrolyte was 0.1 M tetrabutlyammoniumfluoroborate (TBAF). Previous to each measurement, the working electrode was polished by the BAS polishing kit followed by several minutes of sonication in double distilled water and a thorough washing with methanol and electrolyte solutions.

Spectroelectrochemical Measurements. Spectroelectrochemical measurements of WST11 in AN were performed in a specially designed cell (optical path length of 500 μm) that was fitted to the cuvette holder of a Thermo Evolution 300 UV−VIS−NIR spectrophotometer. A transparent indium titanium oxide slide (ITO, sigma-Aldrich) served as the working electrode and a platinum wire as the auxiliary electrode. Potentials were measured vs a thin Ag/Ag^+ reference electrode (custom-made, 0.1 M $AgNO_3$, 0.6 V vs NHE). The ITO slide and the Pt wire were attached to electrical connectors that were mounted to a Teflon cover. The reference electrode and a thin tube (2 mm diameter, used for N_2 purging) were inserted into

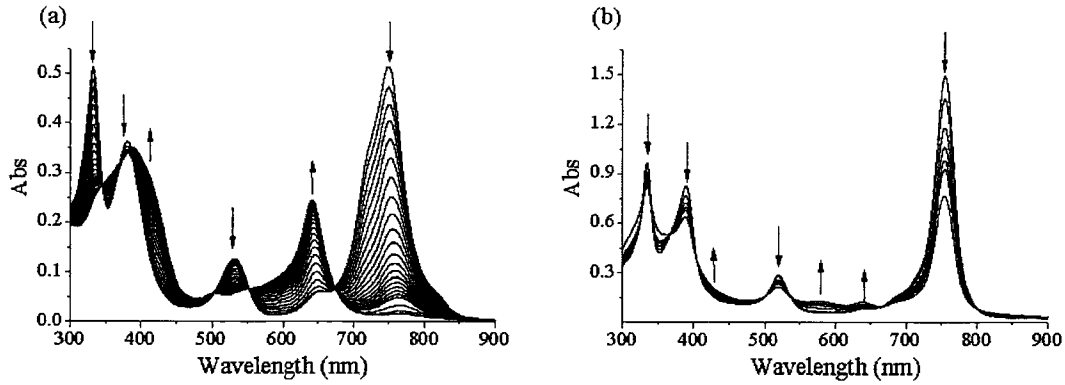

Figure 1. Photodegradation of 25 μM WST11 solutions under illumination at 755 nm (20 mW) for 10 min in (a) PBS and (b) PBS + 500 μM HSA.

the solution through dedicated apertures in the Teflon cover. The sample solutions were thoroughly degassed by N_2 for 30 min. To maintain anaerobic conditions, a moderate gas flow was maintained within the cuvette on top of the solution. The supporting electrolyte was 0.1 M tetrabutlyammoniumfluoroborate (TBAF). Monocationic and monoanionic species of WST11 were electrochemically generated by setting constant oxidative or reductive potentials (+600 and −1100 mV vs NHE, respectively). The measurements were performed at 25 °C.

Dissolved Molecular Oxygen Measurements. Oximetry measurements were performed by an ISO_2 dissolved oxygen sensor (Clark type, 2 mm diameter, World Precision Instruments). The electrode tip was inserted into the spectroscopic cuvette through an appropriate aperture, allowing concomitant monitoring of dissolved oxygen concentration and optical UV−VIS−NIR absorption.

Fluorescence Analysis. Fluorescence analysis was performed using a Cary Eclipse Fluorescence Spectrophotometer from Varian (Australia, Pty Ltd.). Samples were analyzed using a quartz cuvette. The results represent the mean of five measurements.

Results

Spectral Changes of WST11 in Aqueous Solutions, In Response to Continuous VIS−NIR Illumination. Figure 1 illustrates the response of WST11 in different solutions to continuous illumination at 755 nm.

The UV−VIS−NIR spectra of [M]−Bchls are composed of four well-resolved transition bands,[30−33] designated in order of increasing energy as Q_y, Q_x, B_x, and B_y (the x and y captions assign the symmetry axis along the pi system of the Bchl molecule). In PBS solution (Figure 1a), the four transitions are located at 750, 530, 390, and 340 nm, respectively. Upon illumination, these transition bands rapidly bleach, whereas new transitions at 647 and 410 nm emerge. These two transition bands are typical to chlorines the oxidized form of [Pd]-substituted Bchls,[24] indicating that WST11 undergoes photo-oxidation upon illumination. Under anaerobic conditions, this process does not occur, as implied by the stability of the corresponding optical absorption spectrum (data not shown). Addition of HSA to the aerobic solution greatly retards the photo-oxidation process (Figure 1b). Moreover, the photochemical products are different, presenting very weak absorption in the VIS region with a maximum at 580 nm. Importantly, at the working concentration of WST11 (25 μM), the Q_y transition undergoes broadening and exciton splitting, typical of Bchl aggregates.[34−36] These aggregates undergo monomerization upon adding HSA, and the excitonic transitions collapse as depicted by Figure 1b, consistent with our previous report.[14]

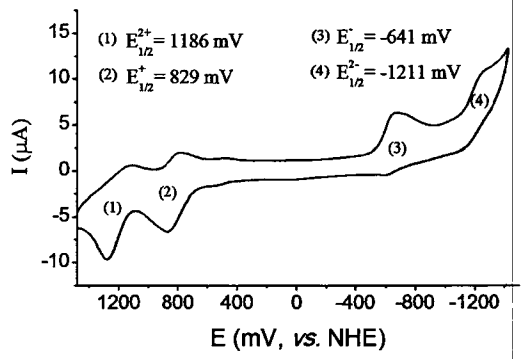

Figure 2. Cyclic voltammetry measurement of WST11 (500 μM) in aerated AN recorded at a scan rate of 75 V/s. The four detectable waves and the corresponding half-wave potential values are indicated and reported vs NHE. The positive half-wave potentials, designated as $E^{+}_{1/2}$ and $E^{2+}_{1/2}$, refer to the first and second oxidation of the Bchl pi system, respectively (formation of cation radical and dication species). The negative half-wave potentials, designated as $E^{-}_{1/2}$ and $E^{2-}_{1/2}$, refer to the first and second reduction of the pi system, respectively (anion radical and dianion species).

Electrochemistry and Spectroelectrochemistry of WST11. Figure 2 shows the CV response of WST11 in AN under anaerobic conditions.

The voltammogram features four quasi-reversible ring-centered (ring-centered refers to oxidation or reduction of the Bchl pi system as opposed to metal-centered reactions that occur on the central metal) oxidation waves.[37] The half-wave potentials of the mono- and dication species (mono- and dication species are products of first and second ring-centered oxidation processes, respectively) are 484 and 841 mV vs NHE, respectively. The half-wave potentials of the mono- and dianion species are −986 and −1556 mV vs NHE, respectively. The oxidation potentials of WST11 are less positive by ~100 mV than the corresponding oxidation potentials of previously characterized [M]−Bchl compounds.[37,38] In this respect, this finding implies that WST11 can be oxidized more easily then the WST09 derivative and therefore provides favorable thermodynamic conditions for the formation of the $O_2^{-\bullet}$ radical.

Figure 3 depicts the spectral changes introduced by the reversible and irreversible products of one-electron electrochemical oxidation and reduction of WST11 in AN under anaerobic conditions. Figure 3a shows the difference spectra of neutral WST11 and its electrochemical products obtained under a mono-oxidizing or reducing potential. Notably, the Q_y and Q_x of WST11 in AN are blue-shifted relative to their

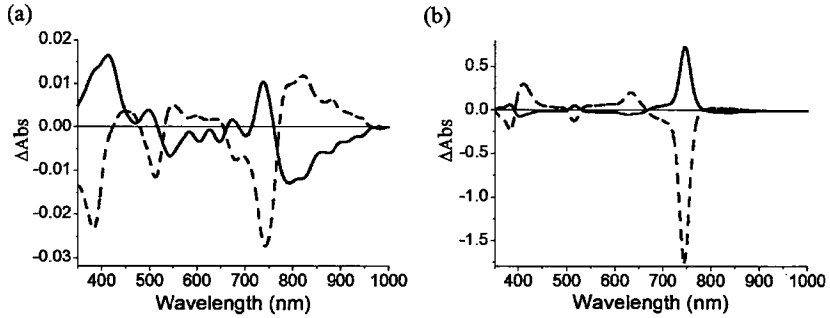

Figure 3. Difference spectra of neutral WST11 and its electrochemically produced species: (a) dashed line, difference of neutral and mono-oxidized species; solid line, difference of mono-oxidized and back-reduced species; (b) dashed line, difference of neutral and monoreduced species; solid line, difference of monoreduced and back-oxidized species.

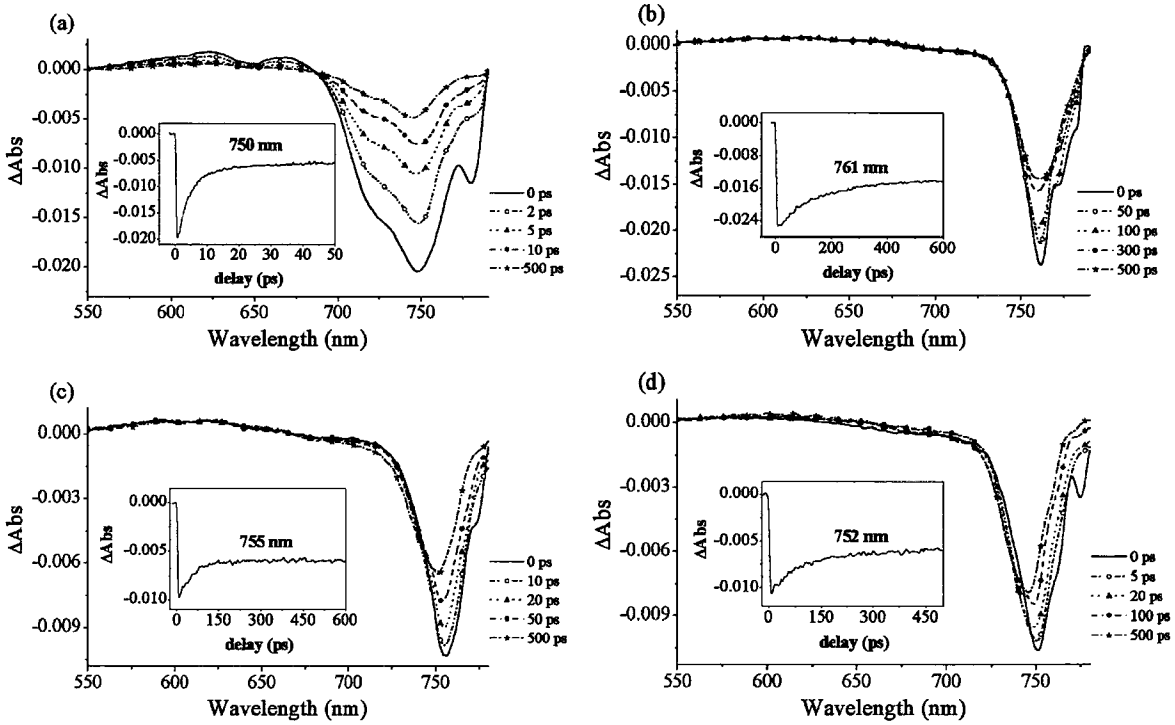

Figure 4. Time-resolved spectra of WST11 in (a) PBS, (b) PBS + 150 μM HSA, (c) MeOH, and (d) AN. The measurements were carried out under anaerobic conditions. Data collection time was 45 min per transient.

position in PBS and peak at 744 and 514 nm, respectively, while the B_x and B_y slightly red-shifted and peak at 383 and 326 nm, respectively. The electrochemical oxidation induces bleaching of the major transition bands of WST11 at 382, 514, and 744 nm and an absorption increase at 448, 548, and 821 nm, where the latter is the most prominent transition band. Upon the back reduction process, the bleaching of these bands allows their assignment to the cationic $WST11^+$. The electrochemical reduction results in a similar bleaching pattern but a significantly different absorption increase, with major transitions at 411 (strong) and 824 (weak) nm (Figure 3b). The reaction reversibility is ~50% and ~30% for the oxidation and reduction processes, respectively. The rest of the compound was irreversibly degraded to the bacteriochlorine form, indicated by the transition band at ~640 nm.[24,30,32,33]

Time-Resolved Changes in the Optical Absorption of WST11 in Response to Pulsed Illumination at the Femto- to Picosecond Time Domain. Figure 4 illustrates the ultrafast response of 25 μM WST11 in different solutions to 120 fs light pulses at 525 nm (pump pulse energy 2.3 μJ, which did not induce significant degradation after several measurement sets). The corresponding kinetic parameters of the transient absorption and bleaching recovery are given in Table 1.

The 750 nm absorption and the accompanying shoulder at 715 nm undergo instantaneous bleaching. The bleaching is accompanied by an absorption increase at 585, 625, and 670 nm. Between 10 and 15 ps, about 75% of the bleached spectrum recovers, and the transient absorption decays to a longer-living state (at 585 nm, Figure 4a), at a rate of 1.2×10^{11} s^{-1} (Table 1). In the presence of HSA (Figure 4b), the absorption in the Q_y domain bleaches as a single band (in agreement with the proposed monomerization of the compound),[14] and 20% of the bleached spectrum recovers at a rate of 4.5×10^{10} s^{-1} (Table 1). An additional 10% recovers at a rate of 6.6×10^9 s^{-1} (Figure 4b and Table 1). The rest appears as a long-living state that decays in the nano/millisecond time domain (see below), fairly similar to the yield and decay rate of the long-living excited form of WST09.[24] The transient absorption and bleaching of WST11 in response to the 120 fs pulses in MeOH and AN (Figure 4c and d, respectively) appear similar to those observed in the HSA solutions, but the corresponding rate constants for 30% recovery are about half (2×10^{10} s^{-1}, Table 1). Importantly,

TABLE 1: Kinetic Parameters of the Transient Absorption and Bleaching Recovery of WST11 in Different Solutions

	WST11 in PBS				
	585 nm[a,b]	625 nm[a,b]	670 nm[a,b]	715 nm[b]	750 nm[b]
τ (ps) [k (1/s)]	7.9 ± 2 [1.2 × 10^{11}]	5.2 ± 0.5 [1.9 × 10^{11}]	4.7 ± 0.4 [2 × 10^{11}]	5.4 ± 0.1 [1.8 × 10^{11}]	4.8 ± 0.1 [2 × 10^{11}]
R^2	0.32	0.66	0.70	0.99	0.99

	WST11 in PBS + 150 μM HSA	WST11 in MeOH	WST11 in AN
	761 nm[b]	755 nm[b]	752 nm[b]
τ (ps) [k (1/s)]	24 ± 11, 152 ± 6 [4.5 × 10^{10}, 6.6 × 10^{9}]	50 ± 3 [2 × 10^{10}]	50 ± 13, 226 ± 75 [2 × 10^{10}, 4.4 × 10^{9}]
R^2	0.98	0.79	0.96

[a] Absorption band. [b] Bleaching.

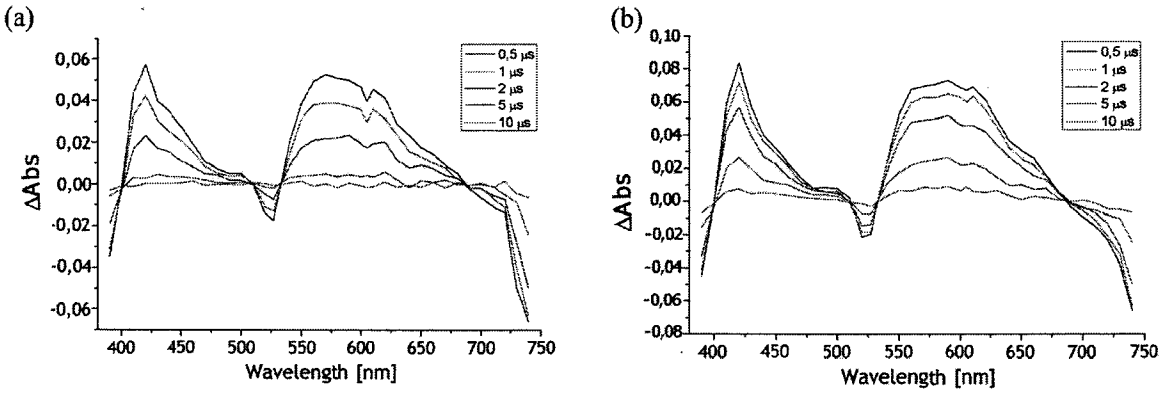

Figure 5. Time-dependent changes in optical absorption of 25 μM WST11 + 150 μM HSA in PBS after 532 nm pulsed excitation (5 ns pulse duration). (a) Oxygen-saturated solution; (b) argon-saturated solutions. During this experiment, total exposure time to white monitoring light did not exceed 5 s. Each data point was obtained by a single laser flash (energy ~1.5 mJ).

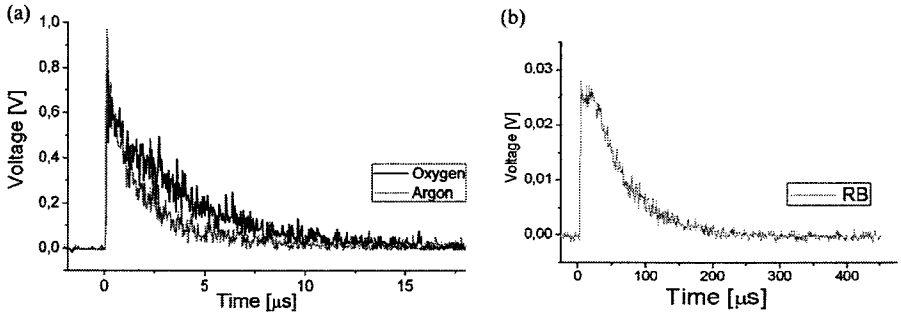

Figure 6. (a) The 1272 nm emission due to a single, 5 ns flash excitation at 532 nm of WST11/HSA/D2O solution saturated with argon (red line) or molecular oxygen (black line). (b) The 1272 nm emission due to excitation of Rose Bengal in oxygen-saturated solutions.

the transient absorption of WST11 in PBS features peaks between 500 and 700 nm (Table 1). This can be carefully attributed to the cationic form of WST11 as derived from Figure 3a, with some red shift that reflects the solvent effect.

Measurements at the Sub-microsecond to Millisecond Time Domain. Figure 5 presents the long-living transient optical absorption of WST11 in PBS\HSA solutions, under oxygen or argon saturation, from the submicro- to the millisecond time range.

While the two spectra appear similar, saturation with argon gives rise to an absorption increase at 605 nm that partly bleaches during the first microsecond after excitation in the oxygen-saturated solutions. Although the difference between the ground and long-living excited state of WST11 resembles the one observed for WST09,[24] there are several profound differences. First, WST11 presents transient absorption at 418 nm that is several times stronger than the absorption of WST09 at this wavelength region. Second, the VIS absorption of WST11 includes shoulders that extend beyond 605 nm, whereas WST09 presents a single absorption increase at 575 nm. To gain a better insight into the origin of the long-living transient absorption, we examined the NIR emission of WST11 in PBS/HSA solution under argon or oxygen saturation. The results are presented in Figure 6a.

Typical to both Bchl triplets is the fairly strong emission (phosphorescence) at ~1160−70 nm that extends up to 1272 nm.[24,39] This emission can overlap the emission of singlet oxygen.[24,39] Thus, the 1272 nm emission of aerobic solutions of Bchl derivatives can be contributed by both the Bchl triplet state and photodynamically generated singlet oxygen molecules. Fortunately, the decay rate of the Bchl phosphorescence is larger by more than an order of magnitude than the singlet oxygen decay in D_2O solutions, thus enabling good resolution of the two.[24] Table 2 summarizes the corresponding kinetic parameters.

TABLE 2: Kinetic Parameters of WST11 Transient Absorption at the Sub-microsecond to Millisecond Time Domain

	oxygen-saturated solution	argon-bubbled solution
τ (μs) [k (1/s)]	1.72 [5.8 × 10^5]	4.22 [2.4 × 10^5]
standard error	0.04	0.13

The phosphorescence signal in the argon-saturated solution decays at a rate of 2.4 × 10^5 s^{-1} and at a double rate of 5.8 × 10^5 s^{-1} in the oxygen-saturated solution. No significant change in the signal amplitude was observed in the presence of oxygen. Figure 6b illustrates the decay of the 1272 nm emission (excitation at 532 nm) generated by Rose Bengal in PBS/HSA/D_2O solution that have the same OD at 532 nm. The rate constant of the 1272 nm generated by Rose Bengal, which is uniquely identified with singlet oxygen emission, is by far smaller (0.1 × 10^5 s^{-1}), as we previously reported.[24] Cumulatively, our data exclude the formation of singlet oxygen by photoexcited WST11 in aqueous solutions. In the absence of singlet oxygen generation, only $OH^•$ and $O_2^{-•}$ radicals can be generated by the photoexcited WST11. To better identify the evolved ROS, we utilized the ESR technique.

Generation of ROS by Photoexcited WST11 in the Absence of Serum Albumin. Figure 7 shows the ESR spectra of the photogenerated and spin-trapped $OH^•$ and $O_2^{-•}$ radicals upon illumination of WST11 in PBS solution, using DMPO as the spin trap.

Verifying the Genuine Production of $O_2^{-•}$ and $OH^•$ Radicals. A shortcoming of using DMPO as a spin trap is the rapid decomposition of the DMPO−OOH adduct to DMPO−OH. To overcome this problem and to verify the production of a genuine $OH^•$ radical in our system, we used the selective 5-diethoxyphosphoryl-5-methyl-1-pyrroline *N*-oxide (DEPMPO) spin-trap, as previously described.[24] The DEPMPO−OOH adduct does not degrade to the DEPMPO−OH adduct, therefore allowing selective trapping of $OH^•$ and $O_2^{-•}$ radicals. Figure 8 presents the experimental and corresponding simulated ESR signals of the DEPMPO−OOH and DEPMPO−OH spin adducts, obtained upon illumination of WST11 in PBS.

This result confirms that WST11 produces both $OH^•$ and $O_2^{-•}$ radicals in aqueous solutions. The concentrations of the photogenerated radicals were calculated using the following equations:

$$[OH^•] = \frac{S_{DEPMPO-OH}}{S_{stn}}[stn] \text{ and } [O_2^{-•}] = \frac{S_{DEPMPO-OOH}}{S_{stn}}[stn]$$

In these expressions, $S_{DEPMPO-OH}$ and $S_{DEPMPO-OOH}$ are the integrated ESR signal of DEPMPO−OH and DEPMPO-OOH, respectively. S_{stn} is the integrated ESR signal of a standard ([3-carboxy-PROXYL]). Accordingly, the obtained concentration values for the $OH^•$ and $O_2^{-•}$ radicals are 5 and 10 μM, respectively. The number of radicals generated in the entire experimental volume V is

$$N_{OH^•} = N_A[OH^•]V = 1.5 \times 10^{14} \text{ and } N_{O_2^{-•}} = N_A[O_2^{-•}]V = 3.0 \times 10^{14}$$

where N_A is the Avogadro number and $V = 50$ μL. The energy needed to generate these radicals, 2.4 J, was delivered by 9 × 10^{18} photons at 755 nm through an optical path of 0.2 cm. Using eq 13 in Vakrat et al.[24] for 100 μM WST11, and assuming a similar cross section of absorption for WST11 and WST09 (1.2 × 10^{-16} cm^2), we found that the delivered energy could generate 5 × 10^{17} WST11 molecules in the excited triplet state (e.g., under anaerobic conditions). Figure 4b shows that ~70% of WST11 molecules that were excited to their first excited singlet state (in one 120 fs pulse) relaxed into their triplet state. Upon collision with ground-state oxygen, ~66% of the formed complexes (i.e., those having a spin multiplicity of 1) can make ion pairs.[40,41] Thus, the apparent quantum yield of $O_2^{-•}$ and $OH^•$ radicals can reach 4.5 × 10^{14}/2.3 × 10^{17} ~ 2 × 10^{-3} or 0.2% in the PBS solution (using eq 14 in Vakrat et al.).[24] However, each oxidized WST11 undergoes irreversible degradation under aerobic conditions and in the absence of compensating reducing agents, as previously explained for WST09.[24] Following these constraints, the integrated number of the photoexcited WST11 molecules in the singlet state is significantly reduced, and the quantum yield for radical formation should be markedly higher than the above value. Indeed, such higher yields are demonstrated below in the presence of HSA.

Generation of ROS by Photoexcited WST11 in the Presence of Human Serum Albumin. Figure 9 shows the effect of HSA on $OH^•$ radical generation by WST11 upon consecutive illumination−reoxygenation cycles in the presence and absence of HSA.

The sample (1 mL of 100 μM WST11) was placed in an optical cuvette of 0.5 cm path length where it was periodically illuminated for 2 min at 755 nm (20 mW). After each illumination period, an aliquot of 50 μL was examined by ESR while the sample in the cuvette was introduced to a stream of oxygen under dark conditions until saturation of dissolved oxygen was reached. This light−dark−reoxygenation cycle was repeated until the complete degradation of the WST11−HSA complex (monitored spectroscopically as in Figure 1b). After the first period of illumination, the concentration of DMPO−OH

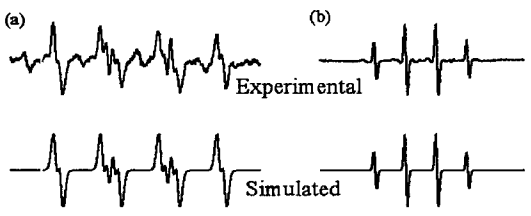

Figure 7. ESR spectra of the photogenerated ROS upon illumination of WST11 (100 μM) at 755 nm (20 mW, 2 min) in PBS. (a) Signal of DMPO−OOH. The signal was acquired in the presence of 10% DMSO used as an $OH^•$ radical quencher. Simulation parameters: a_N = 13.98, $a_{H\beta}$ = 11.26, $a_{H\gamma}$ = 1.27, R = 0.91. (b) Signal of DMPO−OH; simulation parameters: a_N = 14.88, a_H = 14.68, R = 0.99. DMPO concentration was 80 mM.

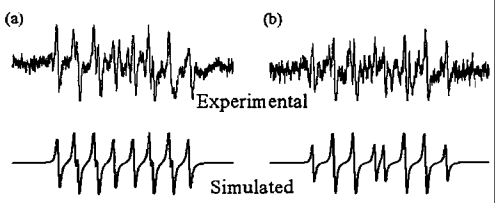

Figure 8. ESR spectra of DEPMPO−OOH and DEPMPO−OH adducts obtained upon illumintion of WST11 (100 μM) at 755 nm (20 mW, 2 min). (a) Signal of DEPMPO−OOH. The signal was acquired in the presence of 10% DMSO used as an $OH^•$ radical quencher. Simulation parameters: a_p = 50.3 G, a_N = 13.8 G, a_H = 11.1 G. (b) Signal of DEPMPO−OH, obtained by subtracting the pure DEPMPO−OOH signal from the original mixed signal. Simulation parameters: a_p = 47.0 G, a_N = 13.5 G, a_H = 14.0 G. DEPMPO concentration was 170 μM.

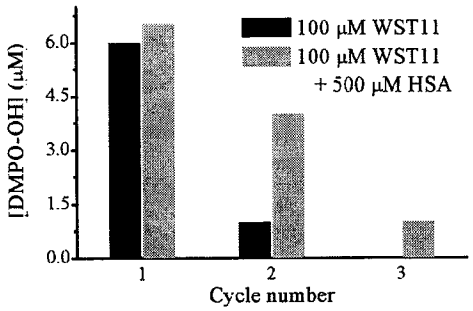

Figure 9. Effect of HSA (500 μM) on the photogeneration of OH$^{\bullet}$ radical by WST11 (1 mL of 100 μM WST11 in PBS, placed in an optical cuvette). The sample was illuminated periodically for 2 min at 755 nm (20 mW). After each illumination period, an aliquot of 50 μL was examined by ESR, while the cuvette was introduced to a stream of molecular oxygen. This was repeated until the complete degradation of the WST11−HSA complex (monitored spectroscopically).

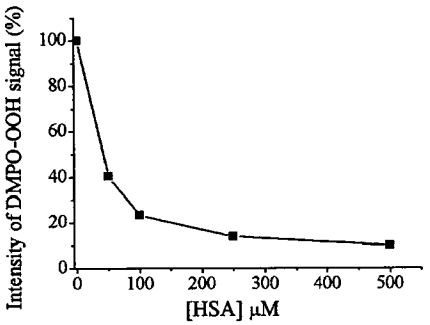

Figure 10. Effect of HSA on the DMPO−OOH ESR signal. [WST11] = 100 μM, [DMPO] = 80 mM. Illumination was performed for 10 min at 755 nm (20 mW).

reached a fairly similar level as in the sample that did not contain HSA. However, after a second period of illumination, in the absence of HSA the concentration of DMPO−OH decreased by 85% relative to the first illumination period, whereas in the presence of HSA, the concentration decreased only by 40%. In the third cycle, no radicals were produced in the non-HSA solution, while in the presence of HSA, OH$^{\bullet}$ radicals were produced at 15% of the initial yield. Altogether, the concentration of the trapped OH$^{\bullet}$ radical increased by more than 2-fold in the presence of HSA, reaching a total value of 12 μM under the applied experimental conditions.

Figure 10 shows that addition of HSA quenched the spin-trapped $O_2^{-\bullet}$ to about 10% of its value in the absence of HSA.

The addition of oxygen and the application of periodic illumination as described above did not affect the concentration of the DMPO−OOH adduct. These findings suggest that either the generation of $O_2^{-\bullet}$ radicals is significantly lowered in the presence of HSA or that the radicals rapidly interact with the protein.

Effect of HSA on Oxygen Consumption during WST11 Illumination in Aqueous Solutions. Generation of reactive oxygen species upon illumination of WST11 is accompanied by rapid consumption of molecular oxygen. In fact, we have recently found that this is an important part of the VTP mechanism in vivo.[42] Hence, we independently explored the consumption of molecular oxygen under illumination of WST11−HSA solutions. Figure 11a (left side) shows that in the absence of HSA molecular oxygen is consumed at a rate of 0.23 μM s^{-1} and levels off after 11 min of illumination. At that time, WST11 undergoes complete bleaching and is converted into a bacteriochlorine type molecule (Figure 11a, right side). Figure 11b (left side) shows that upon adding HSA to WST11/PBS solution the light-induced consumption of molecular oxygen is significantly enhanced in terms of kinetics and yield. Under these conditions, 20 min of illumination brought about the complete depletion of 270 μM of dissolved molecular oxygen at a rate of 0.86 μM s^{-1}. Yet, only ~30% of the WST11−HSA complex has been degraded (Figure 11b, right side). Oxygen replenishment of the solution to the level of saturation during a short dark period (15 s) followed by 6.5 min of illumination resulted in the consumption of additional 270−300 μM molecular oxygen at a rate of 1.7 μM s^{-1} (Figure 11c, left side) and additional 30% degradation of WST11 (Figure 11c, right side). An additional oxygen replenishment and illumination of the sample ended after 4.5 min with another depletion of 230 μM molecular oxygen at a rate of 2.15 μM s^{-1} (Figure 11d, left side) and the complete degradation of the WST11−HSA (Figure 11d, right side).

Altogether, 750−800 compared to 50 μM of molecular oxygen was consumed upon illumination of 100 μM WST11 in the presence and absence of HSA, respectively.

Quantum Yield for Oxygen Consumption by WST11 in Aqueous Solutions Containing HSA. Using the second and third cycles, we calculated the apparent quantum yield for oxygen consumption by light-excited WST11. The linear consumption of oxygen in each of these cycles continued for ~60 s during which 4.5 × 10^{18} photons at 755 nm were delivered. This delivery generated 1.3 μM of OH$^{\bullet}$ radicals (Figure 9) and consumed 150 μM of molecular oxygen (Figure 11c and d). Since the calculated quantum yield for OH$^{\bullet}$ generation by WST11 in the excited triplet state is 0.2% (see above), the calculated quantum yield for oxygen consumption by this compound in the presence of HSA is 21%, one-third of the upper limit expected (assuming a charge transfer mechanism that involves the spin 1 multiplicity of the collision complex between molecular oxygen and WST11 at the excited triplet state).[40,41] Since no singlet oxygen could be detected both in the absence (data not shown) and in the presence of HSA (Figure 6), we can conclude that the oxygen consumption involved only reduction by the noncovalent WST11−HSA complexes. However, since only 1.3 μM of such radicals was trapped, the rest should interact with the protein molecules.

Oxidation of HSA by ROS, Generated through Excitation of WST11−HSA Noncovalent Complexes. Although both oxygen consumption and spin-trapped radical concentrations are increased upon adding HSA to the WST11 solutions, the former is ~15 times higher than the latter. At the same time, the photochemical degradation of WST11 is dramatically attenuated. Thus, the value of [consumed WST11]/[consumed O_2] is 1.5 and 0.1 in the absence and presence of HSA, respectively. Still, there is no apparent difference in the overall concentration of spin-trapped ROS ($O_2^{-\bullet}$ and OH$^{\bullet}$) in the two examined solutions. This discrepancy prompted us to look for possible interactions of the photogenerated ROS with the HSA molecules.

Reactions of ROS with serum proteins are common in biological contexts; the oxidation of Trp residues by ROS is the most commonly reported pathway.[43,44] Moreover, interaction of singlet oxygen with HSA during PDT with porphyrins has been reported.[45] Nevertheless, to the best of our knowledge, this interaction has never been quantified. Peroxidation of serum proteins may slightly increase their molecular weight and/or drive cross-link formation between several HSA monoproteins. The above should result in mass changes that can be monitored by gel electrophoresis if large enough or by mass spectrometry if the peroxidation involves small changes.

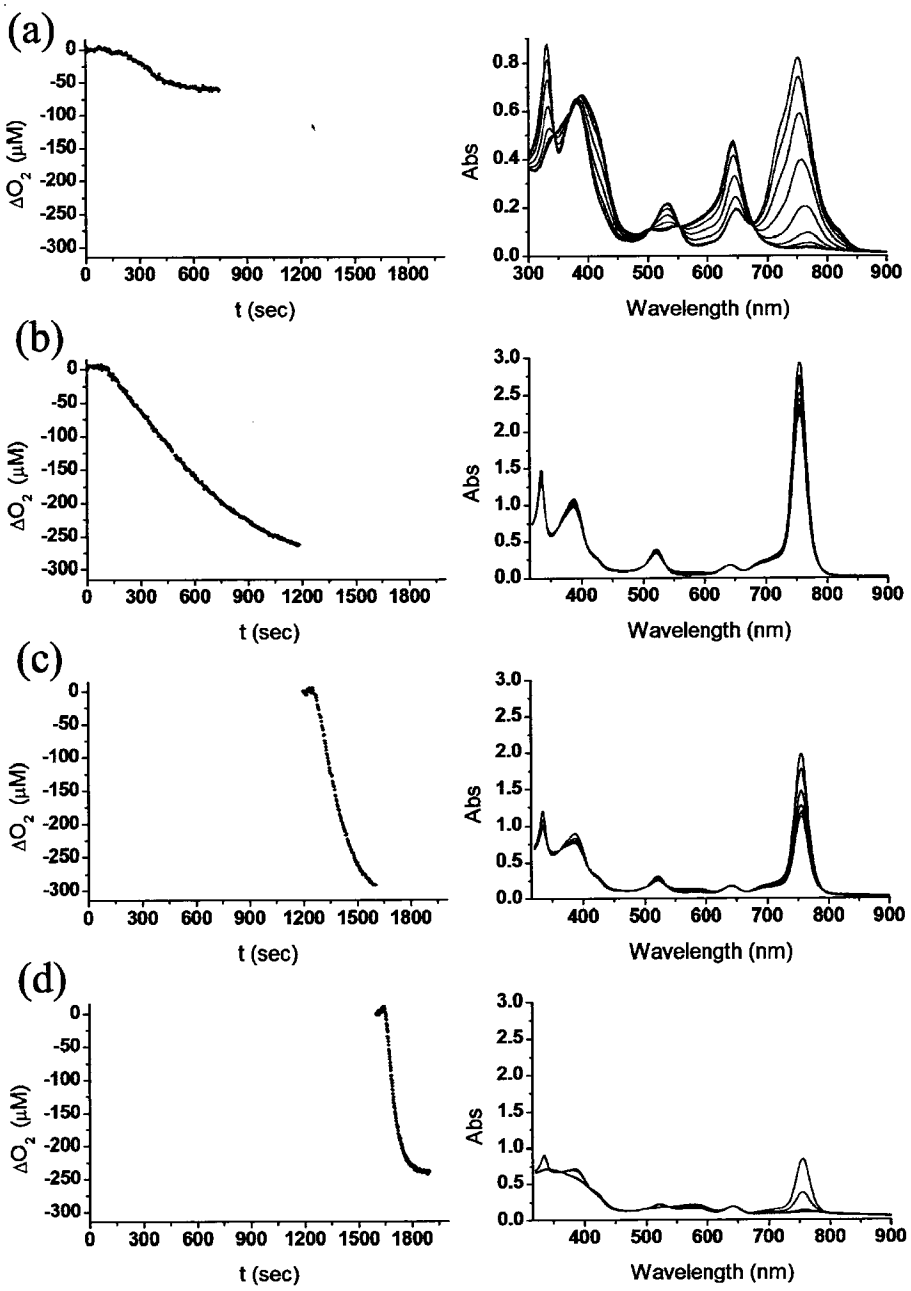

Figure 11. Light-induced oxygen consumption of WST11 (100 μM) during illumination at 755 nm (20 mW) and the corresponding spectral evolution: (a) oxygen consumption during 11 min illumination of WST11 in the absence of HSA; (b) first cycle of oxygen consumption in the presence of HSA (500 μM) and 20 min of illumination; (c) second cycle of light-induced oxygen consumption: after cycle b ended, the solution was replenished by oxygen (dark period of 15 s) and then illuminated for a period of 6.5 min; (d) additional cycle of light-induced oxygen consumption: following the ending of cycle c, the solution was replenished by oxygen (dark perdion of 15 s) and then illuminated for a period of 4.5 min.

Gel electrophoresis of HSA collected from samples of WST11 after extensive illumination did not reveal any significant cross-link formation (not shown). However, ESI−mass spectrometry of HSA before and after PDT was monitored revealed a mass increase of 224 g/mol (Figure 12) in the HSA fraction that was bound to WST11 during illumination (collected as the colored fraction).[14]

This additional mass corresponds to seven molecules of oxygen added to each molecule of HSA during the entire period of illumination. Since more than 90% of the WST11 molecules are bound in a 1:1 complex with HSA, the WST11−HSA concentration is ~100 μM, accounting for ~700 μM out of the 750−800 μM of consumed oxygen molecules.

Unfortunately, we were not able to isolate and directly identify the affected residues; however, HSA contains a single tryptophan (Trp) that was involved in different redox reactions with attached ligands[46,47] and is close to one of the putative porphyrin binding sites in HSA. To determine whether this Trp residue is close to the bound WST11, we followed its fluorescence at different relative HSA and WST11 concentrations, both in aerobic and anaerobic solutions (after extensive purging with argon). To avoid any fluorescence admixing from the multiple Tyr residues in the HSA scaffold, excitation was performed at 295 nm which is sufficiently far from Tyr absorption at 280 nm (as recently reported by Rolinsky et al.[48] and previously suggested by Lakowitz[49]) using narrow slits. As illustrated in Figure 13,

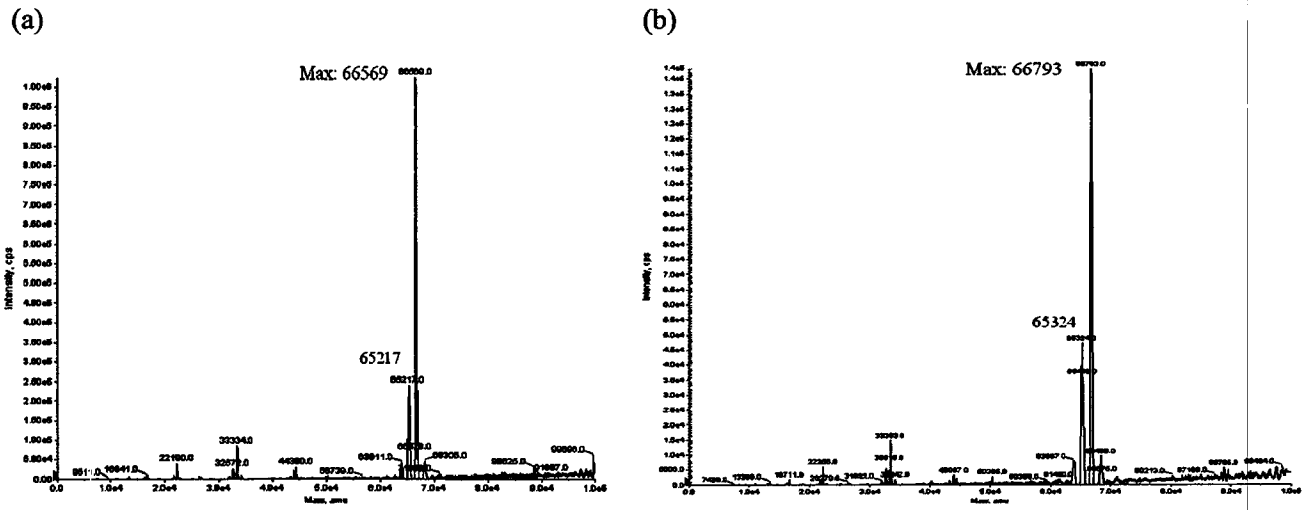

Figure 12. ESI−MS spectra of HSA before (a) and after (b) the introduction of WST11 in PBS. The analysis was done after illumination of the samples at 755 nm (20 mW, 10 min).

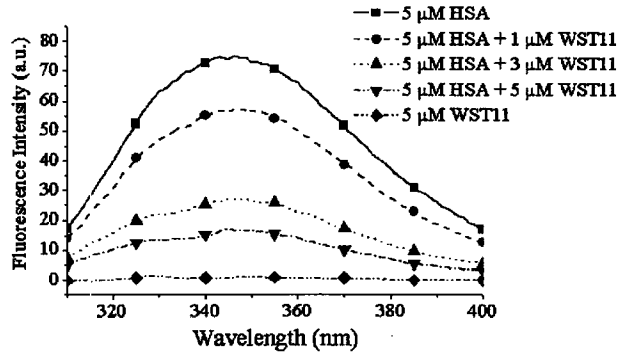

Figure 13. Fluorescence of the HSA's tryptophan residue at different concentrations of WST11. λ_{Ex}, 295 nm; λ_{Em}, 310−400 nm. [HSA] = 5 μM.

we could clearly monitor the quenching of the fluorescence of this Trp residue upon adding WST11 regardless of the oxygen content, suggesting energy transfer to the very weakly NIR fluorescing WST11.

We therefore propose that WST11 is bound at a close distance to the Trp and that part of the generated radicals interact with this residue. This hypothesis as well as the search for other specific interactions is currently under investigation in our group (see Discussion below).

Discussion

In this study, we monitored ROS photogeneration by WST11 in buffered aqueous solutions with no added amphiphilic agents. Specifically, we examined the effect of HSA, the major carrier of WST11 in the circulation and a well-recognized antioxidant agent,[50−55] on the profile and dynamics of the photogenerated ROS as well as regarding the details of the concomitant oxygen consumption. We showed that in both the absence and presence of HSA the primary photogenerated ROS are $O_2^{-\bullet}$ and $OH^{\bullet}$ radicals with no detectable singlet-oxygen generation. This observation infers that WST11−VTP, where the sensitizer is illuminated in the lumen as a WST11−HSA noncovalent complex, is most probably mediated by type I (electron transfer) and not type II (energy transfer) processes. In PBS solutions, oxygen consumption and the related generation of $OH^{\bullet}$ and $O_2^{-\bullet}$ radicals were accompanied by consumption and degradation of a similar number of WST11 molecules. In contrast, upon adding HSA (at physiological concentrations), each molecule of WST11 drove the consumption of 8−9 molecules of oxygen before degradation by radical formation. Since each molecule of WST11 can provide only 1−2 electrons upon monochromatic excitation before undergoing oxidative degradation, additional electrons had to be provided, most probably from the HSA proteins that underwent complexation with WST11. This suggests that WST11 photocatalyzed the electron transfer from the bound HSA molecule into the colliding oxygen molecules through several cycles. As Figure 3 illustrates, both the cation and anion of WST11 are fairly stable and can participate in reversible redox reactions. If electrons are rapidly provided, minimal degradation occurs. Thus, we propose that electron transfer from the excited WST11 (noncovalently bound to HSA) to a colliding oxygen molecule is immediately followed by a compensating electron transfer to the formed $WST11^+$ cation species. Overall, such oxidation and compensating reduction should result in only small changes of the ground-state absorption (Figure 3, considering the irreversible degradation to the oxidized form of WST11 as depicted by the 640 nm transition band) but should accelerate the decay of the excited triplet state, as obtained here (Table 2 and Figures 5 and 6). There are several possible sources for the electrons provided by the HSA. Bound metals such as Fe^{2+} or Cu^{1+} are one such source. However, addition of the metal chelator desferroxamine[56] (20 mM) to the PBS/HSA solution did not reduce neither the rate nor the amount of oxygen consumption, and although the amount of trapped $OH^{\bullet}$ radicals reduced, it was adequately compensated by a steep concentration increase of trapped $O_2^{-\bullet}$ radicals (data not shown). Thus, amino acid residues of the binding HSA are the most likely providers of the electrons.[46] The oxidized HSA can undergo immediate nucleophilic reduction by the generated $O_2^{-\bullet}$ radicals but not by the $OH^{\bullet}$ radicals. Additionally, the $O_2^{-\bullet}$ radicals can oxidize different residues of the HSA such as the nearby tryptophan, cystein, tyrosine, and methionin side chains. In this regard, the well-recognized antioxidative activity of HSA is most relevant.[50−55] Several such cycles should result in significant generation of $OH^{\bullet}$ radicals but minimal traces of $O_2^{-\bullet}$ species.

Conclusions

An excited WST11 molecule, noncovalently bound to the HSA skeleton, can transfer an electron to molecular oxygen to form the $O_2^{-\bullet}$ radical. In turn, the bound $WST11^+$ cation accepts an electron from an HSA residue. This cyclic light-induced process proceeds until the protein loses its capacity to donate electrons as a result of extensive peroxidation in agreement with the observed HSA

damage. This finding and the accompanied detailed analysis suggest that WST11−HSA can be regarded as a simple reaction center unit that photocatalyzes oxidoreductive reactions as needed for ROS generation in VTP. Other evidence supporting the capacity of HSA as an electron donor to different photoexcited molecules was recently published.[46] However, we are not aware of any evidence of a two-step process like the one suggested here. In view of our findings, it is expected that under fractionated light and in the presence of agents that can rapidly reduce the oxidized HSA, the ROS yield may be highly increased, having clear clinical implications and ramifications.

Furthermore, the regeneration of the WST11 photocatalytic redox center by electron mobilization from the protein closely resembles the regeneration of the active primary donors in PSII RC and genetically engineered RC of purple bacteria as reviewed in the Introduction. Thus, further studies of the presented HSA/WST11 and similar systems is expected to shed light on the development of the light conversion machinery in biological photosynthesis and artificial systems.

Acknowledgment. A.S. and Y.S. are the incumbents of the Robert and Yaddele Sklare Professorial Chair in Biochemistry and the Tillie and Charles Lubin Professorial Chair in Biochemical Endocrinology, respectively. I.A. and R.G. have equally contributed to this study. WST11 was prepared by STEBA LABORATORIES (Israel). Transient absorption studies were performed at the Dr. J. Trachtenberg laboratory for photobiology and photobiotechnology (The Weizmann Institute). We are grateful to Prof. E. Riedle, from LMU, Munich, Germany, for helping us in designing the white light generator for the femto−picosecond experiment. The study was supported by research grants from STEBA-BIOTECH (France) and from Sharon Zuckerman (Toronto, Canada) and by the Ministry of Science and Higher Education (DS 4.1.874, Poland).

References and Notes

(1) Moser, C. C.; Page, C. C.; Chen, X.; Dutton, P. L. *Subcell. Biochem.* **2000**, *35*, 1.
(2) Beretan, D. N.; Onuchic, J. N. *Protein Electron Transfer*; Bios Scientific Publishers: Oxford, 1996.
(3) Takahashi, S.; Murata, N. *Trends Plant Sci.* **2008**, *13*, 178.
(4) Battle, A. M. D. *Photochem. Photobiol. B* **1993**, *20*, 5.
(5) McCaughan, J. S. *Drugs & Aging* **1999**, *15*, 49.
(6) Silva, A. R. d.; Ribeiro, J. N.; Rettori, D.; Jorge, R. A. *J. Braz. Chem. Soc.* **2008**, *19*, 1311.
(7) Foote, C. S. *Am. Chem. Soc. Symp. Ser.* **1987**, *339*, 22.
(8) Wilkinson, F.; Brummer, J. G. *J. Phys. Chem. Ref. Data* **1981**, *10*, 809.
(9) Jori, G. *Lasers in Photomedicine and Photobiology*; Springer-Verlag: Berlin, 1980; Vol. 22.
(10) Rossi, E.; Vandevorst, A.; Jori, G. *Photochem. Photobiol.* **1981**, *34*, 447.
(11) Skalkos, D.; Hampton, J. A.; Keck, R. W.; Wagoner, M.; Selman, S. H. *Photochem. Photobiol.* **1994**, *59*, 175.
(12) Solban, N.; Rizvi, I.; Hasan, T. *Lasers Surg. Med.* **2006**, *38*, 522.
(13) Solban, N.; Selbo, P. K.; Sinha, A. K.; Chang, S. K.; Hasan, T. *Cancer Res.* **2006**, *66*, 5633.
(14) Brandis, A.; Mazor, O.; Neumark, E.; Rosenbach-Belkin, V.; Salomon, Y.; Scherz, A. *Photochem. Photobiol.* **2005**, *81*, 983.
(15) Mazor, O. Synthesis of Phototoxicity of Novel Sulfonated Bacteriochlorophyll Derivatives. Ph.D., The Weizmann Institute of Science, 2004.
(16) Mazor, O.; Brandis, A.; Plaks, V.; Neumark, E.; Rosenbach-Belkin, V.; Salomon, Y.; Scherz, A. *Photochem. Photobiol.* **2005**, *81*, 342.
(17) Berdugo, M.; Bejjani, R. A.; Valamanesh, F.; Savoldelli, M.; Jeanny, J.; Blanc, D.; Ficheux, H.; Scherz, A.; Salomon, Y.; Ben-Ezra, D.; Behar-Cohen, F. *Invest. Ophthalmol. Visual Sci.* **2008**, *49*, 1633.
(18) Gross, S.; Gilead, A.; Scherz, A.; Neeman, M.; Salomon, Y. *Nat. Med.* **2003**, *9*, 1327.
(19) Lepor, H. *Rev. Urol.* **2008**, *10*, 254.
(20) Trachtenberg, J.; Bogaards, A.; Gertner, M.; Weersink, R. A.; Yue, C.; Scherz, A.; Savard, J.; Evans, A.; McLusky, S.; Haider, M. A.; Aprikian, A.; Wilson, B. C.; Elhilali, M. *J. Urol.* **2007**, *178*, 1974.
(21) Trachtenberg, J.; Weersink, R. A.; Davidson, S. R. H.; Haider, M. A.; Bogaards, A.; Gertner, M. R.; Evans, A.; Scherz, A.; Savard, J.; Chin, J. L.; Wilson, B. C.; Elhilali, M. *BJU International*, **2008**, *102*, 556.
(22) Eggener, S. E.; Coleman, J. A. *ScientificWorldJournal* **2008**, *8*, 963.
(23) MacDonald, I. J.; Dougherty, T. J. *J. Porphyrins Phthalocyanines* **2001**, 5.
(24) Vakrat-Haglili, Y.; Weiner, L.; Brumfeld, V.; Brandis, A.; Salomon, Y.; McIlroy, B.; Wilson, B. C.; Pawlak, A.; Rozanowska, M.; Sarna, T.; Scherz, A. *J. Am. Chem. Soc.* **2005**, *127*, 6487.
(25) Brun, P. H.; DeGroot, J. L.; Dickson, E. F. G.; Farahani, M.; Pottier, R. H. *Photochem. Photobiol. Sci.* **2004**, *3*, 1006.
(26) Grabolle, M.; Dau, H. *Biochim. Biophys. Acta* **2005**, *1708*, 209.
(27) Tommos, C.; Babcock, G. T. *Biochim. Biophys. Acta* **2000**, *1458*, 199.
(28) Kalman, L.; Williams, J. C. *Photosynth. Res.* **2008**, *98*, 643.
(29) Halliwell, B.; Gutteridge, J. M. C. ESR and spin trapping. In *Free Radicals in Biology and Medicine*; Oxford University Press: Oxford, UK, 1999; p 357.
(30) Gouterman, M. *J. Mol. Spectrosc.* **1961**, *6*, 138.
(31) Gouterman, M.; Wagniere, G. H. *J. Mol. Spectrosc.* **1963**, *11*, 108.
(32) Scherz, A.; Roshenbach-Belkin, V.; Fisher, J. R. E. In Chlorophylls. In *chlorophylls*; CRC Press: Boca Raton, 1991; p 273.
(33) Hanson, L. K. In Chlorophylls. In *chlorophylls*; CRC Press: Boca Raton, 1991; p 993.
(34) Scherz, A.; Parson, W. W. *Biochim. Biophys. Acta* **1984**, *766*, 653.
(35) Scherz, A.; Rosenbachbelkin, V. *Proc. Natl. Acad. Sci. U.S.A.* **1989**, *86*, 1505.
(36) Scherz, A.; Parson, W. W. *Biochim. Biophys. Acta* **1984**, *766*, 666.
(37) Noy, D.; Fiedor, L.; Hartwich, G.; Scheer, H.; Scherz, A. *J. Am. Chem. Soc.* **1998**, *120*, 3684.
(38) Geskes, C.; Hartwich, G.; Scheer, H.; Mantele, W.; Heinze, J. *J. Am. Chem. Soc.* **1995**, *117*, 7776.
(39) Hartwich, G.; Fiedor, L.; Simonin, I.; Cmiel, E.; Schafer, W.; Noy, D.; Scherz, A.; Scheer, H. *J. Am. Chem. Soc.* **1998**, *120*, 3675.
(40) Dzhagarov, B. M.; Sagun, E. I.; Ganzha, V. A.; Gurinovich, G. P. *Khim. Fiz.* **1987**, *6*, 919.
(41) Dzhagarov, B. M.; Gurinovich, G. P.; Novichenkov, V. E.; Salokhiddinov, K. I.; Shulga, A. M.; Ganzha, V. A. *Khim. Fiz.* **1987**, *6*, 1069.
(42) Madar-Balakirski, N.; Tempel-Brami, C.; Kalchenko, V.; Scherz, A.; Salomon, Y. Submitted to the *Int. J. Cancer*.
(43) Dyer, J. M.; Bringans, S. D.; Bryson, W. G. *Photochem. Photobiol.* **2006**, *82*, 551.
(44) Dyer, J. M.; Bringans, S. D.; Bryson, W. G. *Photochem. Photobiol.* **2006**, *5*, 698.
(45) Korinek, M.; Dedic, R.; Molnar, A.; Hala, J. *J. Fluoresc.* **2006**, *16*, 355.
(46) Kobori, Y.; Norris, J. R., Jr. *J. Am. Chem. Soc.* **2006**, *128*, 4.
(47) Davies, K. J. A.; Lin, S. W.; E., P. R. *J. Biol. Chem.* **1987**, *262*, 9914.
(48) Rolinski, O. J.; Martin, A.; Birch, D. J. S. *Ann. N.Y. Acad. Sci.* **2008**, *1130*, 314.
(49) Lakowicz, J. R. *Principles of Fluorescence Spectroscopy*; Plenum Press: New York, 1986.
(50) Cao, G.; Prior, R. L. *Clin. Chem.* **1998**, *44*, 1309.
(51) Jennifer, A.; Irwin, H.; Davies, M. J. *Arch. Biochem. Biophys.* **1999**, *362*, 94–104.
(52) Faure, P.; Tamisier, R.; Baguet, J. P.; Favier, A.; Halimi, S.; Levy, P.; Pepin, J. L. *Eur. Respir. J.* **2008**, *31*, 1046.
(53) Cha, M. K.; Kim, I. H. *Biochem. Biophys. Res. Commun.* **1996**, *222*, 619.
(54) Wayner, D. D.; Burton, G. W.; Ingold, K. U.; Locke, S. *FEBS Lett.* **1985**, *187*, 33.
(55) Armstrong, J. S.; Rajasekaran, M.; Hellstrom, W. J.; Sikka, S. C. *J. Androl.* **1998**, *19*, 412.
(56) Halliwell, B.; Gutteridge, J. M. C. Iron chelators. In *Free Radicals in Biology and Medicine*; Oxford University Press: Oxford, UK, 1999; p 843.

JP900580E